# MOLECULAR MECHANISMS UNDERLYING REGULATION OF TYPE III SECRETION SYSTEM UPSTREAM OF THE MASTER REGULATOR HRPL IN ERWINIA AMYLOVORA

BY

JAE HOON LEE

THESIS

Submitted in partial fulfillment of the requirements
for the degree of Master of Science in Crop Sciences
in the Graduate College of the
University of Illinois at Urbana-Champaign, 2014

Urbana, Illinois

Master's Committee:

Associate Professor Youfu Zhao, Chair
Professor John Juvik
Associate Professor Carl Bradley

## ABSTRACT

*Erwinia amylovora*, the causal agent of fire blight of apples and pears, is a necrogenic bacterium, whose virulence is dependent upon a functional hypersensitive response and pathogenicity (*hrp*)-type III secretion system (T3SS). It has been previously demonstrated that HrpL, an ECF sigma factor, is the master regulator of *hrp*-T3SS. Recently, it is reported that expression of *hrpL* is under the control of sigma 54 complex, including $\sigma^{54}$ (RpoN), its modulation protein YhbH and $\sigma^{54}$-enhancer binding protein HrpS. In this study, we investigated the role of integration host factors (IHFs) in regulating $\sigma^{54}$-dependent *hrpL* and other T3SS gene expression. IHFs are nucleoid-associated proteins and consist of two subunits, i. e. IHFα and IHFβ. IHFα and IHFβ usually form heterodimers, which could influence nucleoid structure and gene expression via DNA bending. Two single mutants (*ihfA* and *ihfB*) were generated and characterized in *E. amylovora*. Results showed that both *ihfA* and *ihfB* mutants failed to colonize and produce necrotic lesions on immature pear fruits. Bacterial growth of both mutants in pear fruits was greatly reduced and expression of *hrpL*, *dspE*, *hrpA* and *hrpN* was also significantly down-regulated as compared to wild type (WT) strain. In addition, both *ihfA* and *ihfB* mutants exhibited slower growth in rich medium and showed hypermotile phenotype as compared to WT strain. Furthermore, results showed that both IHFs positively regulated the expression of small non-coding regulatory RNA *rsmB*/*csrB*, which negatively regulates motility as previously reported. These results indicate that IHFs are required for $\sigma^{54}$-dependent *hrpL* and other T3SS gene expression and virulence in *E. amylovora*.

On the other hand, the bacterial enhancer binding protein (bEBP) HrpS plays a central role in regulating T3SS gene expression by activating the transcription of *hrpL* gene in *E. amylovora*. Upon binding to upstream activator sequence (UAS) at the *hrpL* promoter, HrpS interacts with the $\sigma^{54}$-RNA polymerase holoenzyme through conserved GAYTGA motif, which allows the initiation of *hrpL* transcription. However, where HrpS binds to the promoter of *hrpL* and what is the role of the conserved GAYTGA motif in regulating *hrpL* and other T3SS gene expression remain elusive. In this study, our goals were to identify the HrpS binding site and to characterize the role of conserved GAYTGA motif of HrpS in transcription activation of *hrpL* in *E. amylovora*. First, eight 5’ deletion constructs of *hrpL* promoter fused to a promoter-less *gfp* were made, and promoter activities were measured by flow cytometry. The results of promoter

screening suggested a potential region for HrpS binding. Second, complementation of *hrpL* mutant using twelve constructs containing *hrpL* gene and various lengths of *hrpL* promoter further delineated the UAS region for HrpS binding. Bioinformatic analysis of this region revealed a dyad symmetry sequence between -141 to -122 nt (AT-N-TGCAA-$N_4$-TTGCA-N-AT), which is characteristic for bEBP binding. Third, site-directed mutation analyses and quantitative real time-PCR (qRT-PCR) assays demonstrated that the complete-dyad symmetry sequence was all required for T3SS gene expression and complementation of *hrpL* mutant. Finally, electrophoretic mobility shift assay (EMSA) with purified truncated HrpS protein containing its DNA binding domain further verified that HrpS binds to this sequence, indicating that *hrpL* promoter from -141 to -122 is the HrpS binding site. In addition, results from site-directed mutagenesis analyses of the conserved GAYTGA motif of HrpS showed that Y100F substitution did not affect the function of HrpS, whereas Y100A and Y101A mutations completely abolished HrpS activity. These results suggest that tyrosine and phenylalanine can compensate functionally for each other in the GAYTGA motif of HrpS in *E. amylovora*.

## ACKNOWLEDGEMENTS

First and foremost, I would like to express my sincere appreciation to my advisor Professor Youfu 'Frank' Zhao. This work would not have been possible without his enthusiastic supervision, support and patience. Throughout my M.S. degree, his words and passion for research have always inspired me to take my academic ability to the next level. I feel truly lucky to be able to continue my Ph.D. studies under his guidance.

I also would like to thank my committee members, Prof. Jack Juvik and Prof. Carl Bradley, for their valuable suggestions and comments, which provided me with correct directions and helped to improve the clarity of this thesis. My special thanks also go to Ingersoll Fellowship, USDA-SCRI, and USDA-NIFA-AFRI, for financial assistance of my degree and the research projects. I am also grateful to Dr. Steven Huber and Dr. Man-Ho Oh for their help on protein experiments. Furthermore, I would like to thank Dr. Jack Widholm for letting me use his lab equipment and reagent.

I also appreciate my lab members for their cheerful support. My special thanks to Dr. Veronica Ancona for teaching me experiments from basics to applications. I really have learnt a lot from her, which includes not only research but also attitude as a scientist. I am also thankful to Dr. June Chatnaparat and Mr. Jeffrey Nian for all kinds of discussion, help, and friendship.

Finally, my deepest and warmest gratitude goes to my parents. Their support, trust, love and smile always encourage me to do my best in all matters of life. Thank you all for your love.

## TABLE OF CONTENTS

## LIST OF FIGURES

## LIST OF TABLES

# CHAPTER 1

# INTRODUCTION

## 1.1 Fire blight and *Erwinia amylovora*

### 1.1.1 Fire blight disease and symptoms

Fire blight is one of the most devastative diseases of plants in the *Rosaceae* family, such as apple (*Malus* sylvestris) and pear (*Pyrus communis* L.), and has become a serious economic concern in pome fruit production globally. The first incidence of fire blight was reported in the Hudson Valley of New York in the late 1700s (Denning, 1794). It has since been observed throughout the United States and in other regions of the world, including New Zealand, Europe, the Middle east and Asian countries (Bonn and Zwet, 2000). The causal agent of fire blight, *Erwinia amylovora* (Burrill) Winslow et al., was first discovered in the late 1800s (Burill, 1880) and proven by Koch's postulates a few years later (Arthur, 1885). The bacterium *E. amylovora* is regarded as the first known bacterium to cause a plant disease.

Disease symptoms of fire blight are characterized by water soaking of infected tissue, followed by wilting and rapid tissue necrosis. These result in a blackened and scorched appearance in leaves and twigs, thus the name fire blight. Invasion of *E. amylovora* can occur in all parts of the plant through natural openings and wounds, causing various phases of the disease, such as rootstock blight, shoot blight, and blossom blight (Vanneste, 2000; Norelli et al., 2003). The bark or cankers in wood are the site of pathogen survival over the winter, which establish the major source of primary inoculum for a continuing epidemic of secondary rootstock and shoot blight in the spring and summer (Khan et al., 2012). Rootstock blight girdles and eventually kills the limbs or the entire trees, while shoot blight exhibits a characteristic shepherd's crook and

wilting with brown to black necrotic lesions on the affected succulent shoots (Oh and Beer, 2005). Under conditions of high humidity and warm temperature, droplets of sticky bacterial ooze are often exuded from the diseased parts of the plant, and bacteria can be disseminated to other tissues or plants by wind, rain, and insects. Pathogen colonization and multiplication on the stigma of blossom of apples and pears are thought to be an important step for subsequent disease development, including fruit blight and infection of other shoots (Malnoy et al., 2012). A severe outbreak of fire blight is closely associated with not only favorable weather conditions, but also age and susceptibility of the host plant (Thomson, 2000).

### 1.1.2 Causal agent of fire blight: *Erwinia amylovora*

*E. amylovora* is a necrogenic, Gram-negative bacterium. The cells of *E. amylovora* are short rods with rounded ends, weakly fermentative (Holt et al., 1994), and motile by peritrichous flagella in pH- and temperature-dependent manner (Raymundo and Ries, 1981). Optimum growth of *E. amylovora* occurs between 21℃ and 30℃, and a temperature above 18℃ is required for the development and epidemic of blight symptoms (Billing, 1974). *E. amylovora* shows unique chemotactic response toward aspartate and several organic acids of the citric acid cycle, such as succinate, oxaloacette, malate, and fumarate, but not toward the other amino acids and sugars (Raymundo and Ries, 1980). As a member of the family *Enterobacteriaceae, E. amylovora* is closely related to several other plant-associated bacteria, such as *Pantoea*, *Pectobacterium* and *Brennaria* (Smits et al., 2011), and share some common characteristics with many animal enterobacterial pathogens such as *Salmonella* spp. and *Shigella* spp. Although there are other related *Erwinia* species capable of causing blight symptoms, several cultural, physiological and biochemical characteristics, including facultative anaerobe, mucoid growth,

reducing substances from sucrose, acetoin production and gelatin liquefaction, distinguish *E. amylovora* from other *Erwinia* species (Vanneste, 2000). The host range of *E. amylovora* includes more than 180 species from 39 genera (Zwet and Keil, 1979; Bradbury, 1986). Based on different host specificity, *E. amylovora* strains can be further divided into three major groups; strains isolated from the *Rosaceae* subfamily Spiraeoideae (e.g., *Crataegus*, *Malus*), from *Rubus* (e.g., raspberries and blackberries), and from Asian pear (a new species *E. pyrifoliae*) (Zhao and Qi, 2011).

*E. amylovora* has a circular genome of about 3.8 Mb which is relatively small as compared to 4.5 to 5.5 Mb of sequenced enterobacterial genomes (Sebaihia et al., 2010). Different strains of *E. amylovora* may contain different plasmids, such as pEA29, pEA72, and pE170, but the specific roles of the plasmids in virulence have not been characterized (Malnoy et al., 2012). The complete genome sequence of *E. amylovora* was first revealed in 2010 for strain CFBP1430, isolated in France from *Crataegus* (Smits et al., 2010). Since then, more than 20 different strains infecting hosts within *Rosaceae* and *Rubus* families have been fully sequenced, allowing in-depth comparative and evolutionary genomic studies. A comparison of two different *E. amylovora* strains CFBP 1430 and Ea273, isolated in New York from apple, revealed more than 99.99% nucleotide sequence identity, suggesting a high homogeneity of this species (Smits et al., 2010). Through comparative genomic analysis of 12 distinct strains of *E. amylovora*, it was also reported that the core genome of the pathogen contains about 89% conserved coding sequences and shares more than 99% amino acid identity among all strains (Mann et al., 2013). In addition, comparative analysis of *E. amylovora* with two other *Erwinia* species, *E. pyrifoliae* and *E. tasmaniensis*, has revealed that major virulence factors, such as type III secretion systems

(T3SS), sorbitol metabolism, and levan biosynthesis are highly conserved between the species. However, it has been proven that four *E. amylovora* wild-type strains (Ea1189, Ea273, Ea110, and CFBP1430) exhibit different levels of disease symptoms and expression of genes related to pathogenesis of fire blight pathogens (Wang et al., 2010). For example, Ea273 and Ea110 caused more severe blight symptoms on apple cv. Golden Delicious, which is a relatively tolerant genotype, and expressed higher levels of amylovoran biosynthesis and T3SS genes, as compared to Ea1189 and CFBP1430, suggesting variation in pathoadaptation on different host plants (Khan et al., 2012).

### 1.2 Type III secretion system (T3SS) in *Erwinia amylovora*

#### 1.2.1 Type III secretion system as a virulence factor

The T3SS of most Gram-negative, phytopathogenic bacteria generally consists of four components: cytoplasmic ATPase, secretion apparatus spanning the two bacterial membranes (inner membrane and outer membrane), extracellular pilus for the penetration of plant cell wall and translocon for the transport of effector proteins (Büttner and He, 2009). As the T3SS functions in delivering bacterial effector proteins into the eukaryotic cells, many plant pathogenic bacteria, such as *Pseudomonas syringae*, *Xanthomonas* spp, and *Erwinia* spp. employ this mechanism for their pathogenicity and interaction with host plants (Büttner and Bonas, 2006).

*E. amylovora* contains three pathogenicity islands (PAIs; PAI-1, PAI-2 and PAI-3), but only PAI-1, i.e. *hrp* (hypersensitive response and pathogenicity) pathogenicity island 1, has been shown to be essential for virulence in host plants (Oh et al., 2005; Bocsanczy et al., 2008; Zhao

et al., 2009a; Smits et al., 2010). The T3SS of *E. amylovora*, including both structural and effector proteins, are encoded by the *hrp* PAI-1 (Oh et al., 2005). They are so named since strains with mutation in some of these genes failed to elicit the hypersensitive response (HR), a rapid, local death of plant cell at the site of infection, in resistant plants (Lindgren et al., 1986). In *E. amylovora*, the *hrp* PAI-1 is composed of four distinct clusters of genes (Figure 1.1): the hypersensitive response and conserved (*hrp*/*hrc*) region, the Hrp effectors and elicitors (HEE) region, the Hrp-associated enzymes (HAE) region and the island transfer (IT) region (Oh and Beer, 2005).

Among them, the genes important for T3SS function and regulation are mainly located in the *hrp*/*hrc* region and the HEE region. The *hrp*/*hrc* region contains 25 genes, including four genes (*hrpL*, *hrpS*, and *hrpXY*) responsible for regulation of T3SS gene expression and nine *hrc* genes largely involved in the T3SS assembly (Bogdanove et al., 1996; Oh et al., 2005). The HEE region is found to harbor seven genes, including two major effectors for virulence (*hrpN* and *dspA*/*E*) (Oh et al., 2005). Since the *hrp*/*hrc* region and the HEE region include most *hrp* and *dsp* genes, the two regions together are called the *hrp*/*dsp* gene cluster. Unlike the *hrp* PAI-1, two other PAIs in *E. amylovora*, PAI-2 and PAI-3, were not involved in virulence in immature pear fruits and apple seedlings, although they encode complete sets of T3SS apparatus proteins (Bocsanczy et al., 2008; Zhao et al., 2009a). Both PAI-2 and PAI-3 belong to *inv*/*spa*-type T3SS found in the insect endosymbiont *Sodalis glossidinius* (Triplett et al., 2006). Some genes associated with mobile genetic elements are also located on the upstream region of PAI-2 and PAI-3, suggesting that horizontal gene transfer occurred in the evolution of *E. amylovora* (Zhao et al., 2009a).

In addition to T3SS, it is well known that exopolysaccharide amylovoran, an acidic heteropolymer composed of pentasaccharide repeating units, is a major virulence factor of *E. amylovora* and produced by an *ams* (amylovoran synthesis) operon (Oh and Beer, 2005; Khan et al., 2012). Both *ams* and *hrp* PAI deletion mutants have been shown to fail to cause fire blight disease on immature pear fruits (Zhao et al., 2009a). However, previous studies reported that T3SS mutants could not induce an HR in tobacco and a local necrotic reaction in apple leaf mesophyll, while an *ams* mutant could still elicit both reactions (Metzger et al., 1994; Malnoy et al., 2012). Furthermore, it has been shown that T3SS is responsible for inducing oxidative stress responses, such as accumulation of superoxide anion and lipid peroxidation, at the beginning of the infection process in pears (Venisse et al., 2001).

### 1.2.2 Type III-secreted proteins of *Erwinia amylovora*

The T3SS of *E. amylovora* secretes several proteins, which mediate host-pathogen interactions and contribute to disease development in host plants. Since HrpN was identified as the first cell-free elicitor of HR (Wei et al., 1992a), at least 15 proteins have since been known to be secreted by the T3SS in *E. amylovora*, including not only effectors but also helper proteins which play a role in effector translocation (Bogdanove et al., 1998; Zhao et al., 2006; Nissinen et al., 2007).

One of the well-known type III-secreted proteins in *E. amylovora* is the harpin family proteins. Harpins are a unique subset of the type III proteins found only in plant pathogenic bacteria. Although most harpin proteins exhibit a low degree of sequence homology and may function differently in different bacteria, they are all acidic, glycine-rich, heat-stable, lack

cysteine and have few aromatic amino acids (Alfano and Collmer, 1997). Harpins are secreted in the apoplast, not in the cytoplasm, during infection process to presumably act on plant cell wall and/or plasma membrane (Perino et al., 1999; Tampakaki and Panopoulos, 2000). In *E. amylovora*, two harpins, HrpN and HrpW, have been identified, but virulence functions are detected only in the HrpN protein (Wei et al., 1992a). HrpN has been reported to trigger oxidative stress (Venisse et al., 2003) and contribute either directly or indirectly to callose deposition and translocation of other effector proteins (Bocsanczy et al., 2008). However, the exact function of HrpN remains to be explored. Nevertheless, HrpN on non-host plants has been relatively well characterized and shown to induce various cellular responses which are related to plant defense reactions, including oxidative burst (Baker et al., 1993; Cessna and Low, 2001), myelin basic protein kinase activation (Adam et al., 1997), increase of internal Ca2+ concentration (Cessna et al., 2001), defense gene activation (Dong et al., 1999; Peng et al., 2003), modulation of ion channel activity in the cell (Popham et al., 1995) and mitochondrial dysfunction (Xie and Chen, 2000).

The DspA/E effector is another major type III-secreted protein in *E. amylovora* required for pathogenicity. The *dspA/E* gene exhibits homology with *avrE* gene of *P. syringae* pv. *tomato*, which confers cultivar specificity on host plants (Gaudriault et al., 1997; Bogdanove et al., 1998). During infection on host plants, DspA/E of *E. amylovora* is found to interact with intracellular domains of host plant receptor kinases (Meng et al., 2006) and precursor of the host chloroplast protein ferredoxin (Bonasera et al., 2004), resulting in oxidative stress (Venisse et al., 2003) and suppression of salicylic acid (SA)-dependent innate immunity and promotion of cell death (DebRoy et al., 2004). The *dspA/E* mutant is also shown to have a significantly reduced capacity

to trigger electrolyte leakage in apple and tobacco leaves, indicating that DspA/E plays a major role in causing cell death after translocation into plant cells (Boureau et al., 2006). Secretion of DspA/E is partially dependent on DspB/F which acts as a DspA/E specific chaperone and inhibits intrabacterial DspA/E degradation (Gaudriault et al., 2002). In addition, DspA/E is also reported to be more efficiently delivered into plant cells with the help of HrpN (Bocsanczy et al., 2008).

The T3SS of *E. amylovora* requires several type III-secreted helper proteins to be fully functional and/or virulent. Analysis of the secretomes of *E. amylovora* (Nissinen et al., 2007) revealed that HrpJ is important in efficient translocation or extracellular accumulation of two harpin proteins (HrpN and HrpW), and HrpK may contribute to formation of the secretion apparatus. Function of HrpJ was further identified as an essential virulence factor of *E. amylovora* for virulence and elicitation of the HR through *hrpJ* mutation analysis (Nissinen et al., 2007). *E. amylovora* also has several other type III-secreted proteins involved in pilus formation, such as HrpA (Kim et al., 1997), FlgL (Nissinen et al., 2007), and TraF (Haase and Lanka, 1997), and virulence, such as $AvrRpt2_{Ea}$ (Zhao et al., 2006) and effector-like proteins (Eop1 and Eop3) (Nissinen et al., 2007); however, despite several studies, current understanding of their properties and function in T3SS and virulence is still limited.

### 1.2.3 Regulation of type III secretion system

In many plant pathogens including *E. amylovora*, the extracytoplasmic function (ECF) sigma factor, HrpL, is a master regulator that controls the expression of genes encoding the T3SS components (Figure 1.2) (Shen and Keen, 1993; Wei and Beer, 1995; Chatterjee et al., 2002). It

has been shown that ECF is one of the most abundant signal transduction pathways to mediate specific gene expression in response to environmental stimuli (Mascher, 2013). Significant down-regulation of T3SS gene expression associated with a loss of ability to cause disease and HR was observed in *hrpL* mutant of *E. amylovora* (Ancona et al., 2014). As an alternative sigma factor belonging to the sigma 70 ($\sigma^{70}$) family, HrpL binds to a consensus nucleotide sequence (GGAACC-$N_{16}$-CCACNNA), called the *hrp* box or *hrp* promoter, at the -35 and -10 promoter regions to direct transcription by RNA polymerase at a target site (Wei and Beer, 1995). To date, 30 putative *hrp* promoters including all known genes encoding T3SS components have been identified in *E. amylovora* (McNally et al., 2012).

Regulation of T3SS gene expression in many phytopathogenic bacteria including *E. amylovora* is subject to transcriptional control of *hrpL* expression (Figure 1.2) (Xiao et al., 1994; Wei and Beer, 1995). In *E. amylovora*, *hrpL* transcription is positively regulated by alternative sigma factor 54 ($\sigma^{54}$) (RpoN), HrpS and YhbH (Figure 1.2) (Wei et al., 2000; Ancona et al., 2014). HrpS, a member of the NtrC family, acts as a bacterial enhancer binding protein (bEBP) which is a $\sigma^{54}$-dependent transcription activator, whereas YhbH of *E. amylovora* is annotated as a $\sigma^{54}$ modulation protein (Smits et al., 2010). Deletion of *rpoN*, *hrpS* and *yhbH* in *E. amylovora* resulted in a dramatic decrease in *hrpL* and other T3SS gene expression, thus a non-pathogenic mutant strain on immature pear fruits and apple shoots (Ancona et al., 2014). Consistently, the ability to elicit HR on nonhost tobacco leaves was also abolished in these mutants, but restored after *hrpL* expression using arabinose inducible-*hrpL* complementation (Ancona et al., 2014). These results indicate that RpoN, YhbH and HrpS are essential activators of *hrpL* transcription and other T3SS gene expression.

The signal cascade leading to *hrpL* transcription may begin with environmental stimuli, such as low pH, low temperature, and low concentrations of ammonium ions and certain carbon sources (Wei et al., 1992b). It has been shown that *hrp* gene expression of *E. amylovora* is repressed in nutrient-rich media, but induced in minimal media and *in planta*, indicating that nutritional condition is important for transcription of *hrp* genes (Wei et al., 1992b). In *E. amylovora*, HrpXY two-component signal transduction system has been proposed to perceive *hrp*-inducing stimuli and either directly or indirectly induce *hrpS* transcription for the subsequent *hrpL* gene induction (Figure 1.2), but this remains to be determined (Wei et al., 2000; Zhao et al., 2009b).

## 1.3 Sigma 54-dependent transcription

### 1.3.1 Sigma factors

Regulation of transcription initiation process is a major point in controlling gene expression in both prokaryotes and eukaryotes. Transcription in bacteria generally requires two components for initiation: core RNA polymerase (RNAP), composed of five subunits ($\alpha_2\beta\beta'\omega$), and sigma factor, a sixth dissociable subunit of RNAP. Association of the two components forms a holoenzyme that is capable of initiating transcription. Bacteria have only one form of the core RNAP, and the specificity for promoter recognition of the holoenzyme is primarily determined by a sigma factor. Therefore, expression of individual genes and gene groups can be effectively regulated by different holoenzyme species (Haugen et al., 2008). There are multiple forms of sigma factors in most bacteria. The number of sigma factors is highly diverse between different bacterial species depending on the complexity and/or lifestyle of the organism, ranging from 1 in *Mycoplasma genitalium* to 63 in *Streptomyces coelicolor* (Fraser et al., 1995; Bentley et al., 2002;

Gruber and Gross, 2003). In order to promote a proper transcriptional response to various environmental stimuli, it has been shown that bacteria can manipulate the holoenzyme composition through several different mechanisms, including regulation of sigma factor expression, anti-sigma factors and small regulatory proteins (Ö sterberg et al., 2011). Sigma factors, thus, play a central role in controlling gene expression in bacteria.

Bacterial sigma factors can be grouped into two families based on their domain structure and promoter specificity: the $\sigma^{70}$ family and the $\sigma^{54}$ family. Most sigma factors, including 'housekeeping' sigma factor, $\sigma^{70}$, belong to the $\sigma^{70}$ family; while only a single member, $\sigma^{54}$, is classified into the $\sigma^{54}$ family. The $\sigma^{70}$ family members bind to and direct a holoenzyme to their own specific, consensus binding sequences at positions -35 and -10 of the promoter, followed by the formation of holoenzyme-promoter complex with a default closed form called a closed complex (Figure 1.3A) (Guo et al., 2000; Bush and Dixon, 2012). The closed complex must be converted into the open complex in order for the holoenzyme to access single-stranded DNA as a template. In $\sigma^{70}$ family-dependent transcription, the transition from closed complex to open complex (isomerization) occurs spontaneously because the closed complex in this system is energetically unfavorable (Guo et al., 2000; Bush and Dixon, 2012). Therefore, the holoenzyme with the $\sigma^{70}$ family does not need any energy input for isomerization and transcription initiation. However, the closed complex in $\sigma^{54}$-dependent transcription is an energetically stable structure, which requires bEBP and integration host factor (IHF), to activate transcription (Figure 1.3B) (Buck et al., 2000; Guo et al., 2000; Cannon et al., 2001; Bush and Dixon, 2012).

### 1.3.2 Sigma 54

RpoN ($\sigma^{54}$) was first reported in glutamine synthetase (*glnA*) gene transcription in *Escherichia coli* and *Salmonella typhimurium* (Hirschman et al., 1985; Hunt and Magasanik, 1985). It is now known to play a major role in regulation of gene expression involved in a wide range of cellular processes in many bacterial species, including nitrogen assimilation (Reitzer and Schneider, 2001), survival under stress environment in *E. coli* (Model et al., 1997), cell-to-cell communication in *P. aeruginosa* (Thompson et al., 2003) and flagella biosynthesis and virulence in *Vibrio anguillarum* (O'Toole et al., 1997). Although 70 RpoN-dependent promoters were identified in *E. coli* strain MG1655 through microarray and computational analysis (Zhao et al., 2010), the RpoN regulon has not been clearly defined in most bacteria presumably due to difficulty in estimating inducible conditions of each gene in the regulon. In phytopathgenic bacteria, the function of RpoN has been emphasized in the regulation of T3SS gene expression. It has been shown that the transcription of *hrpL* gene is dependent on RpoN in *P. syringae*, *Pantoea stewartii*, and *Pectobacterium carotovorum*. Their pathogenicity on host plants and HR-inducing ability on nonhost plants are significantly reduced or abolished in the *rpoN* mutant (Frederick et al., 1993; Hendrickson et al., 2000a; Hendrickson et al., 2000b; Chatterjee and Cui, 2002). Recently, the function of RpoN in activation of *hrpL* gene expression is also confirmed in *E. amylovora* (Ancona et al., 2014). In addition to T3SS gene expression, RpoN has been shown to play a role in regulation of other activities in phytobacteria, such as production of the phytotoxin coronatine in *P. syringae* and resistance to osmotic stress in *P. fluorescens* (Alarcón-Chaidez et al., 2003; Péchy-Tarr et al., 2005).

Unlike $\sigma^{70}$, $\sigma^{54}$ binds to consensus -24 (GG) and -12 (TGC) regions of the promoter sequence (Figure 1.3B). In terms of function, $\sigma^{54}$ protein can be divided into three regions (region I, region II and region III) (Figure 1.4). The N-terminal region I acts as a regulatory domain, interacting with both bEBP and RNAP and also binding to the -12 promoter element (Bordes et al., 2003). Region II is dispensable for $\sigma^{54}$-dependent transcription (Buck et al., 2000). Region III contains several functionally important domains, including determinants of promoter DNA binding, such as RpoN box (Taylor et al., 1996), DNA cross-linking region (Cannon et al., 1994) and RNAP binding (Hsieh et al., 1999). Among the three regions of $\sigma^{54}$, the region I has been proposed to be the main reason of the need for bEBP in $\sigma^{54}$-dependent transcription. Cryo-electron microscopy analysis suggests that region I of the $\sigma^{54}$ blocks the loading of DNA by RNAP within the catalytic cleft, thus preventing the transcription initiation (Bose et al., 2008; Bush and Dixon, 2012).

### 1.3.3 Bacterial enhancer binding protein (bEBP)

In $\sigma^{54}$-dependent transcription, the presence of bEBPs is essential to initiate RNA synthesis (Figure 1.3B). Bush and Dixon (2012) have summarized structural and biochemical analysis of $\sigma^{54}$-dependent transcriptional activation (Guo and Gralla, 1998; Chaney et al., 2001; Bose et al., 2008; Ghosh et al., 2010) and have proposed essential properties of $\sigma^{54}$-dependent transcription activator: The activators must be able to induce both $\sigma^{54}$ remodeling and DNA melting as the region I of $\sigma^{54}$ forms energetically favorable closed complex at the -12 promoter element. The activators also must be able to reposition DNA binding domains of $\sigma^{54}$ within the transcription start site in order for the core RNAP to promote transcription elongation correctly. As a member of $AAA^{+}$ (ATPase associated with various cellular activities) family of proteins

which are capable of converting chemical energy into a mechanical action, bEBPs have been shown to fulfill all the requirements to activate $\sigma^{54}$-dependent transcription as well as regulatory functions.

Most bEBPs are modular proteins composed of three domains, N-terminal regulatory (R) domain, central (C) domain and C-terminal DNA binding (D) domain (Figure 1.5), and generally exist as dimer and hexamer in their inactive and active states, respectively (Klose et al., 1994; Wyman et al., 1997; Schumacher et al., 2006). Since the C domain consists of $AAA^+$ domain responsible for ATP hydrolysis, oligomerization and $\sigma^{54}$ contact, it contains several structurally and functionally conserved motifs, including Walker A, Walker B, sensor I, sensor II, and GAFTGA motifs. The Walker A, Walker B and sensor II motifs have been shown to serve as sites for ATP binding and hydrolysis (Walker et al., 1982; Bush and Dixon, 2012), and sensor I motif has been reported to play a role in conformational changes in the $AAA^+$ domain during nucleotide hydrolysis (Schumacher et al., 2006). The GAFTGA motif is a specific structural characteristic of bEBP that has been specifically implicated in the isomerization of the closed complex via $\sigma^{54}$ contact (Rappas et al., 2005; Bush and Dixon, 2012). Through cryo-electron microscopy and three-dimensional reconstruction studies (Rappas et al., 2005), surface-exposed loop of the GAFTGA motif has been confirmed to interact with $\sigma^{54}$, which subsequently lead to conformational changes in $AAA^+$ domain upon ATP hydrolysis therefore remodeling of the holoenzyme (Bordes et al., 2003; Cannon et al., 2003). Amino acid substitution analysis within the GAFTGA motifs of several different bEBPs revealed that a mutation of any one of six residues results in failure to activate transcription and/or reduced ATPase activity, indicating the requirement for the integrity of GAFTGA motif (González et al., 1998; Li et al., 1999; Zhang et

al., 2009; Bush et al., 2010). The $AAA^+$ C domain also contains R fingers with one or two arginine residues, which contribute to nucleotide sensing and oligomerization of bEBP (Lupas and Martin, 2002).

The R and D domains of bEBPs also have important roles in the activation of $\sigma^{54}$-dependent transcription, although some bEBPs lack either and/or both of these domains, including FlgR in *Helicobacter pylori*, CtcC in *Chlamydia trachomatis* and FleT in *Rhodobacter sphaeroides* (Beck et al., 2007). The N-terminal R domain can regulate the activity of $AAA^+$ domain in response to environmental signals through phosphorylation, ligand binding and protein-protein interactions (Schumacher et al., 2006; Bush and Dixon, 2012). Among them, protein-protein interaction can be used for the regulation of bEBPs lacking R domain (Bush and Dixon, 2012). As an example, HrpS in *P. syringae* pv. *tomato* DC3000 does not contain R domain, but can be negatively regulated by HrpS-specific binding protein, HrpV (Jovanovic et al., 2011). On the other hand, the C-terminal D domain contains a helix-turn-helix (HTH) motif and is responsible for recognition of specific DNA sequences called upstream activator sequences (UASs) (Studholme and Dixon, 2003). Since the dimer form of bEBPs bind to DNA before formation of higher oligomers, all UASs identified are reported to have dyad symmetric sequences (Bush and Dixon, 2012). The binding site of bEBPs is generally located 80 to 150 bp upstream of the transcription start site. Therefore, in some cases, IHF binding and bending of the DNA at a position between promoter and UAS are required to allow interaction of bEBP with the $\sigma^{54}$-RNAP holoenzyme (Figure 1.3B and Fig 1.6) (Claverie-Martin and Magasanik, 1992). In addition to DNA binding, it has been shown that the D domain is also involved in facilitating oligomerization (Austin and Dixon, 1992; Pérez-Martín and de Lorenzo, 1996) and stabilizing

the oligomer (De Carlo et al., 2006). However, the binding sites for HrpS in *E. amylovora* and HrpS/HrpR in *P. syringae* are still unknown.

### 1.3.4 Integration host factor (IHF)

IHF is one of the most abundant nucleoid-associated proteins (NAPs) in Gram-negative bacteria. NAPs are generally referred to small DNA-binding proteins of bacteria that affect genome topology by looping, bending, wrapping or bridging of the DNA (Figure 1.7). These unique properties allow them to control nucleoid structure and gene expression (Dillon and Dorman, 2010). To date, *E. coli* and *Salmonella enterica* have been reported to have twelve species of NAPs varying in size, DNA-binding motif and function (Azam and Ishihama, 1999; Mangan et al., 2011), but their regulation and role in cellular processes are sometimes controversial due to ambiguous results from different bacterial species (Navarre et al., 2006; Oshima et al., 2006; Dillon and Dorman, 2010; Prieto et al., 2012).

Since the first identification of IHF as a factor for the site-specific recombination of bacteriophage-λ in *E. coli* (Miller et al., 1979; Miller and Friedman, 1980), its structural and functional properties have been extensively studied. IHF is about 11 kDa in size and predominantly exists in a heterodimeric form composed of an α subunit (IHFα) and a β subunit (IHFβ) (Swinger and Rice, 2004). Binding of IHF to DNA occurs in a sequence-specific manner ((A/T)ATCAANNNNTT(A/G)), which is highly conserved in Gram-negative bacteria (Yang and Nash, 1995; Murtin et al., 1998), although it was reported that the binding specificity can be also determined by DNA structural features (Travers, 1997). The primary function of IHF is to cause DNA looping and bending up to 160˚ upon binding (Rice et al., 1996; Lorenz et al., 1999; Teter

et al., 2000). With this ability to influence on nucleoid structure, IHF facilitates interaction of transcription factors, RNAP, and other NAPs during transcription of a large number of genes including $\sigma^{54}$-dependent genes (Santero et al., 1992; Macchi et al., 2003; Dillon and Dorman, 2010). Positive and negative regulatory effects of IHFs on transcription can be dependent on its position within the promoter relative to the binding sites of other factors involved in transcription initiation (Browning et al., 2010). In *E. coli*, it was found that IHF binding on DNA can induce open complex formation at the chromosomal origin, *oriC* (Bramhill and Kornberg, 1988; Hwang and Kornberg, 1992), but also can inhibit DNA replication process by promoting formation of initiation titration complex at *datA* locus (Nozaki et al., 2009), indicating that IHF plays an important role in controlling the replication timing. Consistent with this function, it was shown that the intracellular abundance of IHFs changes under different growing phases and reaches peak levels when cells enter stationary phase (Ditto et al., 1994). Therefore, like other NAPs, IHFs contribute to not only maintenance of nucleoid structure, but also control of several DNA-dependent processes.

### 1.4 Research objectives

The *hrp*-T3SS is a major virulence factor required at an early infection of many plant-pathogenic bacteria, including *E. amylovora*. The ECF alternative sigma factor, HrpL, acts as a master regulator of *hrp*-T3SS of *E. amylovora* by regulating the expression of *hrp*-T3SS gene (Wei and Beer, 1995; Oh et al., 2005; McNally et al., 2012). Based on a current model of *hrp*-T3SS regulation (Figure 1.2) (Ancona et al., 2014), *hrpL* transcription is positively regulated by RpoN ($\sigma^{54}$), HrpS (bEBP) and YhbH ($\sigma^{54}$-modulation protein). However, in *hrpL* transcription of

*E. amylovora*, the requirement of IHFs or the binding site of HrpS has not yet been experimentally determined.

Most bEBPs contain the GAFTGA motif which plays a central role in the isomerization during the $\sigma^{54}$-dependent *hrpL* transcription (Bush and Dixon, 2012); whereas about 7% of the annotated bEBPs, including HrpS, contain the GAYTGA motif (Zhang et al., 2009). A recent report showed that substitution of tyrosine (Y) with phenylalanine (F) in the GAYTGA motif of HrpS in *P. syringae* pv. *tomato* DC3000 showed an increase in *hrpL* promoter activity by about 1.5-fold (Jovanovic et al., 2011). This led us to ask whether a tyrosine to phenylalanine substitution in the GAYTGA motif of HrpS in *E. amylovora* also affect *hrpL* expression. Therefore, the specific aims of my thesis research are:

1) To determine the role of IHFs in *hrpL* transcription and virulence in *E. amylovora*;

2) To identify the HrpS binding site on the upstream sequence of the *hrpL* promoter in *E. amylovora*; and

3) To examine the role of tyrosine residue of GAYTGA motif in HrpS of *E. amylovora*

## 1.5 Figures

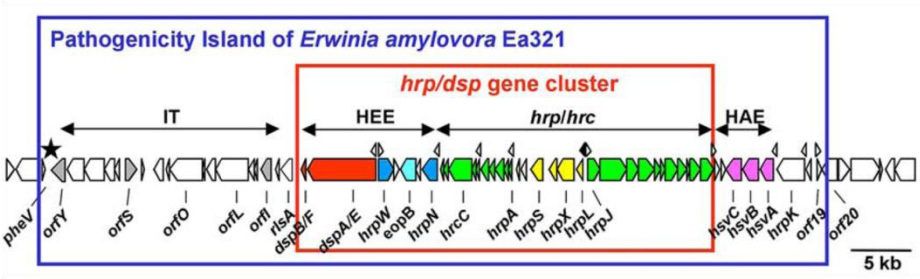


**Figure 1.1 Schematic map of the *hrp* pathogenicity island in *Erwinia amylovora* strain Ea321.** IT, Island transfer region; HEE, Hrp effectors and elicitors region; *hrp/hrc*, hypersensitive reaction and conserved region; HAE, Hrp-associated enzyme region. (From Oh and Beer, 2005)

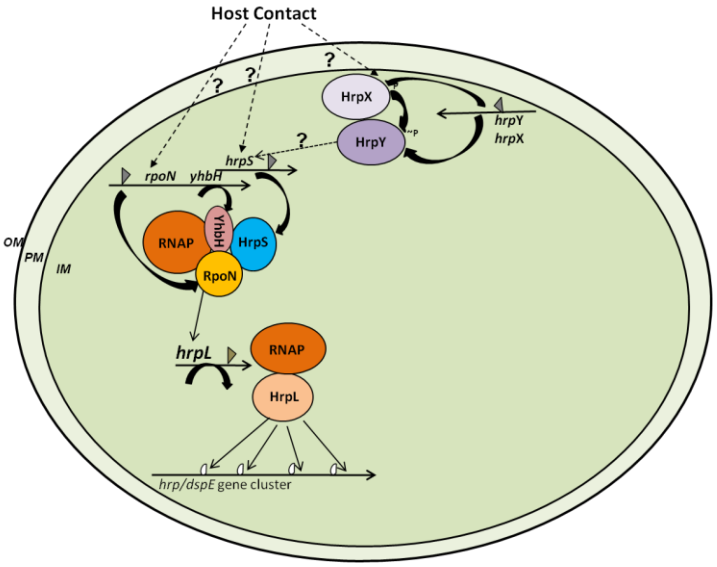


**Figure 1.2 A working model of type III secretion system (T3SS) regulation in *Erwinia amylovora*.** HrpL, an extracytoplasmic functions (ECF) sigma factor; HrpS, a bacterial enhancer binding protein; HrpX/HrpY, two component regulatory systems; RpoN, a sigma 54 ($\sigma^{54}$) alternative sigma factor; RNAP, RNA polymerase; YhbH, a $\sigma^{54}$ modulation protein. OM, outer membrane; PM, plasma membrane; IM, inner membrane; P, phosphorylation; open triangle, $\sigma^{54}$ promoter; filled triangle, $\sigma^{70}$ promoter; circle open triangle, *hrp*-promoter. Positive regulation is indicated by an arrow; '?' and broken line, unknown mechanism. (From Ancona et al., 2014)

**A.**

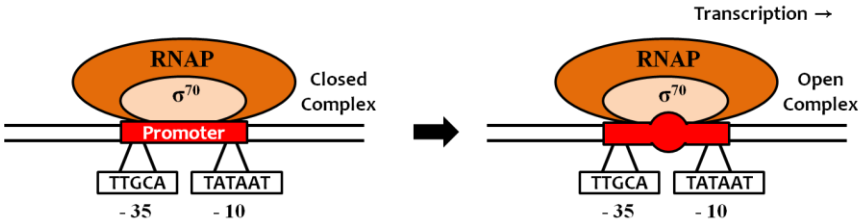


**B.**

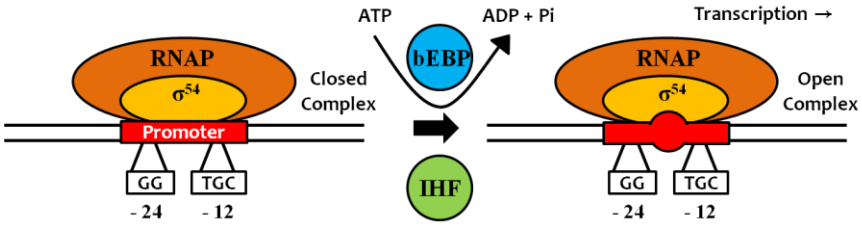


**Figure 1.3 Transcription initiation by the $\sigma^{70}$-RNAP and the $\sigma^{54}$-RNAP holoenzyme.** (A) The $\sigma^{70}$ family members direct RNA polymerase (RNAP) to their consensus DNA binding sequences at positions -35 and -10 region of the promoter. Since the closed complex formed by the $\sigma^{70}$-RNAP holoenzyme and promoter DNA is energetically unfavorable, the open complex is formed without any energy input. (B) The $\sigma^{54}$ directs RNAP to their consensus DNA binding sequences at positions -24 and -12 region of the promoter. Since the closed complex formed in the $\sigma^{54}$-dependent transcription is energetically favorable, bacterial enhancer binding protein (bEBP) is essentially required to provide energy and form the open complex. In some cases, integration host factors (IHFs) are required for interaction between the holoenzyme and bEBP.

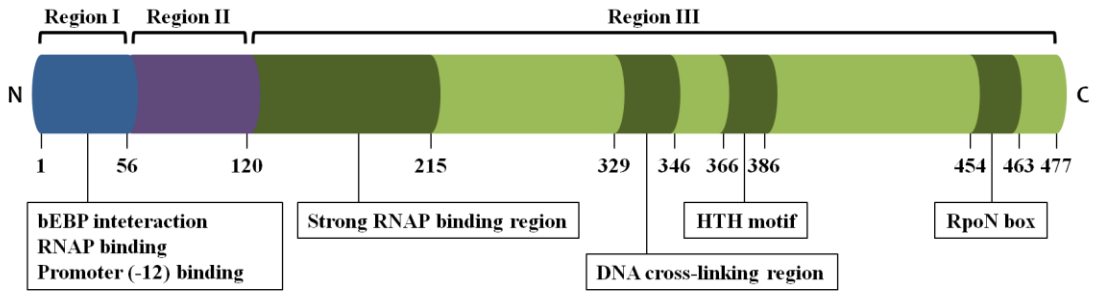


**Figure 1.4 Domain organization of $\sigma^{54}$ in *Escherichia coli*.** The $\sigma^{54}$ of *E. coli* is composed of 477 residues and divided into three regions (region I, II and III). Region I is important for bEBP interaction, RNA polymerase (RNAP) binding and DNA binding at position -12 region of the promoter. Region III contains several motifs responsible for RNAP binding (residues 120 to 215) and promoter DNA binding (residues 329 to 346, 366 to 386 and 454 to 463). No specific function for $\sigma^{54}$-dependent transcription has been described in Region II.

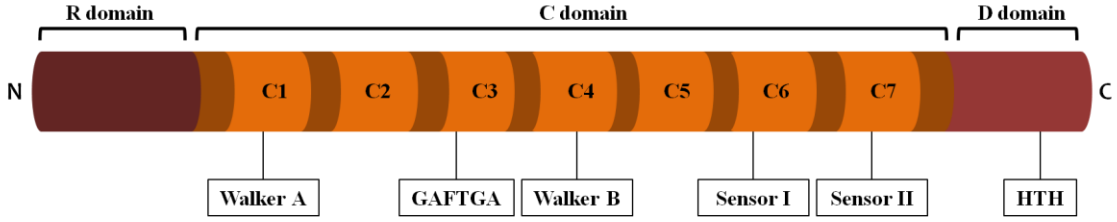


**Figure 1.5 Domain organization of bacterial enhancer binding protein.** Bacterial enhancer binding proteins (bEBPs) generally consist of three domains (R, C and D domain). The N-terminal regulatory (R) domain regulates bEBP function in response to external and internal stimuli. The central (C) domain, also known as $AAA^{+}$ domain, contains highly conserved motifs, including Walker A, GAFTGA, Walker B, Sensor I and Sensor II, which are essential for activation of $\sigma^{54}$-dependent transcription. bEBPs recognize and bind to specific DNA sequence, called upstream activator sequence (UAS) via an helix-turn-helix (HTH) motif in the C-terminal DNA binding (D) domain.

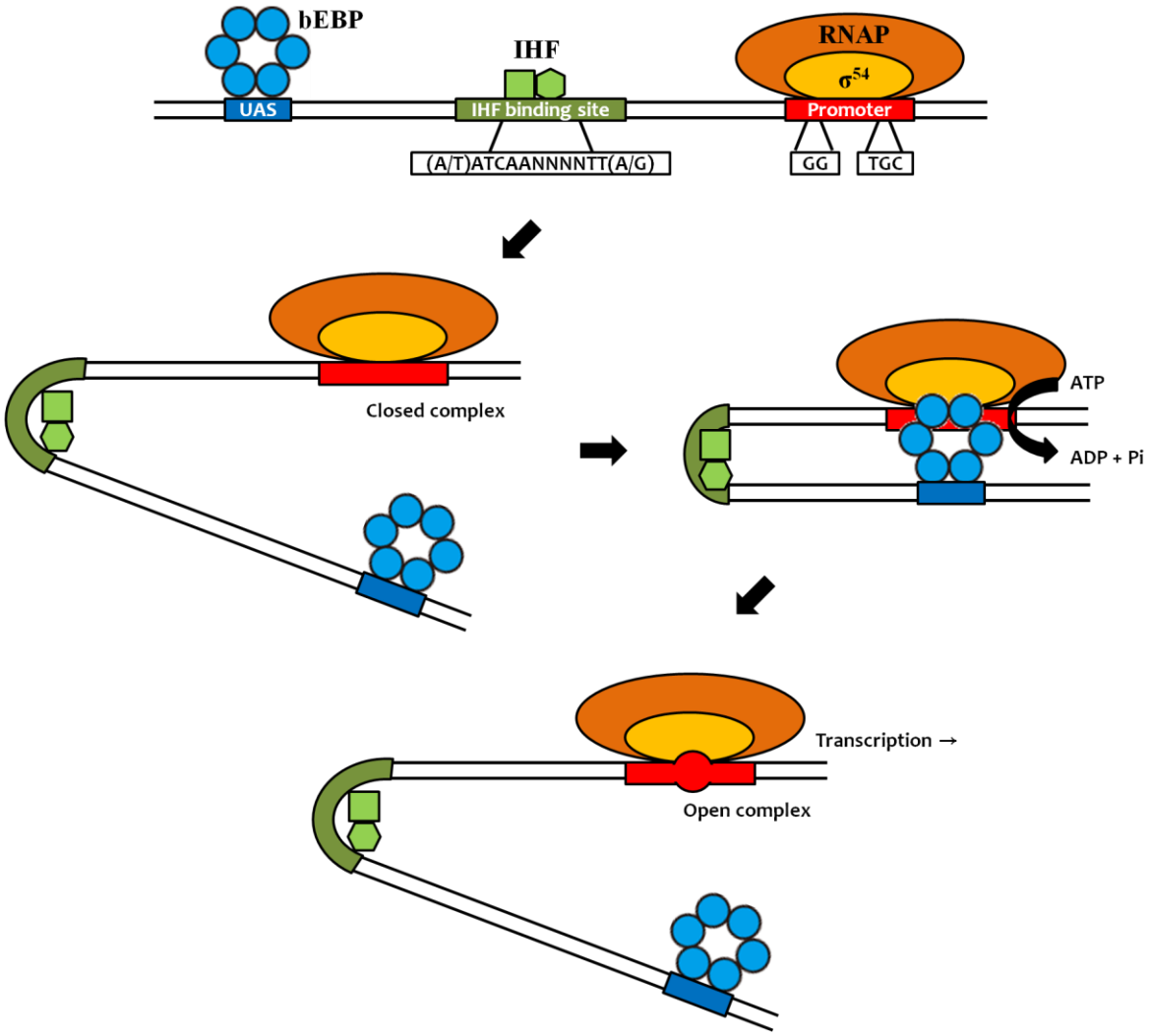


**Figure 1.6 Transcription activation in $\sigma^{54}$-dependent transcription.** The $\sigma^{54}$ directs RNA polymerase (RNAP) to the -24 (GG) and -12 (TGC) promoter region and forms $\sigma^{54}$-RNAP holoenzyme. Bacterial enhancer binding proteins (bEBPs) bind to an upstream activator sequences (UASs) generally located about -80 to -150 position of the promoter DNA. In $\sigma^{54}$-dependent transcription, bEBPs must interact with the closed complex to fulfill the function of coupling ATP hydrolysis to transition to the open complex. DNA bending via integration host factors (IHFs) are often required for correct interfacing between bEBP and $\sigma^{54}$-RNAP holoenzyme. IHFs typically bind as a heterodimer to a consensus sequence [(A/T)ATCAANNNNTT(A/G)] between UAS and $\sigma^{54}$ binding site.

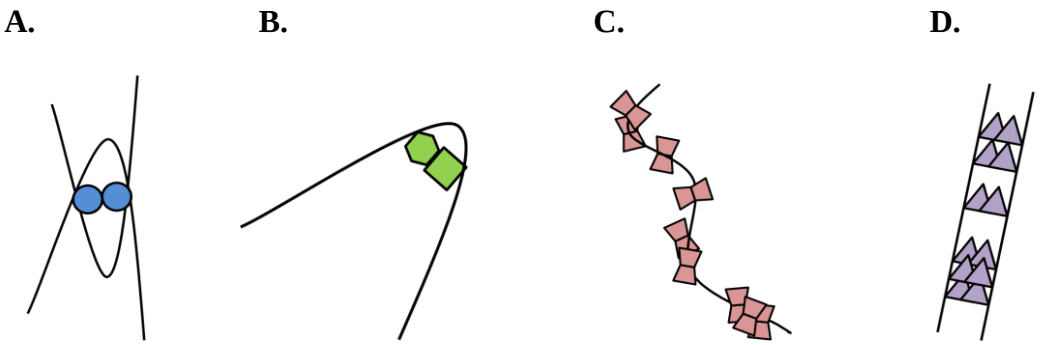


**Figure 1.7 Nucleoid-associated proteins in bacterial genome architecture.** (A) DNA looping. (B) DNA bending. (C) DNA wrapping. (D) DNA bridging. Most nucleoid-associated proteins (NAPs) in Gram-negative bacteria are active as a dimer. DNA binding and structuring properties of NAPs contribute to not only maintaining nucleoid structure, but also a variety of DNA-dependent processes, including gene expression, DNA replication and recombination.

# CHAPTER 2

# INTEGRATION HOST FACTORS ARE REQUIRED FOR SIGMA 54-DEPENDENT *hrpL* GENE EXPRESSION AND VIRULENCE IN *Erwinia amylovora*

## 2.1 Abstract

*Erwinia amylovora*, the causal agent of fire blight of apples and pears, is a necrogenic bacterium, whose virulence is dependent upon a functional hypersensitive response and pathogenicity (*hrp*)-type III secretion system (T3SS). It has been previously demonstrated that HrpL, an ECF sigma factor, is the master regulator of *hrp*-T3SS. Recently, it is reported that expression of *hrpL* is under the control of sigma 54 complex, including $\sigma^{54}$ (RpoN), its modulation protein YhbH and $\sigma^{54}$-enhancer binding protein HrpS. In this study, we investigated the role of integration host factors (IHFs) in regulating $\sigma^{54}$-dependent *hrpL* and other T3SS gene expression. IHFs are nucleoid-associated proteins and consist of two subunits, i. e. IHFα and IHFβ. IHFα and IHFβ usually form heterodimers, which could influence nucleoid structure and gene expression via DNA bending. Two single mutants (*ihfA* and *ihfB*) were generated and characterized in *E. amylovora*. Results showed that both *ihfA* and *ihfB* mutants failed to colonize and produce necrotic lesions on immature pear fruits. Bacterial growth of both mutants in pear fruits was greatly reduced and expression of *hrpL*, *dspE*, *hrpA* and *hrpN* was also significantly down-regulated as compared to wild type (WT) strain. In addition, both *ihfA* and *ihfB* mutants exhibited slower growth in rich medium and showed hypermotile phenotype as compared to WT strain. Furthermore, results showed that both IHFs positively regulated the expression of small non-coding regulatory RNA *rsmB*/*csrB*, which negatively regulates motility as previously reported. These results indicate that IHFs are required for $\sigma^{54}$-dependent *hrpL* and other T3SS gene expression and virulence in *E. amylovora*

## 2.2 Introduction

Fire blight, caused by the Gram-negative enterobacterium *Erwinia amylovora*, is a major threat worldwide to plants in the *Rosaceae* family, including apple and pear. *E. amylovora* infection typically results in disease symptoms characteristic of water soaking and rapid tissue necrosis. Invasion of *E. amylovora* can occur through natural openings and wounds in plants, causing various phases of the disease, including rootstock blight, shoot blight, and blossom blight (Vanneste, 2000; Norelli et al., 2003). Like many other plant pathogenic bacteria, *E. amylovora* employs a hypersensitive response and pathogenicity (*hrp*)-type III secretion system (T3SS) to translocate effector proteins directly into host cells and modulate host cell functions during infection.

Since HrpN was identified as the first cell-free elicitor of hypersensitive response (HR) (Wei et al., 1992a), at least 15 virulence-associated proteins, including HrpA, DspE, HrpW, AvrRpt2, HopC1 and Eop1, have been identified to be secreted by the T3SS in *E. amylovora* (Bogdanove et al., 1998; Zhao et al., 2006; Nissinen et al., 2007). Many genes encoding these effector proteins as well as other components of T3SS in *E. amylovora* are clustered in *hrp* pathogenicity island (PAI), which can be divided into four regions: the *hrp*/*hrc* region, the Hrp effectors and elicitors (HEE) region, the Hrp-associated enzyme (HAE) region and the island transfer (IT) region (Oh and Beer, 2005). Among them, the *hrp*/*hrc* region and the HEE region, together called the *hrp*/*dsp* gene cluster, contain most T3SS structural and regulatory genes. Expression of all known components of the *hrp*-T3SS in *E. amylovora* is regulated by the master regulator HrpL, belonging to the exocytoplasmic functions (ECF) sigma factors (Wei and Beer, 1995; McNally et al., 2012). As an alternative sigma factor within the sigma 70 ($\sigma^{70}$) family,

HrpL binds to the *hrp* box (GGAACC-$N_{16}$-CCACNNA) at the -35 and -10 promoter regions (Wei and Beer, 1995).

Recently, it has been shown that *hrpL* transcription is sigma 54 ($\sigma^{54}$, RpoN)-dependent along with HrpS and YhbH (Ancona et al., 2014). RpoN, initially identified for its role in nitrogen assimilation, is a sigma factor which binds to RNA polymerase (RNAP) and directs a holoenzyme to promoter for transcription initiation (Hirschman et al., 1985; Hunt and Magasanik, 1985; Bush and Dixon, 2012). HrpS, a member of the NtrC family, acts as a bacterial enhancer binding protein (bEBP) or an activator of $\sigma^{54}$-dependent transcription. YhbH of *E. amylovora* is annotated as a $\sigma^{54}$ modulation protein (Smits et al., 2010). Deletion of each of these three genes (*rpoN*, *hrpS* and *yhbH*) in *E. amylovora* resulted in non-pathogenic phenotype on immature pear fruits and apple shoots, with a dramatic decrease in *hrpL* and other T3SS gene expression (Ancona et al., 2014). Transcription mediated by $\sigma^{54}$ is different from other transcription initiation mechanisms in that the $\sigma^{54}$-RNAP holoenzyme forms a transcriptionally silent closed complex and requires energy input to promote transcription initiation (Bush and Dixon, 2012). In order to form an open complex during $\sigma^{54}$-dependent transcription, bEBPs must bind to upstream activator sequences (UASs) and couple ATP hydrolysis to remodeling of the $\sigma^{54}$-RNAP holoenzyme (Bush and Dixon, 2012). Since the binding site of bEBPs (UAS) is generally located 80 to 150 bp upstream of the transcription start site, integration host factors (IHFs) are often required to enhance interactions of bEBP with the $\sigma^{54}$-RNAP holoenzyme during this transition process (Claverie-Martin and Magasanik, 1992; Huo et al., 2006).

IHF is one of the most abundant nucleoid-associated proteins (NAPs) found in Gram-negative bacteria. NAPs are generally referred to small DNA-binding proteins of bacteria that are capable of controlling nucleoid structure and gene expression via DNA looping, bending, wrapping or bridging (Dillon and Dorman, 2010). IHF is about 11 kDa in size and predominantly exists in a heterodimeric form composed of IHFα and IHFβ subunits (encoded by the *ihfA* and *ihfB* genes, respectively) (Swinger and Rice, 2004). IHF binds to DNA at the highly conserved sequence, (A/T)ATCAANNNNTT(A/G) (Yang and Nash, 1995; Murtin et al., 1998) and results in DNA bending up to 160˚ to 180˚ (Rice et al., 1996; Lorenz et al., 1999; Teter et al., 2000). IHF is first reported as a factor for the site-specific recombination of bacteriophage-λ in *Escherichia coli* (Miller et al., 1979; Miller and Friedman, 1980) and has since been found to be involved in several DNA-dependent processes, including DNA replication, maintenance of nucloeid structure and transcription regulation (Bramhill and Kornberg, 1988; Hwang and Kornberg, 1992; Santero et al., 1992; Macchi et al., 2003). Intracellular abundance of IHFs changes under different growing phases and reaches peak levels when cells enter stationary phase in *E. coli* (Ditto et al., 1994). This indicates that IHF function also can influence growth kinetics of bacteria.

The requirement of IHF as a transcription regulator for full virulence has been described in various bacterial species. Transcription of the invasion-specific genes, such as *virB* and *virF*, was activated by IHFs in *Shigella flexneri* (Porter and Dorman, 1997). Expression of the major virulence genes responsible for epithelial cell invasion and systemic infection of the mouse was largely dependent on IHFs in *Salmonella enteric* serovar Typhimurium (Mangan et al., 2006). For *hrpL* and other *hrp*-T3SS gene expression, the presence of IHFs greatly induced the

transcriptional activity of the *hrpL* promoter in *Pseudomonas syringae*, (Jovanovic et al., 2011). The *hrpL* transcription of *Pectobacterium carotovorum* ssp. *carotovorum* was also barely detected in the *E. coli ihf* mutant strains (Chatterjee et al., 2002). However, the role of IHFs in *E. amylovora* virulence is still unknown.

The aim of this study was to determine the role of IHFs in *E. amylovora* virulence. We showed that IHFs positively regulate *hrpL* and other T3SS gene expression and thus virulence. Our results also indicated that IHFs are required for growth and regulates swarming motility.

## 2.3 Materials and methods

### 2.3.1 Bacterial strains and growth conditions

The bacterial strains used in this study are listed in Table 2.1. Luria–Bertani (LB) medium was used for the routine culture of *E. amylovora* and *E. coli* strains. Bacteria were also grown in M9 minimal medium (M9MM) [12.8 g $Na_2HPO_4.7H_2O$, 3.0 g $KH_2PO_4$, 0.5 g NaCl, 1 g $NH_4Cl$, 0.24 g $MgSO_4$ and 0.011 g $CaCl_2$] supplemented with 0.4 % glucose or *hrp*-inducing minimal medium (HMM) [1 g $(NH_4)_2SO_4$, 0.246 g $MgCl_2.6H_2O$, 0.099 g NaCl, 8.708 g $K_2HPO_4$, 6.804 g $KH_2PO_4$] containing 10 mM galactose as indicated in each experiment. When required, antibiotics were added to the medium at the following concentrations: 10 μg/ml chloramphenicol (Cm), 100 μg/ml ampicillin (Ap) and 20 μg/ml kanamycin (Km).

### 2.3.2 DNA manipulation and the construction of plasmids

Plasmid DNA purification, PCR amplification of genes, isolation of fragments from agarose gels, cloning, restriction enzyme digestion and T4 DNA ligation were performed using

standard molecular procedures (Sambrook and Russel, 2001). DNA sequencing was performed at the Keck Center for Functional and Comparative Genomics at the University of Illinois at Urbana-Champaign.

### 2.3.3 Construction of *E. amylovora* mutants by Lambda-Red recombinase cloning

The *ihfA* and *ihfB* mutants of *E. amylovora* were generated using the λ phage recombinase method, as described previously (Datsenko and Wanner, 2000; Zhao et al., 2009). Briefly, *E. amylovora* Ea1189 carrying pDK46 were grown overnight at 28 ℃ and reinoculated into fresh LB broth containing 0.1% arabinose. After growth to exponential phase $OD_{600}$ = 0.8, cells were harvested by centrifugation at 4000 rpm for 10 min, made competent by washing with cold sterile water and stored at -80 ℃. Recombination fragments consisting of Cm resistance gene ($Cm^r$) with its own promoter, flanked by a 50-nucleotide homology arm, were generated by PCR from pKD32 plasmid as a template and transformed into the competent cells by electroporation. Primer pairs (ihfA-F,-R and ihfB-F,-R) were used to amplify $Cm^r$ gene fragments from pKD32 for the generation of *ihfA* and *ihfB* mutants, respectively. Transformants were selected on LB plates supplemented with Ap and Cm, and the mutant construction was confirmed by PCR amplification from internal region of $Cm^r$ gene to the external region of the target gene. The majority of the coding region of each gene in the resulting mutants was replaced by the marker gene, except for the first and last 50 nucleotides. The *ihfA* and *ihfB* mutants were designated as *ΔihfA* and *ΔihfB,* respectively. The primers used for mutant construction and mutant confirmation are listed in Table 2.2

### 2.3.4 Cloning *ihf* genes for complementation of *ihf* mutants

For complementation of the mutants, the regulatory and coding sequences of *ihfA* and *ihfB* genes were amplified by PCR from the *E. amylovora* Ea1189 strain using primer pairs ihfA-CoF, -CoR and ihfB-CoF, -CoR, respectively. The PCR fragments were cloned into high-copy-number pGEM® T-easy vector (Promega, Madison, WI, USA) through A-T ligation according to the manufacturer's instruction. Briefly, the PCR products were ligated into the pGEM® T-easy vector at a 3:1 insert:vector molar ratio in a reaction mixture containing 2X Rapid Ligation Buffer, T4 DNA ligase and water, followed by incubation for 1 h at room temperature. The final plasmids were designated pIhfA and pIhfB, respectively, and transformed into the mutant strain by electroporation. Transformants were selected on LB plates supplemented with Ap and Cm. The primers used for mutant complementation are listed in Table 2.2.

### 2.3.5 Bacterial growth

To measure bacterial growth, overnight cultures of *E. amylovora* WT, mutants and complementation strains were harvested by centrifugation at 4000 rpm for 10 min and washed twice with 0.5X phosphate-buffered saline (PBS). After the final wash, the bacterial pellet was resuspended in fresh medium to be tested and adjusted to $OD_{600}$ = 0.01 for LB and $OD_{600}$ = 0.2 for M9MM and HMM. Bacterial strains were grown at 18℃ (HMM) or 28 ℃ (LB and M9MM) with 250 rpm agitation, and aliquots of the culture were taken at different time points during growth. The bacterial growth rate for each strain was determined by measuring $OD_{600.}$ The experiments were repeated at least twice.

### 2.3.6 Virulence assay and population assay on immature pear fruits

Overnight cultures of *E. amylovora* WT, mutants and complementation strains were harvested by centrifugation at 4000 rpm for 10 min, resuspended in PBS to $OD_{600}$ = 0.1 and then diluted 100-times ($OD_{600}$ = 0.001). Immature Bartlett pear fruits (*Pyrus communis* L. cv. Bartlett) were used for virulence assays, while immature Asian pear fruits were used for population assays. Pears were surface-sterilized with 10% bleach for 10 min and rinsed with sterile distilled water. After air dried, pears were pricked with a sterile needle, inoculated with 2 μl of cell suspensions for each strain and incubated in a humidified chamber at 28 ℃. Symptoms were recorded at 4 and 8 days post-inoculation in virulence assays. For bacterial population studies, the pear tissues surrounding the inoculation site was excised using a no. 4 cork borer and homogenized in 1 ml of PBS. Bacterial growth from 0 to 3 days post-inoculation was monitored by dilution-plating on LB medium supplemented with appropriate antibiotics. For each strain tested, fruits were assayed in triplicate, and the experiments were repeated at least twice.

### 2.3.7 Hypersensitive response assay on tobacco

Bacterial strains grown overnight in LB medium with appropriate antibiotics were harvested by centrifugation at 4000 rpm for 10 min and resuspended in PBS to $OD_{600}$ = 0.1. Eight-week old tobacco (*Nicotiana tobacum*) leaves were infiltrated with bacterial suspension using needleless syringe and kept in a humidified chamber at 28 ℃. HR symptoms were recorded at 24 h post-infiltration. The experiments were repeated at least twice.

### 2.3.8 Motility assay

The motility of each strain was quantitatively determined by measuring diameters on the motility agar plates (10 g tryptone, 5 g NaCl, 2.5 g agar per l L) as previously described (Zhao et al., 2009b). Briefly, overnight cultures of *E. amylovora* WT, mutants and complementation strains were harvested by centrifugation at 4000 rpm for 10 min, washed with PBS and resuspended in PBS to $OD_{600}$ = 1. Bacterial cells were then plated onto the center of agar plates, and diameters were determined at 24 and 48 h post-inoculation. The experiments were repeated at least twice.

### 2.3.9 RNA isolation

To isolate RNA for *in vitro* T3SS gene expression, bacterial cultures grown in LB medium with appropriate antibiotics were harvested by centrifugation at 4000 rpm for 10 min and washed twice with PBS. Bacterial cells were resuspeded in HMM to $OD_{600}$ = 0.2 and incubated at 18 ℃ with 250 rpm agitation. After 6 h in HMM, 4 ml of RNA protect reagent (Qiagen, Hilden, Germany) was added to 2 ml of bacterial cell cultures to avoid RNA degradation. For *in vivo* T3SS gene expression, overnight bacterial cultures were harvested by centrifugation at 4000 rpm for 10 min and resuspended in PBS $OD_{600}$ = 0.2 to 0.3. Immature Bartlett pear fruits (*Pyrus communis* L. cv. Bartlett) were surface-sterilized with 10% bleach for 10 min and rinsed with sterile distilled water. After air dried, pears were cut in half and inoculated with bacterial suspension. Bacterial cells were incubated in a moist chamber at 28 ℃ for 6 h and collected by washing pear surfaces with a solution containing 2 ml RNA protect reagent (Qiagen) and 1 ml water. Cells collected for both *in vivo* and *in vitro* T3SS gene expression were then harvested by centrifugation at 4000 rpm for 10 min. RNA was extracted

using the RNeasy Mini kit (Qiagen), following which the eluted total RNA was DNase-treated using Turbo DNA-free™ (Ambion, Austin, TX, USA) according to the manufacturer's instructions, respectively. Quality and quantity of the RNA was assessed using a Nano-Drop ND-100 spectrophotometer (Nano-Drop Technologies; Wilmington, DE, USA).

### 2.3.10 Quantitative real-time PCR (qRT-PCR)

Reverse transcription for cDNA synthesis was performed using Superscript® VILO™ cDNA synthesis kit (Invitrogen, Carlsbad, CA, USA) on 1 µg of total RNA according to the manufacturer's instruction. The 100 ng of reverse transcription product was used for qRT-PCR analysis in a total volume of 25 µl containing 12.5 µl Power SYBR® Green PCR master mix (Applied Biosystems, Foster City, CA, USA), primers of selected genes (500nM) and water. The primers for qRT-PCR were designated using Primer3 software and listed in Table 2.2. Negative controls were also set up by substituting cDNA with water. The qRT-PCR amplification was carried out in duplicate in MicroAmp® Fast Optical 96-Well plates with Optical Adhesive Films on StepOnePlus Real Time PCR System (Applied Biosystems). The qRT-PCR program was 50 ℃ for 2 min, 95 ℃ for 10 min, followed by 40 cycles of 95 ℃ for 15 s and 60 ℃ for 1 min, and a final dissociation curve analysis step from 65 to 95 ℃. Gene expression levels were analyzed using the relative quantification (ΔΔCt) method, and a 16S rDNA (*rrsA*) gene was used as an endogenous control to normalize gene expression data. A *P* value was calculated based on a moderated *t*-test to measure the significance associated with each relative quantification value. Variations were considered to be statistically significant when $P < 0.05$. The experiments were repeated at least twice using three biological replicates.

## 2.4 Results

### 2.4.1 Generation of *ihf* mutants and effect of *ihf* mutation on bacterial growth

To study the function of IHFs in *E. amylovora*, *ihfA* and *ihfB* knockout mutants were generated using the λ-Red cloning (Zhao et al., 2009a). Despite repeated attempts, we were unable to construct a double mutant lacking both *ihfA* and *ihfB* genes for unknown reasons. In order to assess whether IHFs of *E. amylovora* play a role in bacterial growth, two mutants and their complementation strains were tested for their abilities to grow in three different liquid media (LB medium, M9MM and HMM) and compared with Ea1189 wild-type (WT) stain. Both *ihfA* and *ihfB* mutants initially grew much slower in LB medium than that of WT, but reached maximum population as WT at 24 h post inoculation (Figure 2.1A). However, no significant growth difference was observed between WT and mutants in both M9MM and HMM media (Figure 2.1B, C). Complementation strains showed similar growth patterns as WT in all three conditions. These results indicate that the absence of either IHF subunit does not affect *E. amylovora* growth in nutrient limitation conditions, but slow growth under nutrient rich conditions, suggesting that IHF heterodimer might be required for the rapid growth of *E. amylovora* under favorable conditions.

### 2.4.2 Mutations in *ihfA* and *ihfB* render *E. amylovora* nonpathogenic

To determine the role of IHFs in *E. amylovora* virulence, WT, *ihfA* and *ihfB* mutants and their corresponding complementation strains were inoculated on immature pear fruits, and disease development was assessed for 8 days post inoculation (DPI) (Figure 2.2). The WT strain elicited water soaking symptoms on pears at 2 DPI. Necrotic lesions appeared with bacterial ooze formation at the inoculation sites after 4 days, and the necrotic areas turned black and

covered almost the whole pear fruits after 8 days. However, no disease symptoms were observed for both *ihfA* and *ihfB* mutants on immature pear fruits during 8 DPI. The virulence of the mutants on immature pear fruits was partially recovered in the complementation strains (Figure 2.2). These results indicate that *ihfA* and *ihfB* genes are required for *E. amylovora* virulence.

Bacterial growths of WT, mutant and complementation strains in immature pear fruits were also quantitatively determined for 3 DPI (Figure 2.3). Bacterial number of WT increased up to 1 x $10^9$ CFU/g after 3 days, and complementation strains showed comparable levels of growth as WT following inoculation. However, the number of viable *ihfA* and *ihfB* mutant cells maintained at initial inoculum level or slightly decreased to 5 x $10^3$ CFU/g tissue throughout the incubation period, which represents a six log difference. This indicates that both IHFα and IHFβ subunits are required for *E. amylovora* to colonize and grow on immature pear fruits.

### 2.4.3 IHF positively regulates the expression of *hrpL* and other T3SS genes

We next examined how deletions of *ihfA* and *ihfB* genes affect *hrpL* and other T3SS gene expression using qRT-PCR. Under both *in vitro* and *in vivo* conditions, no expression of *ihfA* and *ihfB* genes was detected in the corresponding mutants (Figure 2.4A, B). However, expression of *ihfA* was increased about 3- and 15-fold in *ihfB* mutant than that in WT *in vitro* and *in vivo*, respectively; whereas expression of *ihfB* remained the same in both *ihfA* mutant and WT, suggesting a potential negative autoregulation of *ihfA* transcription by IHFαβ heterodimer or IHFββ homodimer in *E. amylovora*.

Expression of T3SS genes, including *dspE*, *hrpA*, *hrpN* and *hrpL*, was barely detectable in the two mutants *in vitro* (Figure 2.4C); whereas mutations in *ihfA* and *ihfB* genes also affected expression of *rpoN*, *yhbH* and *hrpS*. Expression of *hrpS* was about 5-fold lower in the two mutants as compared to WT, while expression of *rpoN* and *yhbH* was slightly higher. Overall pattern of T3SS genes in pear was similar to those observed under *in vitro* conditions (Figure 2.4D). The two mutants exhibited reduced expression of T3SS (*dspE*, *hrpA*, *hrpN* and *hrpL*) and *hrpS* genes, while expression of *rpoN* and *yhbH* genes was slightly increased. These results further demonstrated that IHFs act as a positive regulator of T3SS in *E. amylovora* via the activation of *hrpL* transcription. Furthermore, IHFs may also act as a positive regulator of *hrpS* expression.

### 2.4.4 Mutations in *ihfA* and *ihfB* did not affect hypersensitive response (HR) in tobacco

To test the ability to elicit HR in non-host plants, tobacco leaves were infiltrated with cell suspensions of WT, *ihfA* and *ihfB* mutants and their complementation strains and assessed for HR development after 24 h post infiltration (Figure 2.5). As expected, both WT and mutant complementation strains elicited HR on tobacco leaves, while the negative controls, *hrpL* and *hrpS* mutants, failed to produce any visible HR after 24 h. To our surprise, *ihfA* and *ihfB* mutants were still able to induce HR. These were unexpected results given that the two mutants exhibited a significant decrease in the expression of *hrpL* and other T3SS genes. It is possible that an unknown mechanism of T3SS gene regulation exist during incompatible host-pathogen interaction. It is also possible that basal level of *hrpL* transcription may occur in the absence of either IHF subunit, leading to functional T3SS activation that is sufficient to elicit HR on tobacco leaves, but not enough to cause disease on host immature pear fruits.

### 2.4.5 IHF negatively regulates motility in *E. amylovora* by activating expression of *rsmB/csrB*

We also assessed bacterial motility for WT, mutant and complementation strains. Both *ihfA* and *ihfB* mutants exhibited a hypermotile phenotype with a lower density than that of the WT (Figure 2.6). The moving distances were 18 mm and 35 mm for both mutants and 9 mm and 29 mm for WT strain at 24 h and 48 h following inoculation, respectively. Complementation strains returned to normal motility as the WT with a moving distance of about 9 mm and 25 mm at 24 h and 48 h, respectively. These results indicate that IHFα and IHFβ negatively regulate motility in *E. amylovora*.

Given that the RNA-binding protein CsrA/RsmA positively regulates motility, and the non-coding small RNA *csrB*/*rsmB* negatively controls motility (Ancona and Zhao, 2013), we then determined whether the expression of *csrA*/*rsmA* and *csrB*/*rsmB* is dependent upon IHF (Figure 2.7). No significant change in *csrA*/*rsmA* expression was observed, however expression of *csrB*/*rsmB* was barely detectable in *ihfA* and *ihfB* mutants, indicating that IHFα and IHFβ are required for *csrB*/*rsmB* expression and may control motility through regulating its expression.

## 2.5 Discussion

Bacterial chromosomal DNA is highly compacted but organized for genetic activity by small nucleoid-associated proteins (NAPs). The abilities of NAP to remodel nucleoid structure allow not only the alteration in global gene expression, but also the fine tuning of specific gene expression under various conditions (Luijsterburg et al., 2008). NAPs, including IHFs have been described to modulate gene expression for survival and adaptation to changing environments in

many animal and plant pathogenic bacteria (Porter and Dorman, 1997; Chatterjee et al., 2002; Mangan et al., 2006; Stonehouse et al., 2008; Jovanovic et al., 2011). In this study, we, for the first time, demonstrated that IHFs are required for $\sigma^{54}$-dependent *hrpL* and other T3SS gene expression as well as virulence in *E. amylovora.*

The *hrp*-T3SS deletion mutant of *E. amylovora* fails to grow and cause disease on immature pear fruits (Zhao et al., 2009a), indicating that expression of T3SS is essential for virulence of *E. amylovora*. The current model of T3SS regulation in *E. amylovora* suggests that *hrpL* transcription is activated by RpoN ($\sigma^{54}$), HrpS and YhbH (Ancona et al., 2014). Here, we showed that IHFs also positively control the *hrpL* transcription. Both *ihfA* and *ihfB* mutants failed to fully activate the expression of *hrpL* and other T3SS genes, thus failed to grow and cause disease on immature pear fruits. The consensus IHF binding site is also present at the *hrpL* promoter region. These findings suggest that IHF-induced DNA bending at the upstream region of the *hrpL* promoter enhances the interaction between HrpS and the $\sigma^{54}$-RNAP holoenzyme during the $\sigma^{54}$-dependent *hrpL* transcription. Therefore, IHFs are required for the sigma factor cascade that activates T3SS in *E. amylovora* (Ancona et al., 2014).

Furthermore, our results also revealed that mutations in *ihfA* and *ihfB* genes lead to about 5-fold decrease in *hrpS* expression, suggesting that IHF may function as a positive regulator of *hrpS* expression. HrpS, as a member of the $AAA^+$ (ATPases associated with various cellular activities) family of proteins, plays a central role in responding to external stimuli and controlling T3SS gene expression in *E. amylovora* (Wei et al., 2000). Unlike other bEBPs, HrpS lacks an N-terminal regulatory domain, which regulates the activity of the central AAA+ domain

in response to cellular signals. In *Pseudomonas syringae*, a *trans* acting protein HrpV is found to interfere with the HrpS activity via protein-protein interaction, leading to reduced *hrpL* expression (Schumacher et al., 2006; Jovanovic et al., 2011). Despite having *hrpV* gene, the regulation of HrpS activity via HrpV has not been reported in *E. amylovora*. On the other hand, in *Pantoea stewartii*, multiple environmental cues are sensed and integrated by HrpX (sensor kinase) and HrpY (response regulator) two-component signal transduction system (TCST), leading to HrpY-dependent expression of *hrpS* (Merighi et al., 2003). An IHF binding site presents at the *hrpS* promoter region of *P. stewartii*, suggesting that IHF may be important for activating *hrpS* expression (Merighi et al., 2006). *E. amylovora* also contains HrpXY system and shares a similar *hrp*-inducing condition, such as low pH and low concentration of ammonium ions and certain carbon sources (Wei et al., 1992b; Merighi et al., 2003). However, *E. amylovora* HrpXY system may not control the expression of *hrpL* or *hrpS* gene as previously reported (Zhao et al., 2009b). The consensus IHF binding site is also not present at the *hrpS* promoter region of *E. amylovora*. Therefore, more work needs to be done to reveal the mechanisms underlying *hrpS* regulation in *E. amylovora*.

Previous studies of IHFs showed that IHF expression changes under different growing phases and is controlled by various regulatory mechanisms, such as RpoS, ppGpp and autoregulation (Aviv et al., 1994; Ditto et al., 1994; Ali Azam et al., 1999). Expression of both *ihfA* and *ihfB* genes in *Escherichia coli* is shown to be regulated by a negative autoregulation (Aviv et al., 1994). In contrast, we found a potential negative autoregulation only in *ihfA* gene expression. The consensus IHF binding site was also identified only at the *ihfA* promoter region (data not shown). Additionally, under nutrient-rich condition, deletion of *ihfA* and *ihfB* genes in *E.*

*amylovora* reduced bacterial growth, while no changes in growth rate were observed in *ihfA* and *ihfB* mutants of *Salmonella enterica* (Mangan et al., 2006). Together, these results suggest that IHFs of *E. amylovora* have different regulation mechanisms and functions when compared to that of other *Enterobacteriacae* members.

Flagellar motility has been considered as one of the important virulence factors of *E. amylovora* during its invasion of apple flowers and seedlings (Zhao et al., 2009b; Wang et al., 2010). Consistent with the findings from other bacteria, motility of *E. amylovora* have been found to be regulated in a complicated manner by several TCSTs and small regulatory RNAs (Zhao et al., 2009b; Ancona and Zhao, 2013; Li et al., 2014). In this study, we show that IHFs are also involved in controlling motility as negative regulators. *ihfA* and *ihfB* mutants had a hypermotile phenotype and presented a similar swarming pattern as observed in the *gacS*/*gacA* and *rsmB*/*csrB* mutant (Ancona and Zhao, 2013; Li et al., 2014). GacS/GacA system is a TCST that acts as a global regulator in γ-proteobacteria, while *rsmB*/*csrB* is a small regulatory RNA that binds to RsmA/CsrA (RNA binding protein) and regulates its activity (Lapouge et al., 2008). The activated GacA can positively regulate the transcription of *rsmB*/*csrB*, resulting in the inhibition of translational regulator function of RsmA/CsrA (Hyytiäinen et al., 2001; Weilbacher et al., 2003; Kay et al., 2005; Brencic et al., 2009). It has been reported that the expression of FlhDC, the master regulator of flagella biosynthesis, is regulated by this Gac/Rsm/Csr pathway through which RsmA/CsrA enhances the stability and translation of *flhDC* mRNA (Wei et al., 2001). In *E. amylovora*, *rsmB*/*csrB* expression was abolished in *ihfA* and *ihfB* mutants, and the consensus IHF binding site is present in the *rsmB*/*csrB* promoter. Therefore, the increased motility of *ihf* mutants may result from the reduced *rsmB*/*csrB* expression.

In summary, IHFs, as global regulator of several DNA-dependent processes, are essential for *E. amylovora* virulence on host plants. Our results indicate that various virulence traits in *E. amylovora*, including bacterial growth, T3SS and motility, are regulated by IHFs. We have provided undeniable evidence that $\sigma^{54}$-dependent *hrpL* gene expression requires IHFs, therefore the transcription of other *hrp*-T3SS genes is also under positive control of IHFs.

## 2.6 Tables

### Table 2.1 Bacterial strains and plasmids used in this study

| Strains, plasmids, | Relevant characters* | Reference source |
|---|---|---|
| **Strains** | | |
| *Erwinia amylovora* | | |
| Ea1189 | Wild-type, isolated from apple | Burse et al., (2004) |
| Δ*ihfA* | *ihfA::Cm*; $Cm^R$-insertional mutant of *ihfA* of Ea 1189, $Cm^R$ | This study |
| Δ*ihfB* | *ihfB::Cm*; $Cm^R$-insertional mutant of *ihfB* of Ea 1189, $Cm^R$ | This study |
| Δ*hrpL* | *hrpL::Km*; $Km^R$-insertional mutant of *hrpL* of Ea 1189, $Km^R$ | Ancona et al., (2014) |
| Δ*hrpS* | *hrpS::Km*; $Km^R$-insertional mutant of *hrpS* of Ea 1189, $Km^R$ | Ancona et al., (2014) |
| *Escherichia coli* | | |
| DH10B | $F^-$ *mcr*A Δ(*mrr-hsd*RMS-*mcr*BC) Φ80/*ac*Z ΔM15 Δ*lac*X74 *rec*A1 *end*A1 *ara*Δ139 Δ(*ara*, *leu*)7697 *gal*U *gal*K λ-*rps*L ($Str^R$) *nup*G | Invitrogen, Carlsbad, CA, USA |
| **Plasmids** | | |
| pKD46 | $Ap^R$, $P_{BAD}$ gam bet exo pSC101 oriTS | Datsenko and Wanner (2000) |
| pKD32 | $Cm^R$, FRT cat FRT PS1 PS2 oriR6K rgbN | Datsenko and Wanner (2000) |
| pGEM® T-easy | ApR, PCR cloning vector | Promega |
| pIhfA | 1.060-kb PCR fragment containing *ihfA* gene in pGEM® T-easy | This study |
| pIhfB | 1.113-kb PCR fragment containing *ihfB* gene in pGEM® T-easy | This study |

*$Cm^R$, $Km^R$, $Ap^R$, chloramphenicol, kanamycin and ampicilln resistance, respectively.

**Table 2.2 Primers used in this study**

| Primer | Sequences (5'- 3') |
|---|---|
| **Primers for mutation** | |
| ihfA F | ATGGCGCTTACAAAAGCTGAAATGTCTGAATACCTGTTTGAAAAGCTCGGC GATTGTGTAGGCTGGAGCT |
| ihfA R | TTAATCTTCTTTTGGCGTGGCGTTCTCGACCCGGCTTTTGAGTTTCTGGCATT CCGGGGATCCGTCGACC |
| ihfB F | ATGACCAAGTCAGAACTGATTGAGAGGCTTGCAGGCCAGCAATCTCATATC GATTGTGTAGGCTGGAGCT |
| ihfB R | TCAGCCGCCGTATATATTGGCGCGATCGCGCAGCTCTTTTCCGGGCTTGAAT TCCGGGGATCCGTCGACC |
| ihfA C1 | GTACCGTGGTAAGGGCGTAA |
| ihfA C2 | AAGCAAAAACCAGACGGATG |
| ihfB C1 | CGTTGTCAGCCTGTCTGTTC |
| ihfB C2 | ATGATGAGCGCAACACCATA |
| Cm1 | TTATACGCAAGGCGACAAGG |
| Cm2 | GATCTTCCGTCACAGGTAGG |
| **Primers for RT-PCR** | |
| 16S1 | CCTCCAAGTCGACATCGTTT |
| 16S2 | TGTAGCGGTGAAATGCGTAG |
| ihfA-rt1 | TTTTGAAGAAGTGCGTCGTG |
| ihfA-rt2 | TTGAGTTTCTGGCCTGGTCT |
| ihfB-rt1 | CGTTGAGGATGCGGTAAAAG |
| ihfB-rt2 | CTCCACTTTGTCACCCGTCT |
| dspE-rt1 | TCCAGCGAGGGCATAATACT |
| dspE-rt2 | ACAACCGTACCCTGCAAAAC |
| hrpL-rt1 | TTAAGGCAATGCCAAACACC |
| hrpL-rt2 | GACGCGTGCATCATTTTATT |
| hrpN-rt1 | GCTTTTGCCCATGATTTGTC |
| hrpN-rt2 | CAACCCGTTCTTTCGTCAAT |
| hrpA-rt1 | GAGTCCATTTTGCCATCCAG |
| hrpA-rt2 | TGGCAGGCAGTTCACTTACA |
| rpoN-rt1 | AAGCGGTACTGAAACGGGTA |
| rpoN-rt2 | GCATCAGACTGCGAAAATCA |
| yhbH-rt1 | GCGCGAGTTTGTTACCACTA |
| yhbH-rt2 | ATCGCCGCGTACATATCTTT |
| hrpS-rt1 | AATGCTACGCGTGCTGGAAA |
| hrpS-rt2 | AACAATGGCGTTTGCGTTGC |
| **Primers for cloning** | |
| ihfA com F | ACA GCG CAA TGA GGA GCA CT |
| ihfB com F | AGAAAGGCGACGAAATCGCA |

## 2.7 Figures

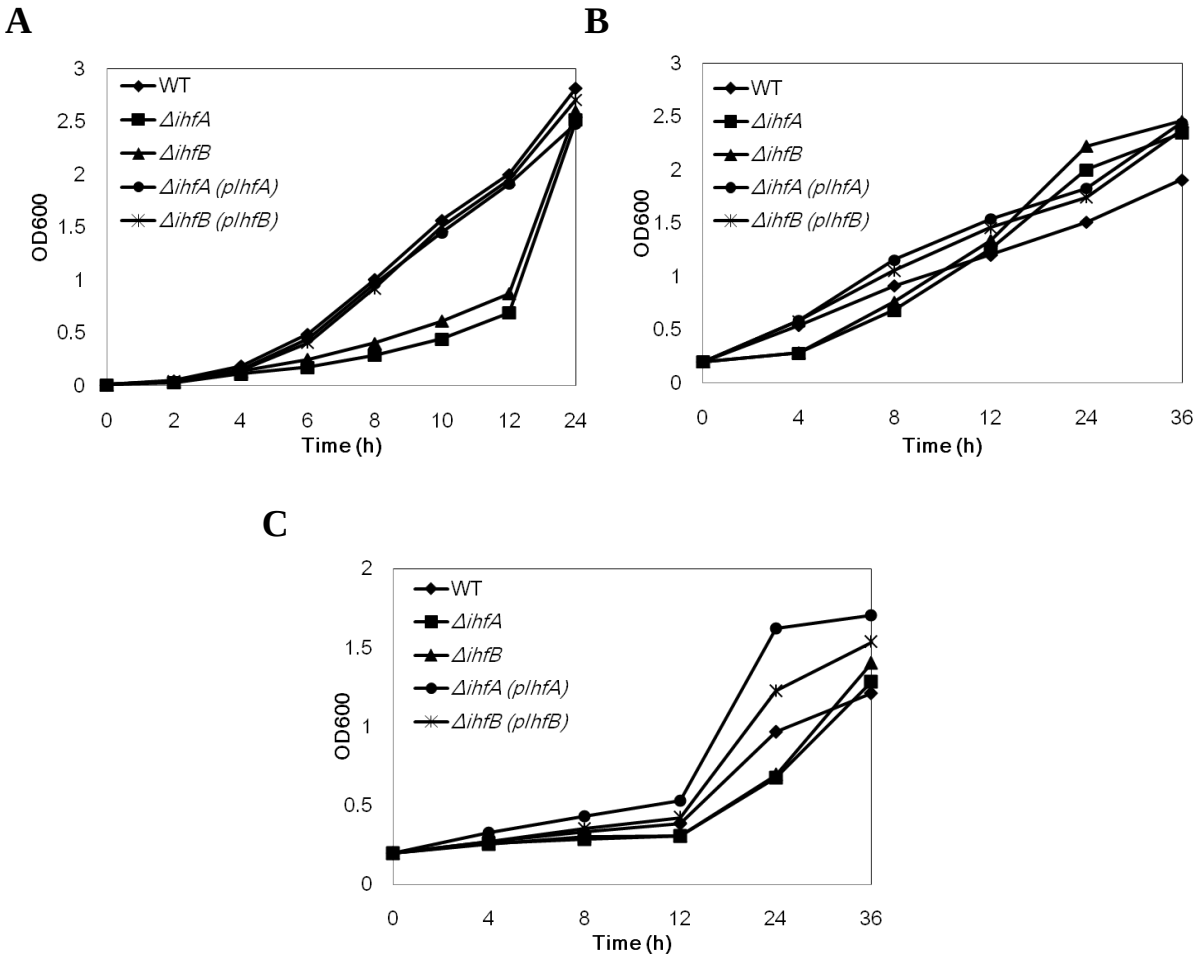


**Figure 2.1 Growth curves of *E. amylovora* wild-type (WT), *ihf* mutants and complementation strains of the *ihf* mutants.** The growth of bacterial strains ($OD_{600}$) was monitored at different time points. (A) Growth curves in LB media at 28℃. (B) Growth curves in M9 minimal media at 28℃. (C) Growth curves in *hrp*-inducing medium at 18℃. Data points represent the means of three replicates ± standard errors. Similar results were obtained in a second independent experiment.

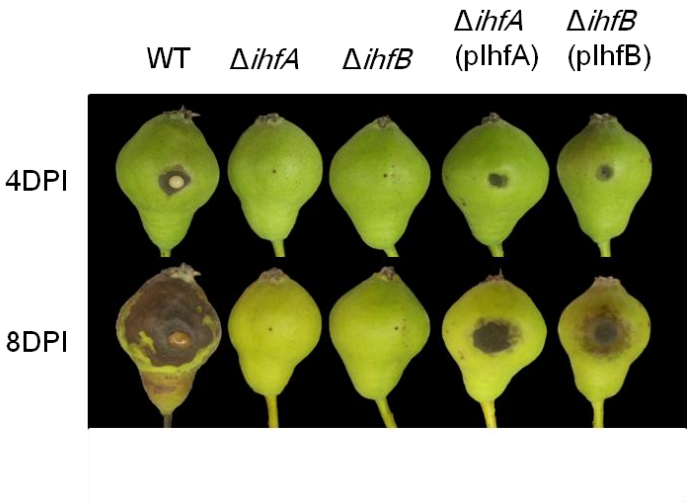


**Figure 2.2 Pathogenicity tests of *E. amylovora* wild-type (WT), *ihf* mutants and complementation strains of the *ihf* mutants on immature pears.** Symptoms caused by WT, *ihfA*, *ihfB* mutants and complementation strains of *ihfA* (pIhfA), *ihfB* (pIhfB) mutants. DPI, days post-inoculation.

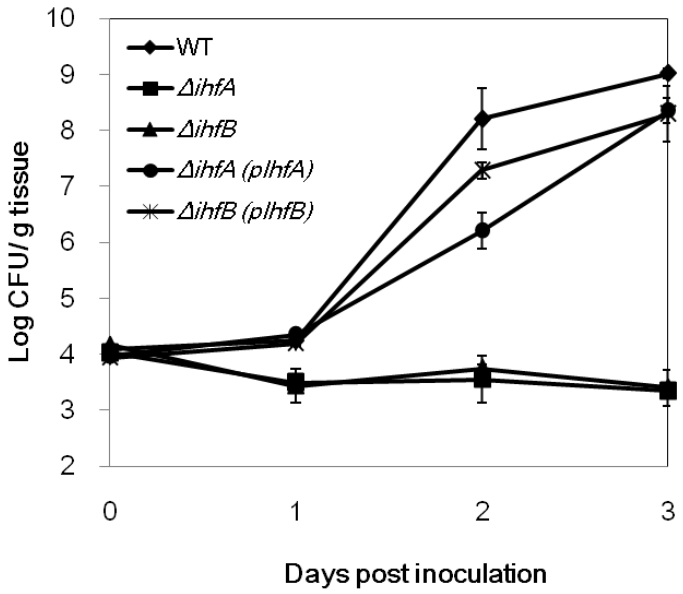


**Figure 2.3 Growth of *E. amylovora* wild-type (WT), *ihf* mutants and complementation strains of the *ihf* mutants during infection of immature pears.** The growth of bacterial strains was monitored at 0, 1, 2 and 3 days after inoculation. Data points represent the means of three replicates ± standard errors. Similar results were obtained in a second independent experiment.

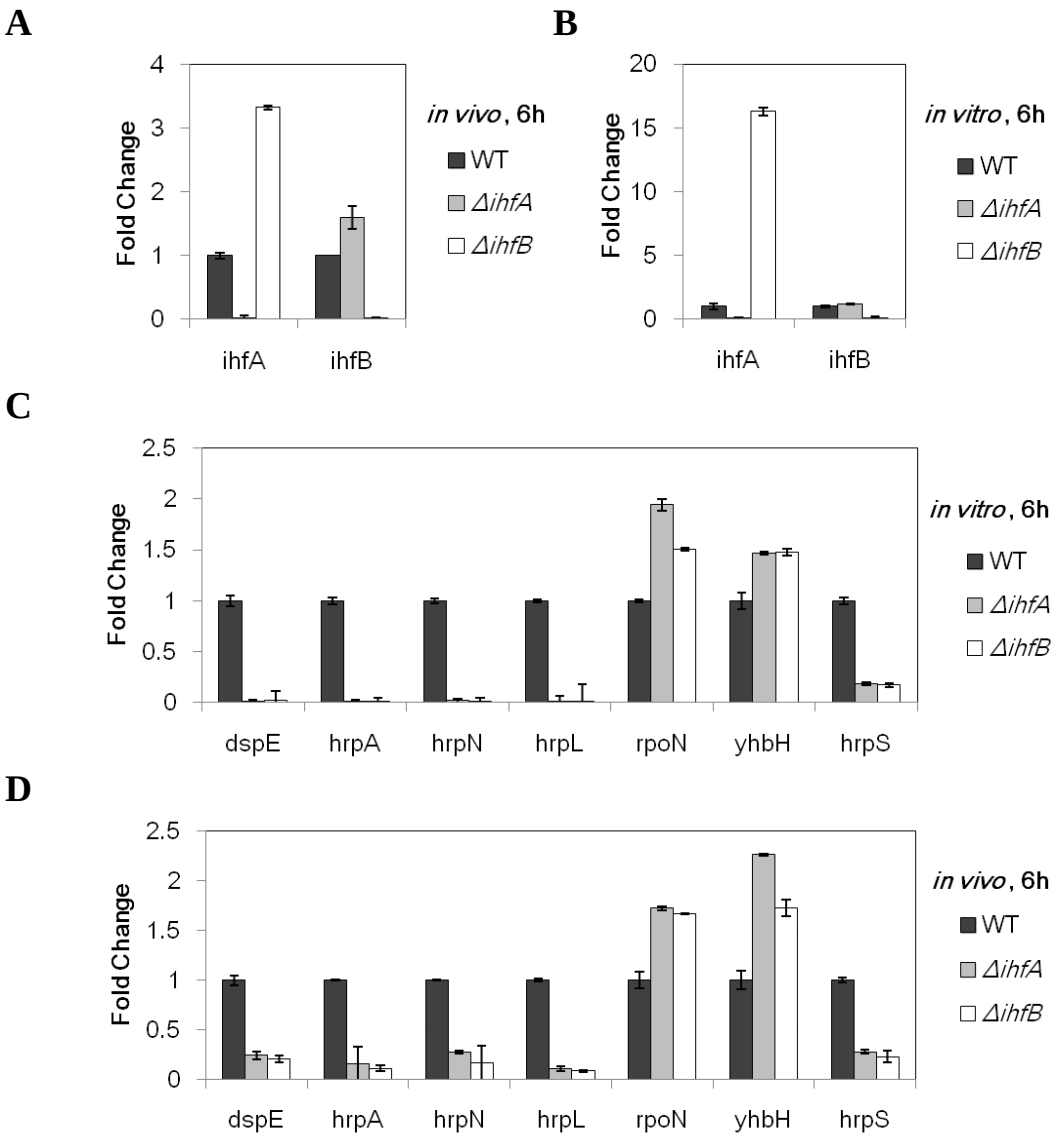


**Figure 2.4 Expression of selected genes *in vivo* and *in vitro* by quantitative real-time reverse transcription-polymerase chain reaction (qRT-PCR).** (A) Relative gene expression of *ihfA* and *ihfB* genes in *ihfA* and *ihfB* mutant strains compared with WT inoculated onto immature pear fruits at 6 h. (B) Relative gene expression of *ihfA* and *ihfB* genes in *ihfA* and *ihfB* mutant strains compared with WT grown in *hrp*-inducing medium at 18℃ at 6 h. (C) Relative gene expression of three T3SS genes and *hrpL*, *rpoN*, *yhbH* and *hrpS* genes in *ihfA* and *ihfB* mutant strains compared with WT grown in *hrp*-inducing medium at 18℃ at 6 h. (D) Relative gene expression of three type III secretion (T3SS) genes (*dspE*, *hrpA*, *hrpN*) and *hrpL*, *rpoN*, *yhbH* and *hrpS* genes in *ihfA* and *ihfB* mutant strains compared with the wild-type (WT) inoculated onto immature pear fruits at 6 h. The relative fold change of each gene was derived from the comparison of mutant strains versus WT control. The 16S rDNA (*rrsA*) gene was used as an endogenous control. The values of the relative fold change were the means of three replicates. The experiments were repeated at least twice with similar results. Error bars indicate standard deviation.

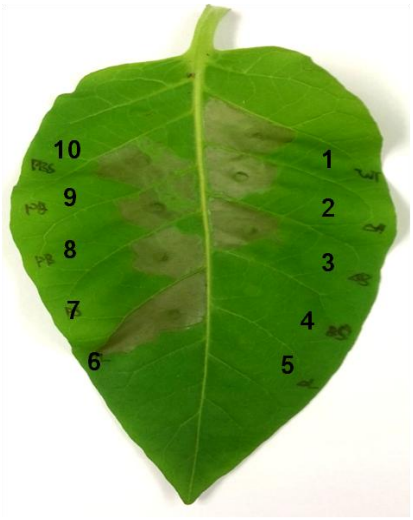


**Figure 2.5 Hypersensitive response (HR) assay of *E. amylovora* wild-type (WT), *ihf* mutants and complementation strains of the *ihf* mutants on tobacco leaves.** Eight-week-old tobacco leaves were infiltrated with WT, mutant strains and complementation strains with cell suspensions at an optical density at 600 nm ($OD_{600}$) of 0.1, 1, WT Ea1189; 2, *ihfA*; 3, *ihfB*; 4, *hrpS*; 5, *hrpL*; 6, *hrpL* (pHrpL); 7, *hrpS* (pHrpS); 8, *ihfB* (pIhfB); 9, *ihfA* (pIhfA); 10, phosphate-buffured saline (PBS).

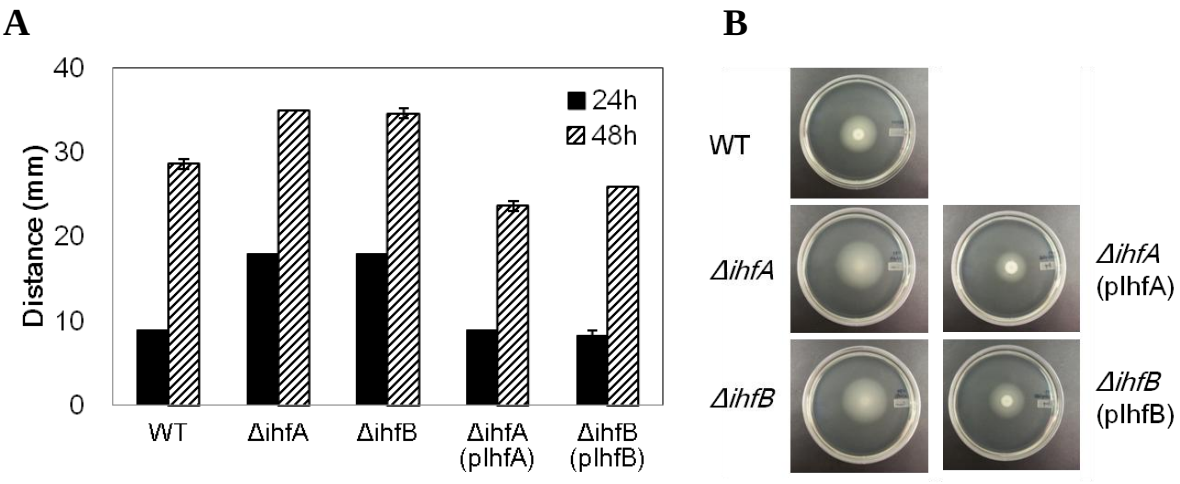


**Figure 2.6 Motility assay of *E. amylovora* wild-type (WT), *ihf* mutants and complementation strains of the *ihf* mutants.** Bacterial strains ($OD_{600}$=1.0) were spotted at the center of the motility plate (0.25% agar) and incubated at 28℃. (A) Comparison of the moving distances of WT, *ihfA*, *ihfB* mutants and complementation strains. Diameters of the circle around the inoculation site (mm) were measured 24h and 48h post inoculation. (B) Comparison of WT, *ihfA*, *ihfB* mutants and complementation strains on the motility plate. Pictures were taken at 48 h post-inoculation.

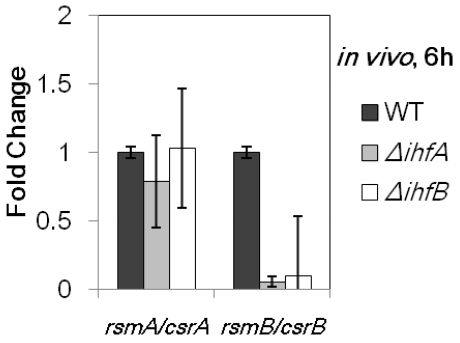


**Figure 2.7 Expression of selected genes *in vivo* by quantitative real-time reverse transcription-polymerase chain reaction (qRT-PCR).** Relative gene expression of *rsmA*/*csrA* and *rsmB*/*csrB* genes in *ihfA* and *ihfB* mutant strains compared with the wild-type (WT) inoculated onto immature pear fruits at 6 h. The relative fold change of each gene was derived from the comparison of mutant strains versus WT control. The 16S rDNA (*rrsA*) gene was used as an endogenous control. The values of the relative fold change were the means of three replicates. The experiments were repeated at least twice with similar results. Error bars indicate standard deviation.

# CHAPTER 3

# CHARACTERIZATION OF ENHANCER BINDING PROTEIN HrpS IN REGULATING TYPE III SECRETION SYSTEM GENE EXPRESSION IN *Erwinia amylovora*

## 3.1 Abstract

The bacterial enhancer binding protein (bEBP) HrpS plays a central role in regulating T3SS gene expression by activating the transcription of *hrpL* gene in *Erwinia amylovora*. Upon binding to upstream activator sequence (UAS) at the *hrpL* promoter, HrpS interacts with the $\sigma^{54}$-RNA polymerase holoenzyme through conserved GAYTGA motif, which allows the initiation of *hrpL* transcription. However, where HrpS binds to the promoter of *hrpL* and what is the role of the conserved GAYTGA motif in regulating *hrpL* and other T3SS gene expression remain elusive. In this study, our goals were to identify the HrpS binding site and to characterize the role of conserved GAYTGA motif of HrpS in transcription activation of *hrpL* in *E. amylovora*. First, eight 5' deletion constructs of *hrpL* promoter fused to a promoter-less *gfp* were made, and promoter activities were measured by flow cytometry. The results of promoter screening suggested a potential region for HrpS binding. Second, complementation of *hrpL* mutant using twelve constructs containing *hrpL* gene and various lengths of *hrpL* promoter further delineated the UAS region for HrpS binding. Bioinformatic analysis of this region revealed a dyad symmetry sequence between -141 to -122 nt (AT-N-TGCAA-$N_4$-TTGCA-N-AT), which is characteristic for bEBP binding. Third, site-directed mutation analyses and quantitative real time-PCR (qRT-PCR) assays demonstrated that the complete-dyad symmetry sequence was all required for T3SS gene expression and complementation of *hrpL* mutant. Finally, electrophoretic mobility shift assay (EMSA) with purified truncated HrpS protein containing its DNA binding domain further verified that HrpS binds to this sequence, indicating that *hrpL* promoter from -

141 to -122 is the HrpS binding site. In addition, results from site-directed mutagenesis analyses of the conserved GAYTGA motif of HrpS showed that Y100F substitution did not affect the function of HrpS, whereas Y100A and Y101A mutations completely abolished HrpS activity. These results suggest that tyrosine and phenylalanine can compensate functionally for each other in the GAYTGA motif of HrpS in *E. amylovora*.

### 3.2 Introduction

*Erwinia amylovora* is the causal agent of fire blight on apples and pears, causing annual economic losses of over 100 million dollars in pome fruit industry in the United States alone (Khan et al., 2012). Trees infected by *E. amylovora* typically show wilting and water soaking symptoms followed by a blackened and scorched appearance in leaves and twigs. As a member of the family *Enterobacteriaceae*, *E. amylovora* shares some common characteristics with many important animal pathogens, such as *Escherichia coli*, and is also closely related to several plant-associated bacteria, such as *Pectobacterium* and *Pantoea*. Like many other Gram-negative plant pathogenic bacteria, the hypersensitive response and pathogenicity (*hrp*)-type III secretion system (T3SS) is one of the major pathogenicity factors in *E. amylovora*. The *hrp*-T3SS functions in delivering effectors into eukaryotic cells, which eventually interferes with host defense mechanisms and cellular metabolism during pathogenesis (Alfano and Collmer, 2004; Büttner and Bonas, 2006).

Structural, functional and regulatory components of the *hrp*-T3SS of *E. amylovora* are encoded in a cluster of genes, known as the Hrp pathogenicity island (PAI) (Oh et al., 2005). Molecular genetic studies of *E. amylovora* have demonstrated that expression of *hrp*-T3SS genes

is regulated by HrpL, one of the exocytoplasmic functions (ECF) subfamily of sigma factors (Shen and Keen, 1993; Wei and Beer, 1995; Chatterjee et al., 2002). The promoter region of genes encoding known components of T3SS possesses the *hrp* box (GGAACC-$N_{16}$-CCACNNA) where HrpL can bind and direct RNA polymerase (RNAP) for transcription initiation (McNally et al., 2012). In *E. amylovora*, *hrpL* transcription is activated by RpoN, HrpS, YhbH and IHFα/β (Ancona et al., 2014; this study). RpoN ($\sigma^{54}$), an alternative sigma factor 54, directs RNAP to consensus -24 (GG) and -12 (TGC) promoter regions. The $\sigma^{54}$-RNAP holoenzyme forms a highly stable, closed complex with DNA that is unable to spontaneously isomerize into an open complex (Buck et al., 2000; Guo et al., 2000). To initiate transcription, specific bacterial enhancer binding proteins (bEBPs) must be present to remodel the $\sigma^{54}$-RNAP holoenzyme, and HrpS serves as a bEBP in *hrpL* transcription (Wei et al., 2000; Cannon et al., 2001). YhbH is annotated as $\sigma^{54}$ modulation protein, but the exact mechanism of action in activating *hrpL* transcription is still unclear (Smits et al., 2010; Ancona et al., 2014).

bEBPs are members of $AAA^+$ (ATPase associated with various cellular activities) family of proteins which can couple chemical energy derived from nucleotide hydrolysis to a mechanical action (Wang, 2004). To activate $\sigma^{54}$-depdendent transcription, the closed complex must be remodeled via $\sigma^{54}$ contact and DNA melting, and the $\sigma^{54}$-RNAP holoenzyme must be relocated near the transcription start site (Bush and Dixon, 2012). This can be met through the $AAA^+$ domain responsible for ATP hydrolysis and $\sigma^{54}$ contact (Bordes et al., 2003). The $AAA^+$ domain of bEBPs is also implicated in oligomerzation so that hexameric or hetameric bEBPs can have increased ATPase activity (Wikström et al., 2001). bEBPs contain several structurally conserved motifs within the $AAA^+$ domain, including the GAFTGA (Bush and Dixon, 2012).

The surface-exposed loop of the GAFTGA motif enables bEBPs to interact with $\sigma^{54}$, leading to conformational changes in the $AAA^+$ domain and substrates remodeling upon ATP hydrolysis (Lew and Gralla, 2002; Zhang et al., 2002; Bordes et al., 2003; Rappas et al., 2005). All six residues of the GAFTGA motif are essentially required for full transcription activity, and the threonine residue is shown to directly interact with $\sigma^{54}$ (Chaney et al., 2001; Dago et al., 2007). However, it has been reported that about 7% of the annotated bEBPs contain tyrosine instead of phenylalanine residue in the GAFTGA motif, including HrpS proteins in *E. amylovora* (Figure 3.1) and *Pseudomonas syringae* pv. *tomato* DC3000 (Zhang et al., 2009). A recent report showed that substitution of tyrosine (Y) with phenylalanine (F) in the GAYTGA motif of HrpS in *P. syringae* pv. *tomato* DC3000 increased *hrpL* promoter activity by about 1.5-fold (Jovanovic et al., 2011). This led us to ask whether a tyrosine to phenylalanine substitution in the GAYTGA motif of HrpS in *E. amylovora* will also affect *hrpL* expression.

In addition to the $AAA^+$ domain, bEBPs also have the N-terminal regulatory domain and the C-terminal DNA binding domain. The regulatory domain is responsible for controlling the $AAA^+$ domain activity in response to environmental signals (Schumacher et al., 2006). To perceive and respond to specific conditions, various signal transduction intermediates, including phosphoryl group, ligands and antiactivator proteins, are shown to be targeted to the regulatory domain (Bush and Dixon, 2012). bEBPs lacking this domain, such as HrpS (Figure 3.1), regulate their activity mainly through protein-protein interaction. In *P. syringae,* HrpS forms heterohexamer complex with HrpR to activate *hrpL* transcription, but HrpV can inhibit the oligomerization via direct interaction with HrpS (Hutcheson et al., 2001; Jovanovic et al., 2011). On the other hand, the DNA binding domain of bEBPs recognizes specific upstream activator

sequence (UAS) near the $\sigma^{54}$-dependent promoter by a helix-turn-helix (HTH) motif (Studholme and Dixon, 2003). All UASs are shown to have dyad symmetry sequence as inactive state of bEBPs binds to DNA in a dimeric form (Bush and Dixon, 2012). DNA-bound bEBPs can promote oligomerization and also contribute to maintain their hexameric or heptameric arrangements (Austin and Dixon, 1992; Pérez-Martín and de Lorenzo, 1996; De Carlo et al., 2006). Since UAS is commonly located at 80 to 150 bp upstream of transcription start site, interactions between the $\sigma^{54}$-RNAP holoenzyme and bEBPs are often achieved by the integration host factor (IHF)-induced DNA bending (Claverie-Martin and Magasanik, 1992; Huo et al., 2006). However, the binding site for HrpS is still unknown.

The goals of this study were to identify the HrpS binding site of *E. amylovora* on the *hrpL* promoter region and to examine the role of the conserved tyrosine residue of the GAYTGA motif in HrpS.

### 3.3 Materials and methods

#### 3.3.1 Bacterial strains and growth conditions

The bacterial strains used in this study are listed in Table 2.1. Luria–Bertani (LB) medium was used for the routine culture of *E. amylovora* and *E. coli* strains. Bacteria were also grown in M9 minimal medium (M9MM) [12.8 g $Na_2HPO_4.7H_2O$, 3.0 g $KH_2PO_4$, 0.5 g NaCl, 1 g $NH_4Cl$, 0.24 g $MgSO_4$ and 0.011 g $CaCl_2$] supplemented with 0.4 % glucose or *hrp*-inducing minimal medium (HMM) [1 g $(NH_4)_2SO_4$, 0.246 g $MgCl_2.6H_2O$, 0.099 g NaCl, 8.708 g $K_2HPO_4$, 6.804 g $KH_2PO_4$] containing 10 mM galactose as indicated in each experiment. When required,

antibiotics were added to the medium at the following concentrations: 10 μg/ml chloramphenicol (Cm), 100 μg/ml ampicillin (Ap) and 20 μg/ml kanamycin (Km).

### 3.3.2 DNA manipulation and the construction of plasmids

Plasmid DNA purification, PCR amplification of genes, isolation of fragments from agarose gels, cloning, restriction enzyme digestion and T4 DNA ligation were performed using standard molecular procedures (Sambrook and Russel, 2001). DNA sequencing was performed at the Keck Center for Functional and Comparative Genomics at the University of Illinois at Urbana-Champaign.

### 3.3.3 GFP reporter assays by flow cytometry

Overnight cultures of *E. amylovora* Ea273 strains carrying different *gfp*-promoter fusion plasmids were harvested and washed with PBS. The bacterial suspensions were re-inoculated into HMM and incubated at 18 ℃ for 18h. GFP intensities were measured by the BD FACSCanto flow cytometer (BD Bioscience, San Jose, CA, USA) and analyzed by flow cytometry software FCS Express V3 (De Novo Sofware, Los Angeles, CA, USA). The experiments were repeated at least twice.

### 3.3.4 Virulence assay on immature pear fruits

Overnight cultures of *E. amylovora* WT, mutants and complementation strains were harvested by centrifugation at 4000 rpm for 10 min, resuspended in PBS to $OD_{600}$ = 0.1 and then diluted 100-fold ($OD_{600}$ = 0.001). Immature Bartlett pears (*Pyrus communis* L. cv. Bartlett) were surface-sterilized with 10% bleach for 10 min and rinsed with sterile distilled water. After dried,

pears were pricked with a sterile needle, inoculated with 2 µl of cell suspensions for each strain and incubated in a humidified chamber at 28 ℃. Symptoms were recorded at 4 and 8 days post-inoculation. For each strain tested, pears were assayed in triplicate, and the experiments were repeated at least twice.

### 3.3.5 Virulence assay on apple shoots

Overnight cultures of *E. amylovora* WT, mutants and complementation strains were harvested by centrifugation at 4000 rpm for 10 min, resuspended in PBS to $OD_{600}$ = 0.1. About 22 to 25 cm length of young 'Gala' apple shoots were pricked with a sterile needle, inoculated with 5 µl of cell suspensions for each strain. Plants were kept at 25 ℃ and 16 h light photoperiod in a greenhouse. The length of the necrotic symptom from the inoculation site was measured at 8 days post-inoculation, and the average value was considered as the disease severity. For each strain tested, 6 or 7 shoots were assayed, and the experiments were repeated at least twice.

### 3.3.6 Hypersensitive response (HR) assay on tobacco

Bacterial strains grown overnight in LB medium with appropriate antibiotics were harvested by centrifugation at 4000 rpm for 10 min and resuspended in PBS to $OD_{600}$ = 0.1. Eight-week old tobacco (*Nicotiana tobacum*) leaves were infiltrated with bacterial suspension using needleless syringe and kept in a humidified chamber at 28 ℃. HR symptoms were recorded at 24 h post-infiltration. The experiments were repeated at least twice.

### 3.3.7 RNA isolation

To isolate RNA for *in vitro* T3SS gene expression, bacterial cultures grown in LB medium with appropriate antibiotics were harvested by centrifugation at 4000 rpm for 10 min and washed twice with PBS. The bacterial cells were resuspended in HMM to $OD_{600}$ = 0.2 and incubated at 18 ℃ with 250 rpm agitation. After 6 h in HMM, 4 ml of RNA protect reagent (Qiagen, Hilden, Germany) was added to 2 ml of bacterial cell cultures to avoid RNA degradation. For *in vivo* T3SS gene expression, overnight bacterial cultures were harvested by centrifugation at 4000 rpm for 10 min and resuspended in PBS $OD_{600}$ = 0.2 to 0.3. Immature Bartlett pear fruits (*Pyrus communis* L. cv. Bartlett) were surface-sterilized with 10% bleach for 10 min and rinsed with sterile distilled water. After dried, pears were cut in half and inoculated with bacterial suspension. The bacterial cells were incubated in a moist chamber at 28 ℃ for 6 h and collected by washing pear surfaces with a solution containing 2 ml RNA protect reagent (Qiagen) and 1 ml water. Cells collected for both *in vivo* and *in vitro* T3SS gene expression were then harvested by centrifugation at 4000 rpm for 10 min. RNA was extracted using the RNeasy Mini kit (Qiagen), following which the eluted total RNA was DNase-treated using Turbo DNA-free™ (Ambion, Austin, TX, USA) according to the manufacturer's instructions, respectively. Quality and quantity of the RNA was assessed using a Nano-Drop ND-100 spectrophotometer (Nano-Drop Technologies; Wilmington, DE, USA).

### 3.3.8 Quantitative real-time PCR (qRT-PCR)

Reverse transcription for cDNA synthesis was performed using Superscript® VILO™ cDNA synthesis kit (Invitrogen, Carlsbad, CA, USA) on 1 μg of total RNA according to the manufacturer's instruction. The 100 ng of reverse transcription product was used for qRT-PCR

analysis in a total volume of 25 µl containing 12.5 µl Power SYBR® Green PCR master mix (Applied Biosystems, Foster City, CA, USA), primers of selected genes (500nM) and water. The primers for qRT-PCR were designated using Primer3 software and listed in Table 3.2. Negative controls were also set up by substituting cDNA with water. The qRT-PCR amplification was carried out in duplicate in MicroAmp® Fast Optical 96-Well plates with Optical Adhesive Films on StepOnePlus Real Time PCR System (Applied Biosystems). The qRT-PCR program was 50 ℃ for 2 min, 95 ℃ for 10 min, followed by 40 cycles of 95 ℃ for 15 s and 60 ℃ for 1 min, and a final dissociation curve analysis step from 65 to 95 ℃. Gene expression levels were analyzed using the relative quantification (ΔΔCt) method, and a 16S rDNA (*rrsA*) gene was used as an endogenous control to normalize gene expression data. A *P* value was calculated based on a moderated *t*-test to measure the significance associated with each relative quantification value. Variations were considered to be statistically significant when $P < 0.05$. The experiments were repeated at least twice using three different biological replicates.

### 3.3.9 Site-directed mutagenesis

Site-directed mutagenesis of the HrpS binding site on the upstream sequence of the *hrpL* promoter and the GAYTGA motif of HrpS was carried out using the QuickChange XL site-directed mutagenesis kit (Stratagene, La Jolla, CA, USA). Briefly, the mutagenic primers containing the desired mutation in the middle were prepared between 25 and 45 bp in length with a melting temperature over 78 ℃. Complementation constructs to be mutated were PCR amplified with 10X reaction buffer, forward and reverse primers, dNPT mix, Quick solution, *PfuTurbo* DNA polymerase, and dd$H_2O$. PCR amplification was carried out at 95 ℃ for 1 min, followed by 18 cycles of 95 ℃ for 50 s, 60 ℃ for 50 s, and 68 ℃ for proper time dependent on

the plasmid length, and a final extension step at 68 ℃ for 7 min. To remove nonmutated, parental DNA template, the reaction was treated with the *Dpn* I restriction enzyme at 37 ℃ for 1 h. The *Dpn* I-treated DNA was transformed into XL10-Gold ultracompetent cells by heat pulse in a 42 ℃ water bath for 30 s. Transformants were selected on LB plates supplemented with appropriate antibiotics. Finally, mutations were confirmed by sequencing, and the mutated complementation constructs were transformed into appropriate mutant strains.

### 3.3.10 Cloning for HrpS protein overexpression

Since overexpression of *E. amylovora* full-length HrpS protein led to formation of insoluble aggregates (inclusion bodies) in *E. coli* BL21 (DE3) strain, truncated $HrpS_{250-325}$ proteins containing only the DNA binding domain was expressed and purified. The corresponding part of *hrpS* gene (748 to 975 nt) was amplified using the primer pairs containing *NdeI* and *XhoI* restriction site (Table 3.2) and cloned into pET28a expression vector (Novagen, Madison, WI, USA). The final plasmid was designated $pHrpS_{250-325}$-His and introduced into the *E. coli* BL21 (DE3) strain which carries the gene for T7 RNA polymerase under control of the IPTG (isopropyl-PD-thiogalactopyranoside)-inducible lacUV-5 promoter. To confirm overexpression of the truncated protein, 1 ml overnight culture was inoculated into 9 ml of fresh LB broth containing 50 μg/ml Km and grown at 37 ℃ for 2 h. The culture was then divided into two aliquots, one of which was induced by IPTG (0.1 mM), and incubated for growth at 37 ℃. After approximately 6 h, bacterial cells from 500 μl of each culture were harvested by centrifugation at 12,000 rpm for 1 min. Cell pellet was then resuspended in the Laemmli buffer containing β-mercaptoethanol, boiled for 5 min and analyzed by sodium dodecyl sulfate-polyacrylamide gel electrophoresis (SDS-PAGE) using 0.75 mm, 10% resolving gel [375 mM

TRIS pH 8.8, 10% (w/v) acrylamide, 0.1% (w/v) SDS, 0.1% (w/v) APS, 1 µl/ml TEMED] and 5% stacking gel [375 mM TRIS pH 8.8, 5% (w/v) acrylamide, 0.1% (w/v) SDS, 0.1% (w/v) APS, 1 µl/ml TEMED]. To visualize proteins separated by SDS-PAGE, the gel was stained with Coomassie blue [25% (w/v) Coomassie Brilliant Blue R, 50% (v/v) methanol, 7.5% (v/v) acetic acid and ddH2O] for 2 h and then destained overnight with destaining solution [60% (v/v) methanol, 20% (v/v) acetic acid and ddH2O].

### 3.3.11 Purification of truncated HrpS protein

Five milliliters of *E. coli* BL21 (DE3) strain carrying protein overexpression vector was grown overnight and inoculated into 500 ml of fresh LB media containing 50 µg/ml Km. After 2-3 h growth at 18 ℃, protein overexpression was induced by IPTG (0.1 mM) and incubated for growth at 18 ℃ with 250 rpm agitation overnight. Cells were harvested by centrifugation at 5000 rpm for 10 min, washed once with cell wash buffer (50mM MOPS, 150mM NaCl), and resuspended [1:10 ratio (w/v)] in cell wash buffer. The cell suspensions were frozen at -80 ℃ until further use. Thawed cell suspensions were treated with 250 µg/ml lysozyme (Promega) for 30 min and cooled to 4 ℃ on ice for at least 30 min. Cells were further treated with Halt™ protease inhibitor cocktail EDTA-free (1X, Thermo Scientific, Rockford, IL, USA), NaCl (300 mM) and imidazole (60 mM), followed by sonication in an ice-water bath. The cell lysates were centrifuged at 35,000 g for 20 min to remove cell debris, and Ni-NTA agarose resin (Qiagen) was added to the supernatants. Columns were washed before use with equilibration/wash buffer (50 mM MOPS, 300 mM NaCl, 60 mM imidazole). Proteins in the supernatant were allowed to bind to the resin at 4 ℃ for 10 min with gentle rocking, and centrifuged at 1000 rpm for 2 min to remove cell debris. After one more wash with equilibration/wash buffer, the proteins were eluted

with elution buffer (50 mM MOPS, 300 mM NaCl, 500 mM imidazole) and dialyzed overnight against buffer containing 20 mM MOPS and 1 mM DTT. Protein concentration was measured using Invitrogen Qubit protein assays.

### 3.3.12 Electrophoretic mobility shift assay (EMSA)

Complementary oligonucleotides comprising the HrpS-binding site from the *hrpL* promoter region of *E. amylovora* (Table 3.2) were 3' biotinylated using the biotin 3' end DNA labeling kit (Pierce, Rockford, IL, USA). Briefly, 50 µl reaction with 100 nM oligonucleotides were incubated with 1X TdT reaction buffer, 0.5 µM Biotin-11-UTP and 0.2 U/µl of TdT at 37 ℃ for 30 min. Reaction mixtures were then mixed with 2.5 µl of 0.2 M EDTA and 50 µl of 24:1 (v/v) chloroform:isoamyl alcohol, and the acqueous phases were stored at -20 ℃ for further use. For annealing, equal amounts of the end-labeled, complementary oligonucleotides were mixed together, denatured at 100 ℃ for 1 min and incubated at room temperature for 1 h before use. The lightshift® chemiluminescent EMSA kit (Pierce) was used for protein-DNA binding assays. Increasing amount of $HrpS_{250\text{-}325}$ (0 to 2.05 µM) was added in reaction volumes of 10 µl containing 20 fmol of labeled oligonucleotides, 1X binding buffer, 50 ng/µl Poly(dI·dC), 0.5mM $MgCl_2$, 0.1% Nonidet P-40, 0.05 mg/ml BSA, and 5% glycerol. Reaction mixtures were incubated at room temperature for 20 min, mixed with 2.5 µl of 5X loading buffer and resolved into a 6% native polyacrylamide gel in 0.5X TBE buffer (44.5 mM Tris-base, 44.5 mM Boric acid and 1 mM EDTA). Resolved binding reactions were transferred to a positively charged nylon membrane and cross-linked using UV-light cross-linking instrument at 120 $mJ/cm^2$ for 1 min. The chemiluminescent signals were developed according to the manufacturer's instructions

and visualized using ImageQuant LAS 4010 CCD camera (GE Healthcare, Piscataway, NJ, USA).

## 3.4 Results

### 3.4.1 Upstream sequence from -153 to -104 nt of the *hrpL* promoter contains potential HrpS binding site

In $\sigma^{54}$-dependent transcription, most bEBPs have been shown to bind at UAS located 80 to 150 bp upstream of the transcription start site (Bush and Dixon, 2012). Based on these previous observations, nine different constructs containing different length of the *hrpL* promoter (within -398 to +86 nt) fused to a promoter-less *gfp* were made, and promoter activity was determined by flow cytometry (Figure 3.2A). Constructs containing the *hrpL* promoter up to position -128 nt in Ea273 (pZW2-1 to 2-4) exhibited basal levels of GFP intensity as compared to vector control, whereas constructs containing the *hrpL* promoter region within position -153 nt in Ea273 (pZW2-5 to 2-9) led to a significant increase of GFP intensity, suggesting that the *hrpL* promoter region spanning -153 to -104 nt is required for HrpS binding and activation of *hrpL* expression. In addition, there was also about 10% increase in GFP intensity between Ea273 (pZW2-6) and Ea273 (pZW2-7), suggesting presence of an unknown factor with a potential role in activating *hrpL* expression at the region between -215 and -153 nt of the *hrpL* promoter.

### 3.4.2 The dyad symmetry sequence between -141 and -121 is required for virulence

To verify the results obtained by reporter gene-based promoter activity and further delineation of the potential binding site, various 5'-deletion constructs of the *hrpL* gene were generated (Figure 3.3) and transformed into Ea1189 *hrpL* mutant. Furthermore, bioinformatic

analysis between -153 to -104 nt of the *hrpL* promoter, a 14 bp dyad symmetry sequence (AT-N-TGCAA-$N_4$-TGCAA-N-AT) spanning -141 to -122 nt of the *hrpL* promoter was identified. Since most bEBPs bind to the dyad symmetry sequence, three additional *hrpL* constructs were generated, which contain the *hrpL* promoter sequence from -121 nt (pHrpL-4), -131 nt (pHrpL-6) and -141 nt (pHrpL-7). These constructs contain no, half and full-dyad symmetry sequence, respectively. The *hrpL* mutant complemented with different constructs was first tested for virulence on immature pear fruits (Figure 3.4). Pear fruits infected by *hrpL* (pHrpL) showed water soaking symptoms at 2 days, necrotic lesions with visible bacterial ooze at 4 days, and black lesions covering almost the entire surface of pear fruits at 8 days post inoculation (DPI). Similar disease severity was observed for *hrpL* mutant complemented with constructs with half- or full-dyad symmetry sequence (pHrpL-5 to 11), whereas no disease was observed for *hrpL* mutant complemented with *hrpL* constructs without the dyad symmetry sequence (pHrpL-1 to 3). Interestingly, construct pHrpL-4, which does not contain the dyad symmetry sequence, could still partially complement *hrpL* mutant and result in reduced disease.

Virulence assays were also carried out on apple shoots for the *hrpL* mutant complemented with different constructs (Figure 3.5, Table 3.3). Visible necrosis around the inoculated site was observed for *hrpL* mutant complemented with full length of promoter construct (pHrpL) at 3 DPI, and its length of necrotic lesion reached 18.25 ± 2.40 cm at 7 DPI. As expected, no disease symptoms were observed for *hrpL* (pHrpL-1 to 3), whereas similar disease severity was observed for *hrpL* (pHrpL-8 to 11) as compared to *hrpL* (pHrpL). The length of necrotic lesions were slightly reduced for *hrpL* (pHrpL-7) (14.38 ± 1.60 cm) and about half for *hrpL* (pHrpL-5, 6) (10.50 ± 0.87 cm, 9.88 ± 2.06 cm, respectively) as compared to *hrpL*

(pHrpL). Similar to results with immature pear fruit, construct pHrpL-4 could partially rescue the *hrpL* mutant, but the length of necrotic lesion was greatly reduced (2.04 ± 0.50 cm) at 7 DPI.

Furthermore, the *hrpL* mutant complemented with selected six constructs (pHrpL-3 to 8) was also tested for their ability to elicit HR on tobacco leaves (Figure 3.6). Consistent with disease causing ability, *hrpL* mutant complemented with pHrpL and pHrpL-7 and 8 induced strong HR, while *hrpL* complemented with pHrpL-3 did not result in any HR at 24 h post infiltration. A gradual weak HR was observed for *hrpL* mutant complemented with pHrpL-4, 5 and 6 construct, respectively.

Together, these results indicate that the complete dyad symmetry sequence of the *hrpL* promoter is critical for full virulence of *E. amylovora*. However, it seems that construct containing half of the dyad symmetry sequence is sufficient to complement *hrpL* mutant and cause disease. In addition, our results suggest that *hrpL* promoter region spanning -121 to -104 nt may also influence either HrpS binding or an unknown factor involved in the activation of *hrpL* transcription. This region contains an 10-bp mirror sequence (TTTGG-N-GGTTT) (Figure 3.8A).

### 3.4.3 The dyad symmetry sequence is required for *hrpL* and other T3SS gene expression

To further evaluate the role of the dyad symmetry sequence in the *hrpL* promoter for T3SS gene expression, the relative expression of *hrpL* and *hrpA* genes was determined by qRT-PCR. Consistent with the above virulence assays, expression of *hrpL* gene in *hrpL* mutant complemented with pHrpL-7 and 8 was similar to or higher than that of *hrpL* complemented with pHrpL in both *in vitro* and *in vivo* conditions (Figure 3.7A, B). Whereas expression of *hrpL*

gene was about 5- to 10-fold and 25- to 50-fold lower in *hrpL* (pHrpL-6) and *hrpL* (pHrpL-4) strains, respectively. The *hrpL* expression was barely detected in *hrpL* (pHrpL-3) and *hrpL* (pWSK29). The overall pattern of *hrpA* expression was similar to that of *hrpL* expression, except that expression of *hrpA* was about 2.5- to 5-fold and 10- to 20-fold lower in *hrpL* (pHrpL-4) and *hrpL* (pHrpL-6), respectively. These results indicate that the dyad symmetry sequence of the *hrpL* promoter is essential for full activation of *hrpL* and other T3SS gene expression. Since expression of *hrpL* and *hrpA* genes was not completely off in *hrpL* (pHrpL-4), further suggesting that the 10-bp mirror sequence may also play a role in *hrpL* activation.

### 3.4.4 Nucleotide substitution of the dyad symmetry sequence further affects *hrpL* gene expression and virulence

To further analyze the role of the dyad symmetry sequence and the mirror sequence of the *hrpL* promoter in activating *hrpL*, site-directed mutagenesis was used to generate nucleotide substitution mutant constructs. The first construct (pHrpL-Mut1) contained one base substitution at each side of the dyad symmetry sequence of the *hrpL* promoter in pHrpL (Figure 3.8B). Disease symptoms on immature pear fruits by *hrpL* (pHrpL-Mut1) were comparable to that caused by *hrpL* (pHrpL) (Figure 3.9). However, expression of *hrpL* and *hrpA* genes was about 3 to 5-fold lower (Figure 3.10A, 3.11A).

The other three mutant constructs (pHrpL6-Mut2, 3, 4) were derived from pHrpL-6 and contained three, two and one base substitution(s) at the half-dyad symmetry sequence, respectively (Figure 3.8B). Significantly reduced necrotic lesions on immature pear fruits was observed for *hrpL* complemented with all three mutant constructs (Figure 3.9). Expression of

*hrpL* and *hrpA* in *hrpL* (pHrpL6-Mut2) was about 5- and 10-fold lower compared to *hrpL* (pHrpL-6) strain *in vitro* and *in vivo*, respectively (Figure 3.10B, 3.11B). Whereas expression of *hrpL* and *hrpA* in *hrpL* (pHrpL6-Mut3) and *hrpL* (pHrpL6-Mut4) strains also exhibited 2.5- to 5-fold and 1.5- to 2.5-fold decrease, respectively. These results suggest that these nucleotides are all important for *hrpL* activation.

On the other hand, construct pHrpL4-Mut5 was derived from pHrpL-4 with base substitutions at the mirror sequence. Bacterial virulence and T3SS gene expression of *hrpL* complemented with this construct appeared to be not affected by the mutations as compared to *hrpL* (pHrpL-4) strain (Figure 3.9, 3.10C, 3.11C). These results suggest that the mirror sequence may not be required for *hrpL* activation.

### 3.4.5 HrpS binds to the dyad symmetry sequence in the *hrpL* promoter

In order to determine that HrpS protein indeed binds to the dyad symmetry sequence, full-length HrpS protein was overexpressed in *E.* coli. However, we found that the full length of *E. amylovora* HrpS protein formed inclusion bodies upon overexpression in *E. coli* BL21 (DE3) strain. The pellet containing inclusion bodies were solubilized by treating with high concentration of urea (8M); however our attempts to refold the denatured protein by stepwise dialysis with less concentration of urea were unsuccessful. Therefore, a truncated HrpS protein containing only the DNA binding domain ($HrpS_{250\text{-}325}$) was overexpressed and purified for our subsequent EMSA assay.

To assess specific binding to truncated $HrpS_{250-325}$ protein to the dyad symmetry sequence, two different 26-bp probes containing the original dyad symmetry sequence and the mutated version of the dyad symmetry sequence were subject to EMSA (Figure 3.12A). EMSA results showed that $HrpS_{250-325}$ bound to the original sequence in a concentration-dependent manner, while no shift was observed for the mutated sequence (Figure 3.12B), suggesting that the helix-turn-helix DNA binding motif of HrpS appears to have specific binding affinity for the dyad symmetry sequence of the *hrpL* promoter.

### 3.4.6 Y100F substitution in the GAYTGA motif did not affect the function of HrpS

Previous reports in *P. syringae* pv. *tomato* DC3000 showed that a single amino acid substitution from tyrosine to phenylalanine within the conserved GAYTGA motif of HrpS led to 50% increase in the *hrpL* promoter activity as compared to WT (Jovanovic et al., 2011). To investigate whether similar substitution within the GAYTGA motif of *E. amylovora* HrpS will result in similar change in *hrpL* transcription and virulence, three mutant variants (Y100F, Y100A and T101A) were constructed and introduced into Ea1189 *hrpS* mutant. Virulence assay on immature pear fruits indicated that *hrpS* (pHrpS (Y100F)) and *hrpS* (pHrpS) strains were equally virulent (Figure 3.14), whereas no disease symptoms were observed for *hrpS* (pHrpS (Y100A)) and *hrpS* (pHrpS (T101A)). Consistently, *hrpS* (pHrpS (Y100F)) strain induced strong HR on tobacco leaves as *hrpS* (pHrpS) strain, while *hrpS* (pHrpS (Y100A)) and *hrpS* (pHrpS (T101A)) strains could not induce any HR (Figure 3.15). Furthermore, although expression of *hrpS* gene was similar in *hrpS* (pHrpS (Y100F), (Y100A), (T101A)) and *hrpS* (pHrpS) strains, expression of *hrpL* and *hrpA* was abolished in *hrpS* (pHrpS (Y100A), (T101A)) strains, but not

affected in *hrpS* (pHrpS (Y100F)) strain. These results suggest that Y100F substitution in GAYTGA motif did not affect the function of HrpS in *E. amylovora.*

### 3.5 Discussion

In many plant pathogenic bacteria, T3SS plays a central role in colonization and infection of their host plants. T3SS-secreted effector proteins have been found to impede host immunity, thus enabling pathogens to overcome host defense barriers and establish successful infection (Alfano and Collmer, 2004). Therefore, comprehensively understanding the function and regulation of T3SS is key to the study of plant-bacterium interactions (Büttner and Bonas, 2006). Based on the current model of T3SS regulation, HrpS acts as a positive regulator of $\sigma^{54}$-dependent *hrpL* transcription in *Pseudomonas* sp., *Erwinia* sp. and the *Pectobacterium* sp. (Grimm et al., 1995; Wei et al., 2000; Chatterjee et al., 2002; Yap et al., 2005; Ancona et al., 2014). In this study, we further characterized HrpS of *E. amylovora* in regulating T3SS gene expression, especially its transcription activation activity of *hrpL* gene.

We, for the first time, identified and determined the binding site for HrpS in plant pathogenic bacteria. A 14-bp sequence (AT-N-TGCAA-$N_4$-TTGCA-N-AT) exhibits nearly perfect dyad symmetry, which is the characteristic binding sequence for many bEBPs. To further confirm our results, the *hrpL* promoter sequences from related plant pathogenic enterobacteria were compared. We found that *Pectobacterium astrosepticum* also contains an 14-bp dyad symmetry sequence (N-ATTGCAA-$N_4$-TTGCAAT-N) at -139 to 120 nt region, *Dickeya dadantii* contains a 10-bp dyad symmetry sequence ($N_3$-TGCAA-$N_4$-TTGCA-$N_3$) at -141 to -122 nt region, and *Pantoea stewartii* contains an 10-bp dyad symmetry sequence ($N_3$-TGCAA-$N_4$-

TTGCA-$N_3$) at -136 to -117 nt region (Figure 3.13). Interestingly, all four contain common dyad symmetry sequence (TGCAA-$N_4$-TTGCA), suggesting that this region probably is the most important part for HrpS binding. Consistently, mutations at the center region of the dyad symmetry sequence (*hrpL* (pHrpL6-Mut2)) had much stronger effect on *hrpL* transcription than mutations at the border region of the sequence (*hrpL* (pHrpL6-Mut3)). However, this dyad symmetry sequence is not present in the *hrpL* promoter of *P. syringae,* indicating that the binding site of HrpS is different in *P. syringae*. Unlike *Erwinia, Dickeya*, *Pantoea* and *Pectobacterium,* in which HrpS forms homohexameric complex to activate $\sigma^{54}$-dependent transcription, HrpS of *P. syringae* is reported to form a heterohexamer via interaction with HrpR, another bEBP (Hutcheson et al., 2001). Although *hrpR* and *hrpS* genes of *P. syringae* are believed to arise from gene duplication events, they share about 60% sequence identity and 75% sequence similarity to each other (Jovanovic et al., 2011), presumably leading to having a non-dyad symmetry binding sequence on the *hrpL* promoter. More research is needed to determine the binding site for HrpR/HrpS in *P. syringae*.

Next to the dyad symmetry sequence, we also found an unusual mirror sequence (TTTGG-N-GGTTT) at -121 to -111 nt region of the *hrpL* promoter. Our results showed that the activation of *hrpL* transcription and a functional T3SS can still be detected in *hrpL* (pHrpL-4), in which the construct contains the mirror sequence, but not the dyad symmetry sequence, while activation of *hrpL* transcription was completely abolished in the *hrpL* (pHrpL-3), in which the construct does not contain both the dyad symmetry and the mirror sequences. However, mutation in right end of the mirror sequence did not affect T3SS gene expression. There are at least two possibilities for the role of the mirror sequence in the regulation of *hrpL* transcription. One is that

the mirror sequence may contribute to the regulation via formation of intramolecular triplex structure of DNA. Under specific conditions, such as the supercoiled DNAs and in the presence of multivalent cations, the homopurine-homopyrimidine mirror sequence in the DNA duplex may allow one strand to fold back onto the duplex, forming the DNA triplexes called H-DNA (Mirkin et al.; Htun and Dahlberg, 1988; Kohwi and Kohwi-Shigematsu, 1988; Floris et al., 1999). Triplex configuration of DNA is often found in sites upstream the promoter and involved in several DNA-dependent processes, including transcriptional regulation (Buske et al., 2011). However, the *hrpL* promoter of *E. amylovora* contains relatively short mirror sequence (11 bp), therefore it is less likely to form triplexes (Collier and Wells, 1990). The other possibility is that the mirror sequence may be a site for binding of an unknown regulator. A comparison between *hrpL* promoter sequences of *E. amylovora* and other plant enterobacteria showed that the mirror sequence appears to be unique in *E. amylovora*. In *Pectobacterium*, *Dickeya* and *Pantoea*, *hrpS* gene expression is controlled by HrpX/HrpY two component system, whereas in *E. amylovora*, expression of *hrpS* is not controlled by HrpX/HrpY (Zhao et al., 2009b). Further analysis of the mirror sequence may provide clues as what the role of this sequence will be.

The conserved GAFTGA motif is a bEBP-specific structural feature within $AAA^+$ domain. The importance of the GAFTGA motif for the activation of $\sigma^{54}$-dependent transcription has been demonstrated through amino acid substitution analyses on several different bEBPs (Bush and Dixon, 2012). All six residues of the GAFTGA motif are essential for full bEBP activity, and mutation in phenylalanine residue has been shown to adversely affect ATPase activity, $\sigma^{54}$ contact and oligomerization of bEBPs (Wang et al., 1997; Wikström et al., 2001; Bordes et al., 2003; Zhang et al., 2009). However, in about 7% of the annotated bEBPs,

including HrpS, tyrosine is shown to replace with phenylalanine residue within the GAFTGA motif (Zhang et al., 2009). Although both tyrosine and phenylalanine share similar aromatic ring structure, substitution of phenylalanine with tyrosine within GAFTGA motif of NifA and PspF results in a significant decrease in bEBP activity in transcriptional activation (González et al., 1998; Zhang et al., 2009). On the other hand, substitution of tyrosine with phenylalanine in GAYTGA motif of HrpS in *P. syringae* pv. *tomato* DC3000 instead increased its activity by 1.5-fold (Jovanovic et al., 2011). In this study, we showed that substitution of tyrosine with phenylalanine within the GAYTGA motif of HrpS has no effect on its function in *E. amylovora.* We suspect this variation might have occurred due to either random natural selection or other regulatory purposes.

Extrapolating from the function of bEBPs, HrpS plays a central role in linking the detection of environmental cues and the activation of T3SS. A comprehensive characterization of HrpS might be key for understanding how *E. amylovora* activates $\sigma^{54}$-dependent *hrpL* transcription during pathogenesis. Our future work will focus on the molecular mechanisms underlying the regulation of *hrpS* gene expression as well as HrpS protein stability. It has been reported that Lon protease of *P. syringae* down-regulates T3SS gene expression by degrading HrpR protein (Lan et al., 2007; Ortiz-Martín et al., 2010). In addition, up-regulation of *hrpS* expression was observed in the *slyA* mutant of *D. dadantii* (Zou et al., 2012), while a down-regulation of *hrpS* expression was observed in the *hrpL*, *ihfA* and *ihfB* mutants of *E. amylovora* (Ancona et al., 2014; this study). Bioinformatics and transcriptomic profiling will be our next step in fully characterizing HrpS function.

## 3.6 Tables

### Table 3.1 Bacterial strains and plasmids used in this study

| Strains, plasmids | Relevant characters* | Reference source |
|---|---|---|
| **Strains** | | |
| *Erwinia amylovora* | | |
| Ea1189 | Wild-type, isolated from apple | Burse et al., (2004) |
| Ea273 | Wild-type, isolated from apple | Wang et al., (2010) |
| Δ*hrpL* | *hrpL::Km*; $Km^R$-insertional mutant of *hrpL* of Ea 1189, $Km^R$ | Ancona et al., (2014) |
| Δ*hrpS* | *hrpS::Km*; $Km^R$-insertional mutant of *hrpS* of Ea 1189, $Km^R$ | Ancona et al., (2014) |
| *Escherichia coli* | | |
| DH10B | $F^-$ *mcr*A Δ(*mrr-hsd*RMS-*mcr*BC) Φ80/*ac*Z ΔM15 Δ*lac*X74 *rec*A1 *end*A1 *ara*Δ139 Δ(*ara, leu*)7697 *gal*U *gal*K λ-*rps*L ($Str^R$) *nup*G | Invitrogen, Carlsbad, CA, USA |
| XL10-Gold | $Tet^R$ Δ(*mcrA*)*183* Δ(*mcrCB-hsdSMR-mrr*)*173 endA1 supE44 thi-1 recA1 gyrA96 relA1 lac* Hte [F´ *proAB lacI*$^q$ZΔ*M15* Tn*10* ($Tet^R$) Amy $Cam^R$] | Applied Biosystems, Foster City, CA, USA |
| BL21 (DE3) | $F^-$ *ompT hsdS*$_B$ ($r_B^-$ $m_B^-$) *gal dcm* (DE3) | Novagen, San Diego, CA, USA |
| **Plasmids** | | |
| pFPV25 | $Ap^R$, GFP based promoter trap vector containing a promoter-less *gfpmut3a* gene | Valdivia and Falkow, (1997) |
| pWSK29 | $Ap^R$, cloning vector, low copy number | Wang and Kushner (1991) |
| pET28a(+) | $Km^R$, T7 expression vector carrying an N-terminal His-Tag/ thrombin/T7 Tag coniguration plus an optional C-terminal His-Tag sequence | Novagen, San Diego, CA, USA |
| pZW2 | 608 bp DNA fragment containing promoter sequence of *hrpL* gene (-398-+210) in pFPV25 | Wang et al., (2010) |
| pZW2-1 | 144 bp DNA fragment containing promoter sequence of *hrpL* gene (-58-+86) in pFPV25 | This study |
| pZW2-2 | 180 bp DNA fragment containing promoter sequence of *hrpL* gene (-94-+86) in pFPV25 | This study |
| pZW2-3 | 190 bp DNA fragment containing promoter sequence of *hrpL* gene (-104-+86) in pFPV25 | This study |
| pZW2-4 | 214 bp DNA fragment containing promoter sequence of *hrpL* gene (-128-+86) in pFPV25 | This study |
| pZW2-5 | 239 bp DNA fragment containing promoter sequence of *hrpL* gene (-153-+86) in pFPV25 | This study |
| pZW2-6 | 263 bp DNA fragment containing promoter sequence of *hrpL* gene (-177-+86) in pFPV25 | This study |
| pZW2-7 | 301 bp DNA fragment containing promoter sequence of *hrpL* gene (-215-+86) in pFPV25 | This study |
| pZW2-8 | 350 bp DNA fragment containing promoter sequence of *hrpL* gene (-264-+86) in pFPV25 | This study |
| pHrpL | 1.317 kb DNA fragment containing *hrpL* gene (-398-+919) in pWSK29 | Ancona et al., (2014) |
| pHrpL-1 | 977 bp DNA fragment containing *hrpL* gene (-58-+919) in pWSK29 | This study |
| pHrpL-2 | 1.013 kb DNA fragment containing *hrpL* gene (-94-+919) in pWSK29 | This study |

**Table 3.1 (Cont.)**

| | | |
|---|---|---|
| pHrpL-3 | 1.023 kb DNA fragment containing *hrpL* gene (-104-+919) in pWSK29 | This study |
| pHrpL-4 | 1.040 kb DNA fragment containing *hrpL* gene (-121-+919) in pWSK29 | This study |
| pHrpL-5 | 1.047 kb DNA fragment containing *hrpL* gene (-128-+919) in pWSK29 | This study |
| pHrpL-6 | 1.050 kb DNA fragment containing *hrpL* gene (-131-+919) in pWSK29 | This study |
| pHrpL-7 | 1.060 kb DNA fragment containing *hrpL* gene (-141-+919) in pWSK29 | This study |
| pHrpL-8 | 1.072 kb DNA fragment containing *hrpL* gene (-153-+919) in pWSK29 | This study |
| pHrpL-9 | 1.096 kb DNA fragment containing *hrpL* gene (-177-+919) in pWSK29 | This study |
| pHrpL-10 | 1.134 kb DNA fragment containing *hrpL* gene (-215-+919) in pWSK29 | This study |
| pHrpL-11 | 1.183 kb DNA fragment containing *hrpL* gene (-264-+919) in pWSK29 | This study |
| pHrpL-Mut1 | 1.317 kb DNA fragment containing *hrpL* gene (-398-+919) with site-directed mutations at position -135 (A→C) and -127 (G→A) in pWSK29 | This study |
| pHrpL6-Mut2 | 1.050 kb DNA fragment containing *hrpL* gene (-131-+919) with a site-directed mutation at position from -128 to -126 (TGC→CAT) in pWSK29 | This study |
| pHrpL6-Mut3 | 1.050 kb DNA fragment containing *hrpL* gene (-131-+919) with a site-directed mutation at position from -124 to -122 (AAT→CCC) in pWSK29 | This study |
| pHrpL6-Mut4 | 1.050 kb DNA fragment containing *hrpL* gene (-131-+919) with a site-directed mutation at position -127 (G→A) in pWSK29 | This study |
| pHrpL4-Mut5 | 1.040 kb DNA fragment containing *hrpL* gene (-121-+919) with a site-directed mutation at position from -115 to -113 (GGT→AAC) in pWSK29 | This study |
| pHrpS | 1.81 kb DNA fragment containing *hrpS* gene in pWSK29 | Ancona et al., (2014) |
| pHrpS (Y100F) | 1.81 kb DNA fragment containing *hrpS* gene with a site-directed mutation (Tyrosine100Phenylalanine) in pWSK29 | This study |
| pHrpS (Y100A) | 1.81 kb DNA fragment containing *hrpS* gene with a site-directed mutation (Tyrosine100Alanine) in pWSK29 | This study |
| pHrpS (T101A) | 1.81 kb DNA fragment containing *hrpS* gene with a site-directed mutation (Threonine101Alanine) in pWSK29 | This study |
| $pHrpS_{250-325}$-His | 238-bp PCR fragment containing *hrpS* gene in pET28a | This study |

*$Km^R$, $Ap^R$, kanamycin and ampicilln resistance, respectively.

**Table 3.2 Primers used in this study**

| Primer | Sequences (5'- 3') |
|---|---|
| **Primers for cloning of 5' deletion constructs** | |
| hrpL-gfp1 | AGTTGAATTCGTTATCAGTGTGTTATGTGAT (EcoRI) |
| hrpL-gfp2 | AGTTGAATTCGCCAGAAATTGCGACAATTT (EcoRI) |
| hrpL-gfp3 | AGTTGAATTCGCAACAAGTTGCCAGAAATTGC (EcoRI) |
| hrpL-gfp4 | AGTTGAATTCTGCAAATTTTGGCGGTTTAT (EcoRI) |
| hrpL-gfp5 | AGTTGAATTCGTCGCCAGCGACATATGCAAC (EcoRI) |
| hrpL-gfp6 | AGTTGAATTCCTGGCCATGCCGCTGTTAAA (EcoRI) |
| hrpL-gfp7 | AGTTGAATTCCAGTTGTCATTGTGTGGTGCGA (EcoRI) |
| hrpL-gfp8 | AGTTGAATTCGGGTAAAACGGGAGCAATTT (EcoRI) |
| hrpL-gfp9 | TCGAGGATCCTCGTTGACCGATGTTGATTC (BamHI) |
| hrpL-121 | AGTTGAATTCTTTGGCGGTTTATCCTGGCA (EcoRI) |
| hrpL-131 | AGTTGAATTCTATTGCAAATTTTGGCGGTT (EcoRI) |
| hrpL-141 | AGTTGAATTCATATGCAACTTATTGCAAAT (EcoRI) |
| hrpL com R | AGTAGAGCTCCGACACGCACATGTTCAACA (SacI) |
| **Primers for RT-PCR** | |
| rpoD-rt1 | CCTCCAAGTCGACATCGTTT |
| rpoD-rt2 | TGTAGCGGTGAAATGCGTAG |
| hrpL-rt1 | TTAAGGCAATGCCAAACACC |
| hrpL-rt2 | GACGCGTGCATCATTTTATT |
| hrpA-rt1 | GAGTCCATTTTGCCATCCAG |
| hrpA-rt2 | TGGCAGGCAGTTCACTTACA |
| hrpS-rt1 | AATGCTACGCGTGCTGGAAA |
| hrpS-rt2 | AACAATGGCGTTTGCGTTGC |
| **Primers for site-directed mutagenesis** | |
| hrpL mut1 F | AGCGACATATGCCACTTATTACAAATTTTGGCGGTTTATCC |
| hrpL mut1 R | GGATAAACCGCCAAAATTTGTAATAAGTGGCATATGTCGCT |
| hrpL mut2 F | CGATAAGCTTGATATCGAATTCTATCATAAATTTTGGCGGTTTATCCTGGCAA |
| hrpL mut2 R | TTGCCAGGATAAACCGCCAAAATTTATGATAGAATTCGATATCAAGCTTATCG |
| hrpL mut3 F | AAGCTTGATATCGAATTCTATTACAAATTTTGGCGGTTTATCCTG |
| hrpL mut3 R | AAGCTTGATATCGAATTCTATTACAAATTTTGGCGGTTTATCCTG |
| hrpL mut4 F | CTTGATATCGAATTCTATTGCACCCTTTGGCGGTTTATCCTGGCAAC |
| hrpL mut4 R | GTTGCCAGGATAAACCGCCAAAGGGTGCAATAGAATTCGATATCAAG |
| hrpL mut5 F | GCTTGATATCGAATTCTTTGGCAACTTATCCTGGCAACAAGTTGCCA |
| hrpL mut5 R | TGGCAACTTGTTGCCAGGATAAGTTGCCAAAGAATTCGATATCAAGC |
| hrpS Y100F F | CATTAATAATGGTGCTTTTACCGGTGCCGGGCAGG |
| hrpS Y100F R | CCTGCCCGGCACCGGTAAAAGCACCATTATTAATG |
| hrpS Y100A F | CATTAATAATGGTGCTGCTACCGGTGCCGGGCAG |
| hrpS Y100A R | CTGCCCGGCACCGGTAGCAGCACCATTATTAATG |
| hrpS T101A F | AATAATGGTGCTTATGCCGGTGCCGGGCAGG |
| hrpS T101A R | CCTGCCCGGCACCGGCATAAGCACCATTATT |
| **Primers for cloning of protein expression constructs** | |
| hrpS 250-325 F | CAGCCATATGTTCGTACTGGGCCTACCGCC (NdeI) |
| hrpS 250-325 R | GATCCTCGAGCTACTGAGCAATAACCCGAC (XhoI) |
| **Primers for EMSA** | |
| HrpS-WT F | GACATATGCAACTTATTGCAAATTTT |
| HrpS-WT R | AAAATTTGCAATAAGTTGCATATGTC |
| HrpS-Mut F | GACATTTTTTACTTATCCCCCATTTT |
| HrpS-Mut R | AAAATGGGGGATAAGTAAAAAATGTC |

**Table 3.3 Disease severity of *E. amylovora* wild-type (WT) strain and 13 complementation strains of the *hrpL* mutant on apple shoots**

| Strain | Necrosis (cm)* |
|---|---|
| WT | 15.5 ± 1.47 |
| Δ*hrpL* (pHrpL) | 18.25 ± 2.40 |
| Δ*hrpL* (pHrpL-11) | 19.67 ± 3.79 |
| Δ*hrpL* (pHrpL-10) | 16.63 ± 2.32 |
| Δ*hrpL* (pHrpL-9) | 18.67 ± 1.75 |
| Δ*hrpL* (pHrpL-8) | 19.10 ± 1.29 |
| Δ*hrpL* (pHrpL-7) | 14.38 ± 1.60 |
| Δ*hrpL* (pHrpL-6) | 9.88 ± 2.06 |
| Δ*hrpL* (pHrpL-5) | 10.50 ± 0.87 |
| Δ*hrpL* (pHrpL-4) | 2.04 ± 0.50 |
| Δ*hrpL* (pHrpL-3) | 0 |
| Δ*hrpL* (pHrpL-2) | 0 |
| Δ*hrpL* (pHrpL-1) | 0 |
| Δ*hrpL* (pWSK29) | 0 |
| PBS | 0 |

*Mean of severity index from 6-7 inoculated shoots ± standard deviation seven days post inoculation

## 3.7 Figures

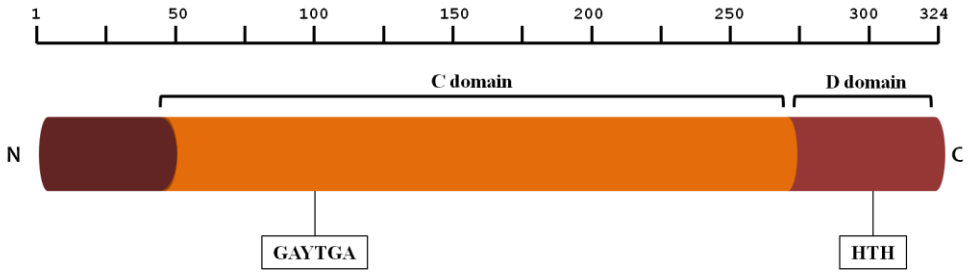


**Figure 3.1 Domain organization of HrpS protein of *E. amylovora*.** Bacterial enhancer binding protein (bEBP) HrpS consists of two domains (central (C) and DNA-binding (D) domain). The GAYTGA motif is located at position 98 to 103 within the C domain. The D domain contributes to binding to the upstream activator sequence (UAS) via an helix-turn-helix (HTH) motif located at position 274 to 312.

**A**


**B**

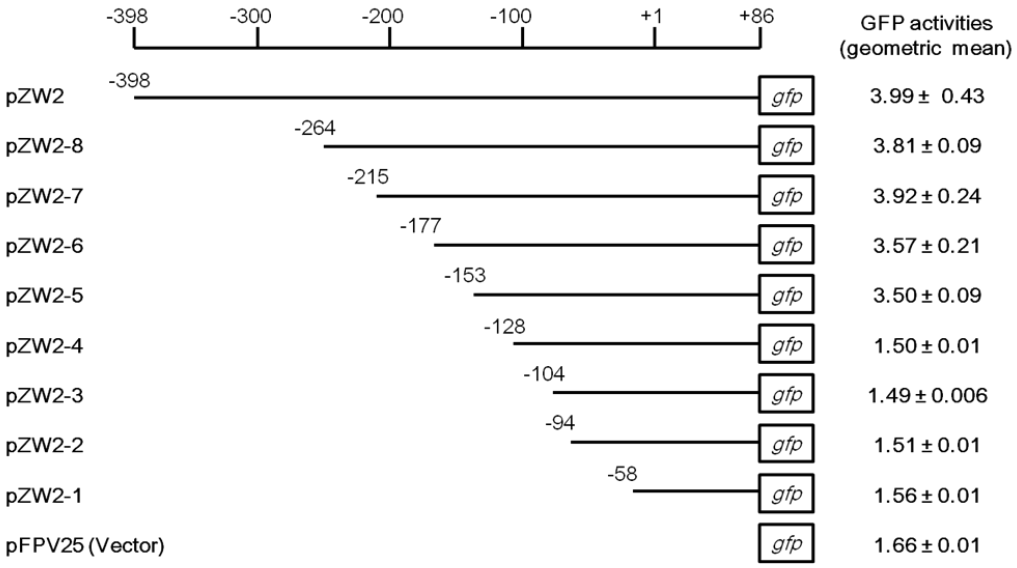


**Figure 3.2 Schematic diagram of *gfp* reporter gene with various lengths of *hrpL* upstream regions in pFPV25 and GFP activity of *E. amylovora* carrying each construct.** (A) DNA sequence of the *hrpL* upstream sequence. The IHF binding site is underlined, and the sigma factor 54 ($\sigma^{54}$) binding site is double underlined. The transcription start site is indicated with an asterisk, and the start codon is indicated in red. (B) Series of deletion of *hrpL* promoter-*gfp* fusion constructs were transformed into *Erwinia amylovora* Ea273 wild-type. Bacterial strains were grown in *hrp*-inducing medium at 18℃ for 18 h, and GFP activity of each strain was measured by flow cytometry. Numbers represent GFP activity means of three replicates ± standard errors. The experiment was repeated at least twice with similar results.

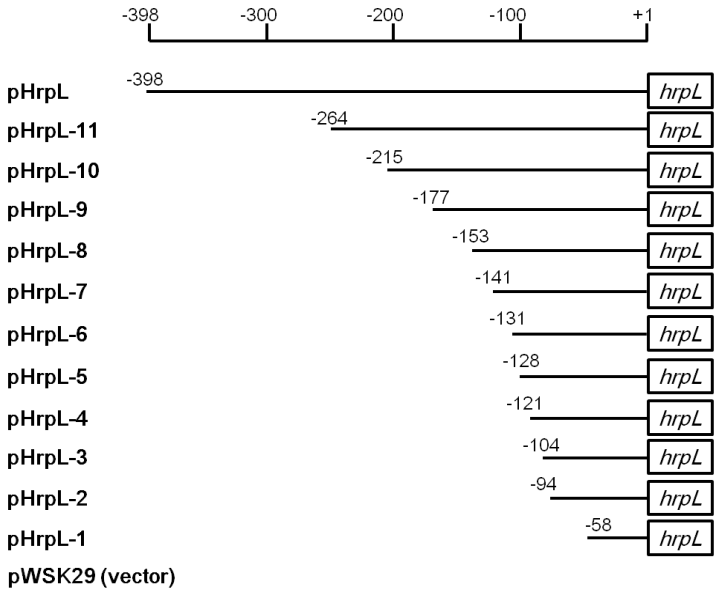


**Figure 3.3 Schematic diagram of *hrpL* gene with various lengths of *hrpL* upstream regions in pWSK29.** Series of *hrpL* gene constructs under the control of different lengths of *hrpL* promoter were generated and transformed into *E. amylovora* Ea1189 *hrpL* mutant.

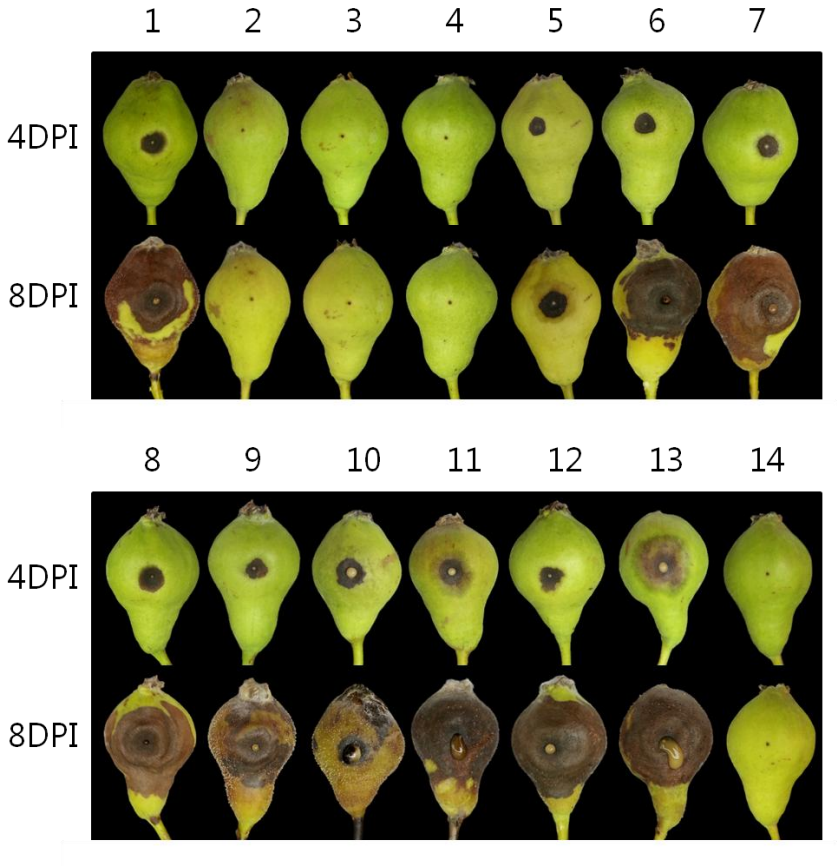


**Figure 3.4 Pathogenicity tests of *E. amylovora* wild-type (WT) and 13 different complementation strains of the *hrpL* mutant on immature pears.** Symptoms caused by WT and 13 different complementation strains of the *hrpL* mutant. The *hrpL* (pWSK29) was used as a negative control, 1, WT Ea1189; 2, *hrpL* (pHrpL-1); 3, *hrpL* (pHrpL-2); 4, *hrpL* (pHrpL-3); 5, *hrpL* (pHrpL-4); 6, *hrpL* (pHrpL-5); 7, *hrpL* (pHrpL-6); 8, *hrpL* (pHrpL-7); 9, *hrpL* (pHrpL-8); 10, *hrpL* (pHrpL-9); 11, *hrpL* (pHrpL-10); 12, *hrpL* (pHrpL-11); 13, *hrpL* (pHrpL); 14, *hrpL* (pWSK29), DPI, days post-inoculation.

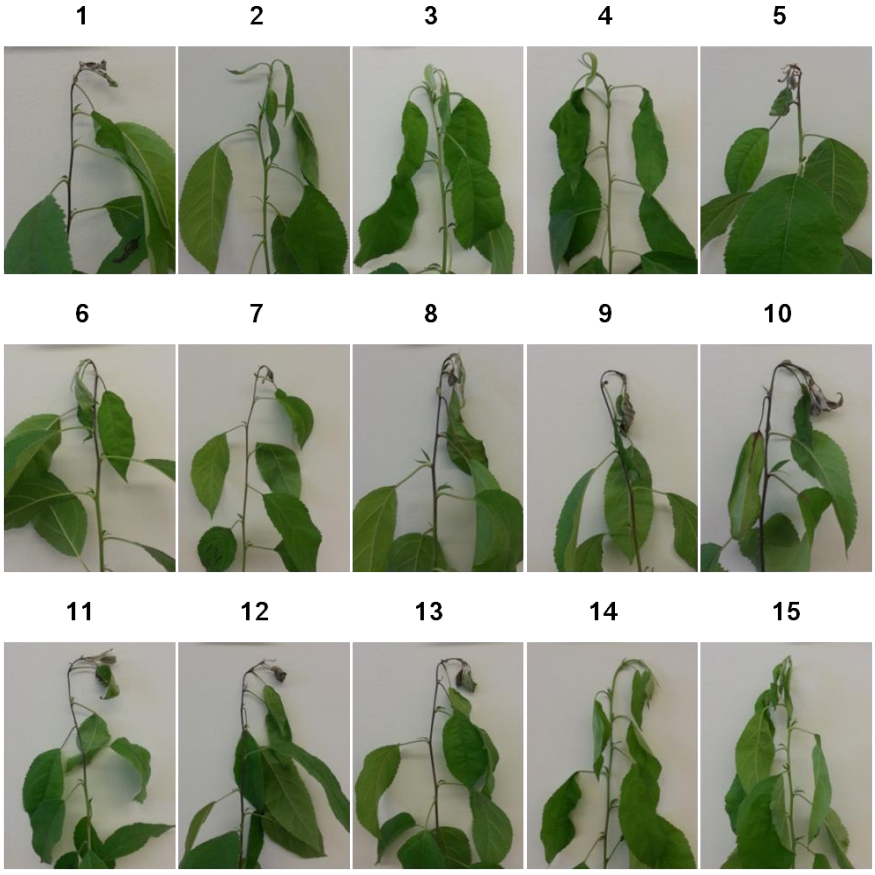


**Figure 3.5 Pathogenicity tests of *E. amylovora* wild-type (WT) and 13 different complementation strains of the *hrpL* mutant on apple shoots.** Symptoms caused by WT and 13 different complementation strains of the *hrpL* mutants at 7 days post-inoculation. The *hrpL* (pWSK29) was used as a negative control, 1, WT Ea1189; 2, *hrpL* (pHrpL-1); 3, *hrpL* (pHrpL-2); 4, *hrpL* (pHrpL-3); 5, *hrpL* (pHrpL-4); 6, *hrpL* (pHrpL-5); 7, *hrpL* (pHrpL-6); 8, *hrpL* (pHrpL-7); 9, *hrpL* (pHrpL-8); 10, *hrpL* (pHrpL-9); 11, *hrpL* (pHrpL-10); 12, *hrpL* (pHrpL-11); 13, *hrpL* (pHrpL); 14, *hrpL* (pWSK29); 15. PBS.

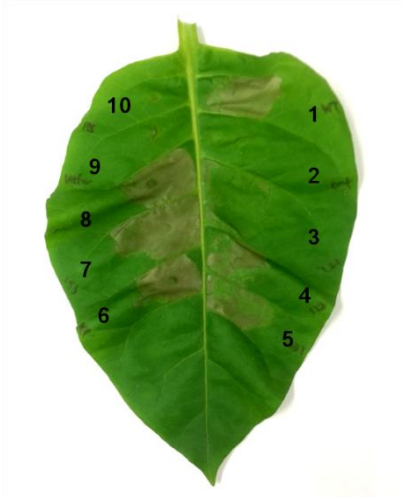


**Figure 3.6 Hypersensitive response (HR) assay of *E. amylovora* wild-type (WT) and seven selected complementation strains of the *hrpL* mutant on tobacco leaves.** Eight-week-old tobacco leaves were infiltrated with wild-type, mutant strain and complementation strains with cell suspensions at an optical density at 600 nm ($OD_{600}$) of 0.1, 1, WT Ea1189; 2, *hrpL* (pHrpL-3); 3, *hrpL* (pHrpL-4); 4, *hrpL* (pHrpL-5); 5, *hrpL* (pHrpL-6); 6, *hrpL* (pHrpL-7); 7, *hrpL* (pHrpL-8); 8, *hrpL* (pHrpL); 9, *hrpL* (pWSK29); 10, PBS.

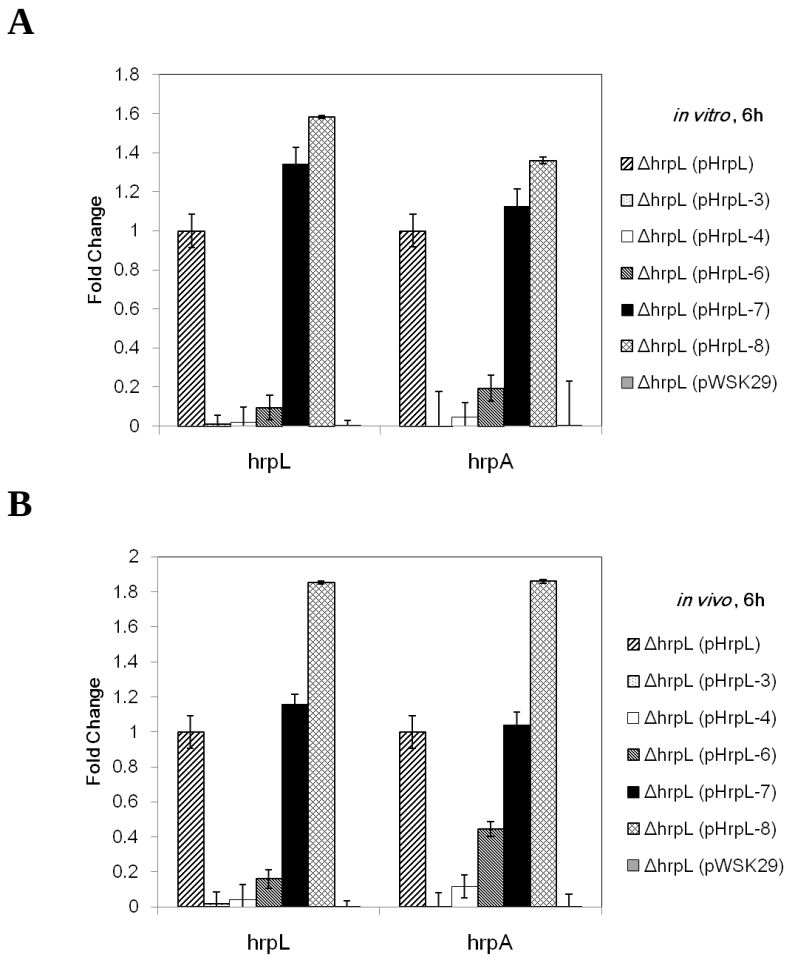


**Figure 3.7 Expression of *hrpL* and *hrpA* genes *in vivo* and *in vitro* by quantitative real-time reverse transcription-polymerase chain reaction (qRT-PCR).** (A) Relative gene expression of *hrpL* and *hrpA* genes in five selected complementation strains of the *hrpL* mutant (pHrpL-3, 4, 6, 7 and 8) as compared with the full *hrpL* complementation strain (pHrpL) grown in *hrp*-inducing medium at 18℃ at 6 h. (B) Relative gene expression of *hrpL* and *hrpA* genes in five selected complementation strains of the *hrpL* mutants (pHrpL-3, 4, 6, 7 and 8) as compared with the full *hrpL* complementation strain (pHrpL) inoculated onto immature pear fruits at 6 h. The relative fold change of each gene was derived from the comparison versus pHrpL. The *hrpL* (pWSK29) was used as a negative control, and the *rpoD* gene was used as an endogenous control. The values of the relative fold change were the means of three replicates. The experiments were repeated at least twice with similar results. Error bars indicate standard deviation.

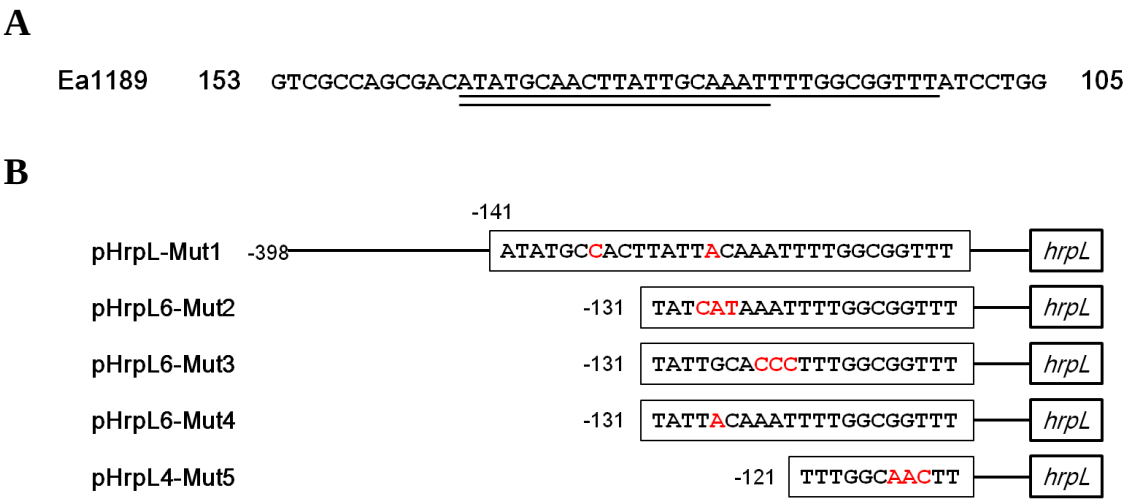


**Figure 3.8 Mutational analysis of potential HrpS binding site.** (A) The HrpS binding site (double underlined) is located at -141 to -122 upstream of the *hrpL* transcription start site. Mirror sequence (underlined) is located at -121 to -111 in the *hrpL* promoter region. (B) Schematic diagram of mutated constructs for the analysis of the potential HrpS binding site and the mirror sequence. Mut1, Mut2 to Mut4, and Mut5 were generated using pHrpL, pHrpL-6, and pHrpL-4 constructs, respectively. Mutated nucleotides are indicated in red.

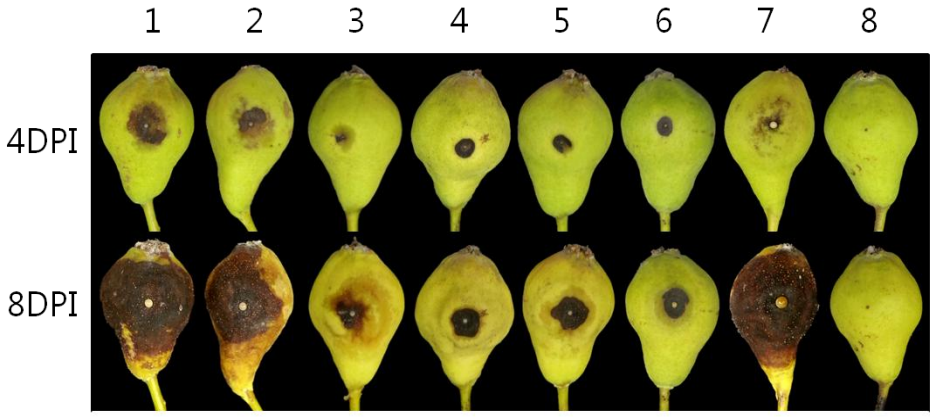


**Figure 3.9 Pathogenicity tests of *E. amylovora* wild-type (WT) and five complementation strains of the *hrpL* mutant on immature pears.** Symptoms caused by WT and five complementation strains of the *hrpL* mutants. The *hrpL* (pWSK29) was used as a negative control, 1, WT Ea1189; 2, *hrpL* (pHrpL-Mut1); 3, *hrpL* (pHrpL6-Mut2); 4, *hrpL* (pHrpL6-Mut3); 5, *hrpL* (pHrpL6-Mut4); 6, *hrpL* (pHrpL4-Mut5); 7, *hrpL* (pHrpL); 8, *hrpL* (pWSK29), DPI, days post-inoculation.

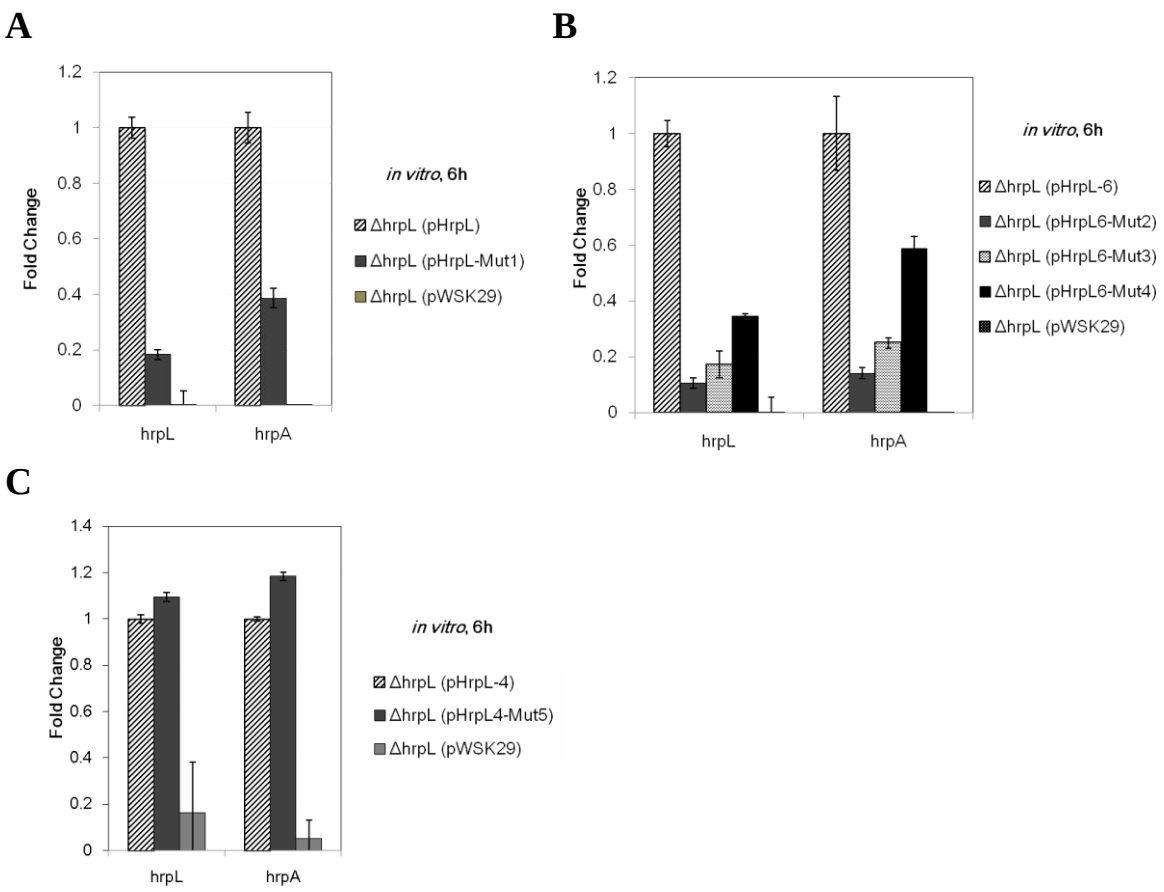


**Figure 3.10 Expression of *hrpL* and *hrpA* genes *in vitro* by quantitative real-time reverse transcription-polymerase chain reaction (qRT-PCR).** (A) Relative gene expression of *hrpL* and *hrpA* genes in *hrpL* mutants (pHrpL-Mut1) as compared with the *hrpL* (pHrpL) grown in *hrp*-inducing medium (HMM) at 18℃ at 6 h. (B) Relative gene expression of *hrpL* and *hrpA* genes in *hrpL* mutants (pHrpL6-Mut2, 3, 4) as compared with the *hrpL* (pHrpL-6) grown in HMM at 18℃ at 6 h. (C) Relative gene expression of *hrpL* and *hrpA* genes in *hrpL* mutants (pHrpL4-Mut5) as compared with the *hrpL* (pHrpL-4) grown in HMM at 18℃ at 6 h. The relative fold change of each gene was derived from the comparison versus pHrpL. The *hrpL* (pWSK29) was used as a negative control, and the *rpoD* gene was used as an endogenous control. The values of the relative fold change were the means of three replicates. The experiments were repeated at least twice with similar results. Error bars indicate standard deviation.

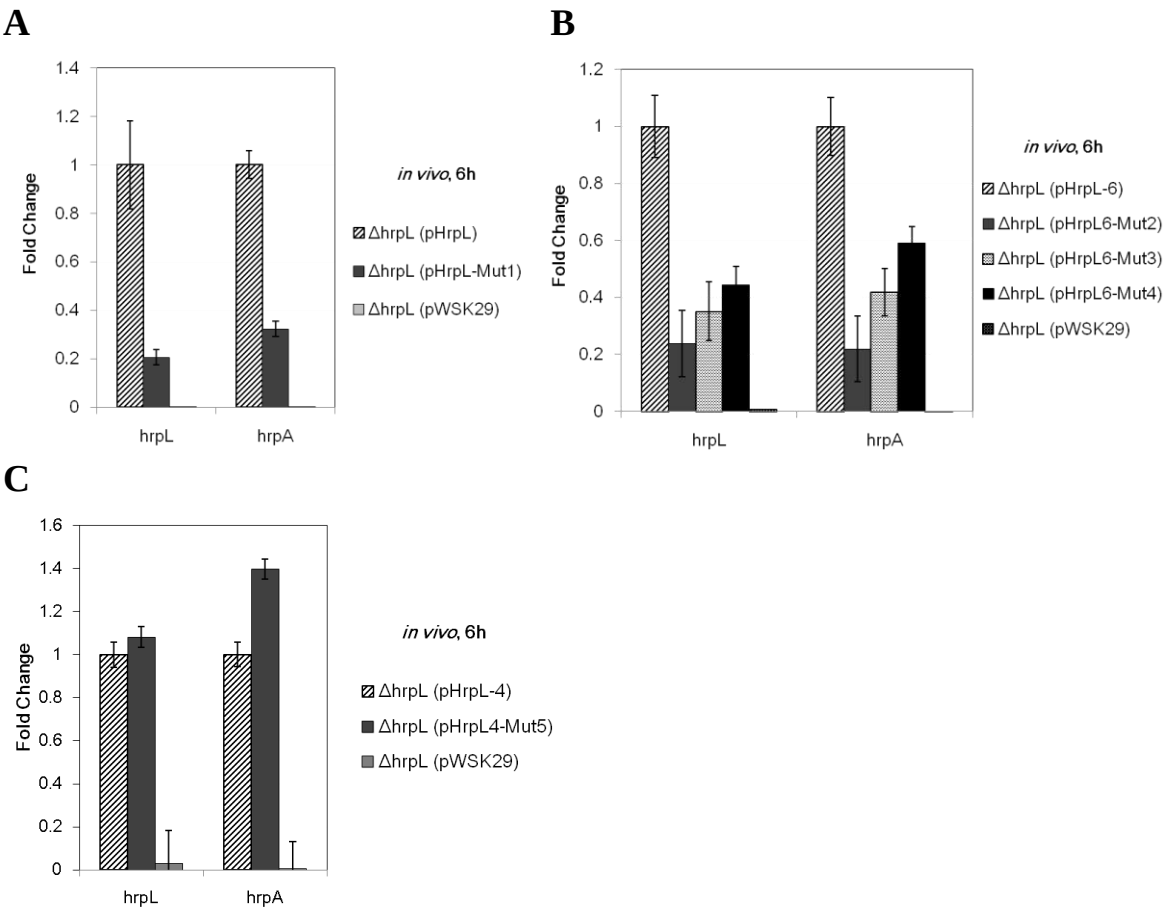


**Figure 3.11 Expression of *hrpL* and *hrpA* genes *in vivo* by quantitative real-time reverse transcription-polymerase chain reaction (qRT-PCR).** (A) Relative gene expression of *hrpL* and *hrpA* genes in *hrpL* mutants (pHrpL-Mut1) as compared with the Δ*hrpL* (pHrpL) inoculated onto immature pear fruits at 6 h. (B) Relative gene expression of *hrpL* and *hrpA* genes in *hrpL* mutants (pHrpL6-Mut2, 3, 4) as compared with the Δ*hrpL* (pHrpL-6) inoculated onto immature pear fruits at 6 h. (C) Relative gene expression of *hrpL* and *hrpA* genes in *hrpL* mutants (pHrpL4-Mut5) as compared with the *hrpL* (pHrpL-4) inoculated onto immature pear fruits at 6 h. The relative fold change of each gene was derived from the comparison versus pHrpL. The *hrpL* (pWSK29) was used as a negative control, and the *rpoD* gene was used as an endogenous control. The values of the relative fold change were the means of three replicates. The experiments were repeated at least twice with similar results. Error bars indicate standard deviation.

**A**

```
HrpS-WT  : GACATATGCAACTTATTGCAAATTTT
HrpS-Mut: GACATTTTTTACTTATCCCCCATTTT
```

**B**

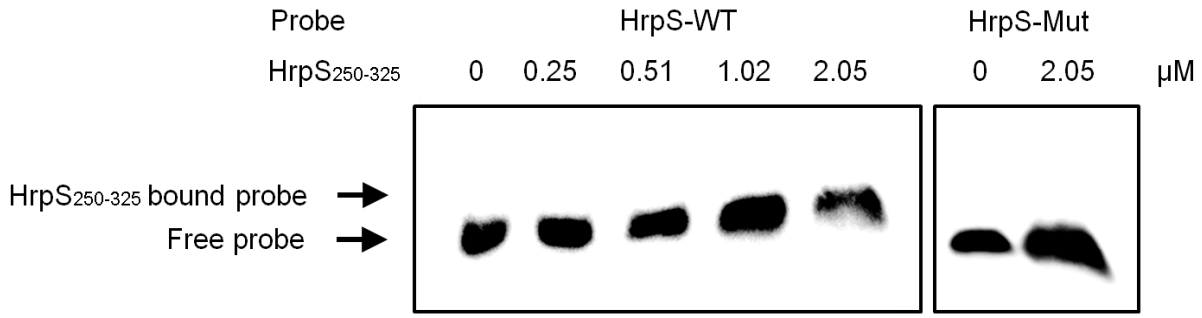


**Figure 3.12 Electrophoretic mobility shift assay (EMSA) using truncated HrpS$_{250-325}$ protein.** (A) The 26 bp of the *hrpL* promoter region (-144 to -119 nt) containing the HrpS binding site (HrpS-WT) and mutations of the HrpS binding site (HrpS-Mut) was tested for binding to HrpS$_{250-325}$. The HrpS binding site is underlined, and mutated nucleotides are indicated in red. (B) The unshifted DNA (free probe) and the protein-DNA complex (HrpS$_{250-325}$ bound probe) are indicated by arrows. The concentration of purified HrpS$_{250-325}$ is indicated above each lane.

```
E. amylovora      : -141 ATATGCAA-CTTA-TTGCAAAT -122
P. atrosepticum   : -139 GATTGCAA-TAAC-TTGCAATT -120
D. dadantii       : -141 TTCTGCAA-AAGC-TTGCAATT -122
P. stewartii      : -136 GATTGCAA-TGAG-TTGCAGAT -117
```

**Figure 3.13 Sequence alignment of the dyad symmetry sequence on the *hrpL* promoter region in *Erwinia amylovora*, *Pectobacterium atrosepticum*, *Dickeya dadantii* and *Pantoea stewartii*.** Dyad symmetry sequences are indicated in red.


**Figure 3.14 Pathogenicity tests of *E. amylovora* wild-type (WT), *hrpS* mutant and *hrpS* mutants complemented with different *hrpS* constructs on immature pears.** Symptoms caused by WT, *hrpS* (pHrpS), *hrpS* (pHrpS (Y100F)), *hrpS* (pHrpS (Y100A)), *hrpS* (pHrpS (T101A)) and *hrpS* mutant. DPI, days post-inoculation.

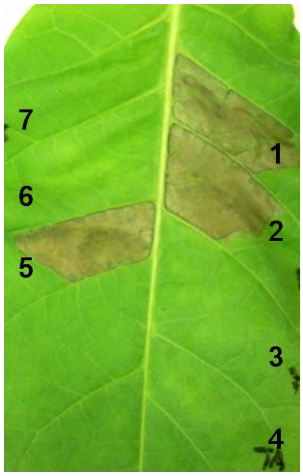


**Figure 3.15 Hypersensitive response (HR) assay of *E. amylovora* wild-type (WT), *hrpS* mutant and *hrpS* mutant complemented with different *hrpS* constructs on tobacco leaves.** Eight-week-old tobacco leaves were infiltrated with wild-type, *hrpS* mutant and different complementation strains with cell suspensions at an optical density at 600 nm ($OD_{600}$) of 0.1, 1, WT Ea1189; 2, *hrpS* (pHrpS (Y100F)); 3, *hrpS* (pHrpS (Y100A)); 4, *hrpS* (pHrpS (T101A)); 5, *hrpS* (pHrpS); 6, *hrpS*; 7, PBS.

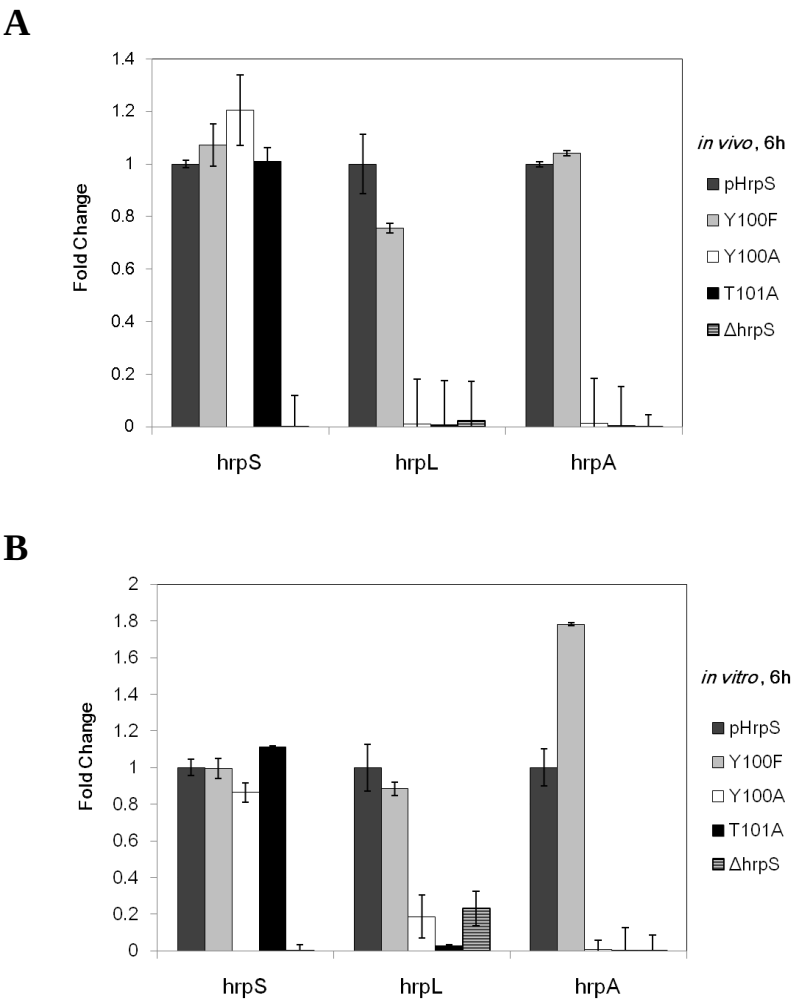


**Figure 3.16 Expression of *hrpL* and *hrpA* genes *in vivo* and *in vitro* by quantitative real-time reverse transcription-polymerase chain reaction (qRT-PCR).** (A) Relative gene expression of *hrpS*, *hrpL* and *hrpA* genes in three different complementation strains of the *hrpS* mutants (pHrpS-Y100F, Y100A and T101A) as compared with the *hrpS* complementation strain (pHrpS) inoculated onto immature pear fruits at 6 h. (B) Relative gene expression of *hrpS*, *hrpL* and *hrpA* genes in three different complementation strains of the *hrpS* mutants (pHrpS (Y100F), pHrpS (Y100A), pHrpS (T101A)) as compared with the *hrpS* complementation strain (pHrpS) grown in *hrp*-inducing medium at 18℃ at 6 h. The relative fold change of each gene was derived from the comparison versus pHrpS. The *hrpS* was used as a negative control, and the *rpoD* gene was used as an endogenous control. The values of the relative fold change were the means of three replicates. The experiments were repeated at least twice with similar results. Error bars indicate standard deviation.

## REFERENCES


Adam AL, Pike S, Hoyos ME, Stone JM, Walker JC, Novacky A (1997) Rapid and transient activation of a myelin basic protein kinase in tobacco leaves treated with harpin from *Erwinia amylovora*. Plant Physiol. 115: 853–861

Alarcón-Chaidez FJ, Keith L, Zhao Y, Bender CL (2003) RpoN ($\sigma^{54}$) is required for plasmid-encoded coronatine biosynthesis in *Pseudomonas syringae*. Plasmid 49: 106–17

Alfano JR, Collmer A (1997) The type III (Hrp) secretion pathway of plant pathogenic bacteria: trafficking harpins, Avr proteins, and death. J. Bacteriol. 179: 5655–62

Alfano JR, Collmer A (2004) Type III secretion system effector proteins: double agents in bacterial disease and plant defense. Annu. Rev. Phytopathol. 42: 385–414

Ali Azam T, Iwata A, Nishimura A, Ueda S, Ishihama A (1999) Growth phase-dependent variation in protein composition of the *Escherichia coli* nucleoid. J. Bacteriol. 181: 6361–70

Ancona V, Li W, Zhao Y (2014) Alternative sigma factor RpoN and its modulation protein YhbH are indispensable for *Erwinia amylovora* virulence. Mol. Plant. Pathol. 15: 58-66

Ancona V, Zhao Y (2013) CsrA is a positive regulator of virulence factors in *Erwinia amylovora*. Phytopathol. 103: S2

Austin S, Dixon R (1992) The prokaryotic enhancer binding protein NTRC has an ATPase activity which is phosphorylation and DNA dependent. EMBO J. 11: 2219–28

Aviv M, Giladi H, Schreiber G, Oppenheim AB, Glaser G (1994) Expression of the genes coding for the *Escherichia coli* integration host factor are controlled by growth phase, rpoS, ppGpp and by autoregulation. Mol. Microbiol. 14: 1021–31

Azam TA, Ishihama A (1999) Twelve species of the nucleoid-associated protein from *Escherichia coli*. Sequence recognition specificity and DNA binding affinity. J. Biol. Chem. 274: 33105–13

Baker CJ, Orlandi EW, Mock NM (1993) Harpin, an elicitor of the hypersensitive response in tobacco caused by *Erwinia amylovora*, elicits active oxygen production in suspension cells. Plant. Physiol. 102: 1341–1344

Beck LL, Smith TG, Hoover TR (2007) Look, no hands! Unconventional transcriptional activators in bacteria. Trends Microbiol. 15: 530–7

Bentley SD, Chater KF, Cerdeño-Tárraga A-M, Challis GL, Thomson NR, James KD, Harris DE, Quail MA, Kieser H, Harper D, et al (2002) Complete genome sequence of the model actinomycete *Streptomyces coelicolor* A3(2). Nature 417: 141–7

Billing E (1974) The effect of temperature on the growth of the fireblight pathogen, *Erwinia amylovora*. J. Appl. Bacteriol. 37: 643–8

Bocsanczy AM, Nissinen RM, Oh C-S, Beer S V (2008) HrpN of *Erwinia amylovora* functions in the translocation of DspA/E into plant cells. Mol. Plant Pathol. 9: 425–34

Bogdanove a J, Bauer DW, Beer S V (1998) *Erwinia amylovora* secretes DspE, a pathogenicity factor and functional AvrE homolog, through the Hrp (type III secretion) pathway. J. Bacteriol. 180: 2244–7

Bogdanove a J, Beer S V, Bonas U, Boucher C a, Collmer A, Coplin DL, Cornelis GR, Huang HC, Hutcheson SW, Panopoulos NJ, et al (1996) Unified nomenclature for broadly conserved hrp genes of phytopathogenic bacteria. Mol. Microbiol. 20: 681–3

Bonasera JM, Meng X, Beer S V, Owens T, Kim WS (2004) Interaction of DspE/A, a pathogenicity/avirulence protein of *Erwinia amylovora*, with pre-ferredoxin from apple and its relationship to photosynthetic efficiency. X Int. Work Fireblight 704 473–478

Bonn W, Zwet T (2000) Distribution and economic importance of fire blight. In: Vanneste, J.L. (Ed.), Fire Blight: The Disease and Its Causative Agent, *Erwinia amylovora*. 37–53

Bordes P, Wigneshweraraj SR, Schumacher J, Zhang X, Chaney M, Buck M (2003) The ATP hydrolyzing transcription activator phage shock protein F of *Escherichia coli*: identifying a surface that binds $\sigma^{54}$. Proc. Natl. Acad. Sci. USA 100: 2278–83

Bose D, Pape T, Burrows PC, Rappas M, Wigneshweraraj SR, Buck M, Zhang X (2008) Organization of an activator-bound RNA polymerase holoenzyme. Mol. Cell 32: 337–46

Boureau T, ElMaarouf-Bouteau H, Garnier A, Brisset M-N, Perino C, Pucheu I, Barny M-A (2006) DspA/E, a type III effector essential for *Erwinia amylovora* pathogenicity and growth in planta, induces cell death in host apple and nonhost tobacco plants. Mol. Plant-Microbe Interact. 19: 16–24

Bradbury JF (1986) Guide to Plant Pathogenic Bacteria. CAB International. Wallingford

Bramhill D, Kornberg A (1988) Duplex opening by DnaA protein at novel sequences in initiation of replication at the origin of the *Escherichia coli* chromosome. Cell 52: 743–55

Brencic A, McFarland KA, McManus HR, Castang S, Mogno I, Dove SL, Lory S (2009) The GacS/GacA signal transduction system of *Pseudomonas aeruginosa* acts exclusively through its control over the transcription of the RsmY and RsmZ regulatory small RNAs. Mol. Microbiol 73: 434–45

Browning DF, Grainger DC, Busby SJ (2010) Effects of nucleoid-associated proteins on bacterial chromosome structure and gene expression. Curr. Opin. Microbiol. 13: 773–80

Buck M, Gallegos MT, Studholme DJ, Guo Y, Gralla JD (2000) The bacterial enhancer-dependent $\sigma^{54}$ ($\sigma^{N}$) transcription factor. J. Bacteriol. 182: 4129–36

Burill TJ (1880) Anthrax of fruit trees: or the so-called fire blight of pear or twig blight of apple trees. Amer. Assoc. Advan. Sci. 29: 583–597

Bush M, Dixon R (2012) The role of bacterial enhancer binding proteins as specialized activators of $\sigma^{54}$-dependent transcription. Microbiol. Mol. Biol. Rev. 76: 497–529

Bush M, Ghosh T, Tucker N, Zhang X, Dixon R (2010) Nitric oxide-responsive interdomain regulation targets the $\sigma^{54}$-interaction surface in the enhancer binding protein NorR. Mol. Microbiol. 77: 1278–88

Buske FA, Mattick JS, Bailey TL (2011) Potential in vivo roles of nucleic acid triple-helices. RNA Biol. 8: 427–39

Büttner D, Bonas U (2006) Who comes first? How plant pathogenic bacteria orchestrate type III secretion. Curr. Opin. Microbiol. 9: 193–200

Büttner D, He SY (2009) Type III protein secretion in plant pathogenic bacteria. Plant Physiol. 150: 1656–64

Cannon W, Bordes P, Wigneshweraraj SR, Buck M (2003) Nucleotide-dependent triggering of RNA polymerase-DNA interactions by an AAA regulator of transcription. J. Biol. Chem. 278: 19815–25

Cannon W, Claverie-Martin F, Austin S, Buck M (1994) Identification of a DNA-contacting surface in the transcription factor sigma-54. Mol. Microbiol. 11: 227–36

Cannon W, Gallegos MT, Buck M (2001) DNA melting within a binary $\sigma^{54}$-promoter DNA complex. J. Biol. Chem. 276: 386–94

De Carlo S, Chen B, Hoover TR, Kondrashkina E, Nogales E, Nixon BT (2006) The structural basis for regulated assembly and function of the transcriptional activator NtrC. Genes Dev. 20: 1485–95

Cessna SG, Low PS (2001) Activation of the oxidative burst in aequorin-transformed *Nicotiana tabacum* cells is mediated by protein kinase- and anion channel-dependent release of $Ca^{2+}$ from internal stores. Planta 214: 126–34

Cessna SG, Messerli MA, Robinson KR, Low PS (2001) Measurement of stress-induced $Ca^{2+}$ pulses in single aequorin-transformed tobacco cells. Cell Calcium 30: 151–6

Chaney M, Grande R, Wigneshweraraj SR, Cannon W, Casaz P, Gallegos MT, Schumacher J, Jones S, Elderkin S, Dago AE, et al (2001) Binding of transcriptional activators to sigma 54 in the presence of the transition state analog ADP-aluminum fluoride: insights into activator mechanochemical action. Genes Dev. 15: 2282–94

Chatterjee AAK, Cui Y (2002) Regulation of *Erwinia carotovora hrpL*$_{Ecc}$ (*sigma-L*$_{Ecc}$), which encodes an extracytoplasmic function subfamily of sigma factor required for expression of the HRP regulon. Mol. Plant-Microbe Interact. 15: 971–80

Chatterjee AAK, Cui Y, Chaudhuri S (2002) Identification of regulators of hrp/hop genes of *Erwinia carotovora* ssp. *carotovora* and characterization of HrpL$_{Ecc}$ (SigmaL$_{Ecc}$), an alternative sigma factor. Mol. Plant Pathol. 3: 359–70

Claverie-Martin F, Magasanik B (1992) Positive and negative effects of DNA bending on activation of transcription from a distant site. J. Mol. Biol. 227: 996–1008

Collier DA, Wells RD (1990) Effect of length, supercoiling, and pH on intramolecular triplex formation. Multiple conformers at pur.pyr mirror repeats. J. Biol. Chem. 265: 10652–8

Dago AE, Wigneshweraraj SR, Buck M, Morett E (2007) A role for the conserved GAFTGA motif of $AAA^{+}$ transcription activators in sensing promoter DNA conformation. J. Biol. Chem. 282: 1087–97

DebRoy S, Thilmony R, Kwack Y-B, Nomura K, He SY (2004) A family of conserved bacterial effectors inhibits salicylic acid-mediated basal immunity and promotes disease necrosis in plants. Proc. Natl. Acad. Sci. USA 101: 9927–32

Denning W (1794) On the decay of apple trees. 219–222

Dillon SC, Dorman CJ (2010) Bacterial nucleoid-associated proteins, nucleoid structure and gene expression. Nat. Rev. Microbiol. 8: 185–95

Ditto MD, Roberts D, Weisberg RA (1994) Growth phase variation of integration host factor level in *Escherichia coli*. J. Bacteriol. 176: 3738–48

Dong H, Delaney TP, Bauer DW, Beer S V (1999) Harpin induces disease resistance in *Arabidopsis* through the systemic acquired resistance pathway mediated by salicylic acid and the NIM1 gene. Plant J. 20: 207–15

Floris R, Scaggiante B, Manzini G, Quadrifoglio F, Xodo LE (1999) Effect of cations on purine.purine.pyrimidine triple helix formation in mixed-valence salt solutions. Eur. J. Biochem. 260: 801–9

Fraser CM, Gocayne JD, White O, Adams MD, Clayton RA, Fleischmann RD, Bult CJ, Kerlavage AR, Sutton G, Kelley JM, et al (1995) The minimal gene complement of *Mycoplasma genitalium*. Science (80) 270: 397–403

Frederick RD, Majerczak DR, Coplin DL (1993) *Erwinia stewartii* WtsA, a positive regulator of pathogenicity gene expression, is similar to *Pseudomonas syringae* pv. *phaseolicola* HrpS. Mol. Microbiol. 9: 477–85

Gaudriault S, Malandrin L, Paulin JP, Barny MA (1997) DspA, an essential pathogenicity factor of *Erwinia amylovora* showing homology with AvrE of *Pseudomonas syringae*, is secreted via the Hrp secretion pathway in a DspB-dependent way. Mol. Microbiol. 26: 1057–69

Gaudriault S, Paulin J-P, Barny M-A (2002) The DspB/F protein of *Erwinia amylovora* is a type III secretion chaperone ensuring efficient intrabacterial production of the Hrp-secreted DspA/E pathogenicity factor. Mol. Plant. Pathol. 3: 313–20

Ghosh T, Bose D, Zhang X (2010) Mechanisms for activating bacterial RNA polymerase. FEMS Microbiol. Rev. 34: 611–27

González V, Olvera L, Soberón X, Morett E (1998) In vivo studies on the positive control function of NifA: a conserved hydrophobic amino acid patch at the central domain involved in transcriptional activation. Mol. Microbiol. 28: 55–67

Grimm C, Aufsatz W, Panopoulos NJ (1995) The hrpRS locus of *Pseudomonas syringae* pv. *phaseolicola* constitutes a complex regulatory unit. Mol. Microbiol. 15: 155–65

Gruber TM, Gross CA (2003) Multiple sigma subunits and the partitioning of bacterial transcription space. Annu. Rev. Microbiol. 57: 441–66

Guo Y, Gralla JD (1998) Promoter opening via a DNA fork junction binding activity. Proc. Natl. Acad. Sci. USA 95: 11655–60

Guo Y, Lew CM, Gralla JD (2000) Promoter opening by $\sigma^{54}$ and $\sigma^{70}$ RNA polymerases: sigma factor-directed alterations in the mechanism and tightness of control. Genes Dev. 14: 2242–55

Haase J, Lanka E (1997) A specific protease encoded by the conjugative DNA transfer systems of IncP and Ti plasmids is essential for pilus synthesis. J. Bacteriol. 179: 5728–35

Haugen SP, Ross W, Gourse RL (2008) Advances in bacterial promoter recognition and its control by factors that do not bind DNA. Nat. Rev. Microbiol. 6: 507–19

Hendrickson EL, Guevera P, Ausubel FM (2000a) The alternative sigma factor RpoN is required for hrp activity in *Pseudomonas syringae* pv. *maculicola* and acts at the level of hrpL transcription. J. Bacteriol. 182: 3508–16

Hendrickson EL, Guevera P, Peñaloza-Vàzquez A, Shao J, Bender C, Ausubel FM (2000b) Virulence of the phytopathogen *Pseudomonas syringae* pv. *maculicola* is *rpoN* dependent. J. Bacteriol. 182: 3498–507

Hirschman J, Wong PK, Sei K, Keener J, Kustu S (1985) Products of nitrogen regulatory genes *ntrA* and *ntrC* of enteric bacteria activate glnA transcription in vitro: evidence that the *ntrA* product is a sigma factor. Proc. Natl. Acad. Sci. USA 82: 7525–9

Holt JG, Krieg NR, Sneath PHA, Staley JT, Williams ST (1994) Bergey's Manual of Determinative Bacteriology, 9th ed. 787

Hsieh M, Hsu HM, Hwang SF, Wen FC, Yu JS, Wen CC, Li C (1999) The hydrophobic heptad repeat in Region III of *Escherichia coli* transcription factor sigma 54 is essential for core RNA polymerase binding. Microbiol. 145: 3081–8

Htun H, Dahlberg JE (1988) Single strands, triple strands, and kinks in H-DNA. Science 241: 1791–6

Hunt TP, Magasanik B (1985) Transcription of glnA by purified *Escherichia coli* components: core RNA polymerase and the products of *glnF*, *glnG*, and *glnL*. Proc. Natl. Acad. Sci. USA 82: 8453–7

Huo Y-X, Tian Z-X, Rappas M, Wen J, Chen Y-C, You C-H, Zhang X, Buck M, Wang Y-P, Kolb A (2006) Protein-induced DNA bending clarifies the architectural organization of the $\sigma^{54}$-dependent *glnAp2* promoter. Mol. Microbiol. 59: 168–80

Hutcheson SW, Bretz J, Sussan T, Jin S, Pak K (2001) Enhancer-binding proteins HrpR and HrpS interact to regulate *hrp*-encoded type III protein secretion in *Pseudomonas syringae* strains. J. Bacteriol. 183: 5589–98

Hwang DS, Kornberg A (1992) Opening of the replication origin of *Escherichia coli* by DnaA protein with protein HU or IHF. J. Biol. Chem. 267: 23083–6

Hyytiäinen H, Montesano M, Palva ET (2001) Global regulators ExpA (GacA) and KdgR modulate extracellular enzyme gene expression through the RsmA-rsmB system in E*rwinia carotovora* subsp. *carotovora*. Mol. Plant Microbe Interact. 14: 931–8

Jovanovic M, James EH, Burrows PC, Rego FGM, Buck M, Schumacher J (2011) Regulation of the co-evolved HrpR and HrpS $AAA^+$ proteins required for *Pseudomonas syringae* pathogenicity. Nat Commun 2: 177

Kay E, Dubuis C, Haas D (2005) Three small RNAs jointly ensure secondary metabolism and biocontrol in *Pseudomonas fluorescens* CHA0. Proc. Natl. Acad. Sci. USA 102: 17136–41

Khan MA, Zhao YF, Korban SS (2012) Molecular mechanisms of pathogenesis and resistance to the bacterial pathogen *Erwinia amylovora*, causal agent of fire blight disease in *Rosaceae*. Plant Mol. Biol. Rep. 30: 247–260

Kim JF, Wei ZM, Beer S V (1997) The *hrpA* and *hrpC* operons of *Erwinia amylovora* encode components of a type III pathway that secretes harpin. J. Bacteriol. 179: 1690–7

Klose KE, North AK, Stedman KM, Kustu S (1994) The major dimerization determinants of the nitrogen regulatory protein NTRC from enteric bacteria lie in its carboxy-terminal domain. J. Mol. Biol. 241: 233–45

Kohwi Y, Kohwi-Shigematsu T (1988) Magnesium ion-dependent triple-helix structure formed by homopurine-homopyrimidine sequences in supercoiled plasmid DNA. Proc. Natl. Acad. Sci. USA 85: 3781–5

Lan L, Deng X, Xiao Y, Zhou J-M, Tang X (2007) Mutation of Lon protease differentially affects the expression of *Pseudomonas syringae* type III secretion system genes in rich and minimal media and reduces pathogenicity. Mol. Plant Microbe Interact. 20: 682–96

Lapouge K, Schubert M, Allain FH-T, Haas D (2008) Gac/Rsm signal transduction pathway of gamma-proteobacteria: from RNA recognition to regulation of social behaviour. Mol. Microbiol. 67: 241–53

Lew CM, Gralla JD (2002) New roles for conserved regions within a $\sigma^{54}$-dependent enhancer-binding protein. J. Biol. Chem. 277: 41517–24

Li J, Passaglia L, Rombel I, Yan D, Kustu S (1999) Mutations affecting motifs of unknown function in the central domain of nitrogen regulatory protein C. J. Bacteriol. 181: 5443–54

Li W, Ancona V, Zhao Y (2014) Co-regulation of polysaccharide production, motility, and expression of type III secretion genes by EnvZ/OmpR and GrrS/GrrA systems in *Erwinia amylovora*. Mol. Genet Genomics 289: 63–75

Lindgren PB, Peet RC, Panopoulos NJ (1986) Gene cluster of *Pseudomonas syringae* pv. *phaseolicola* controls pathogenicity of bean plants and hypersensitivity of nonhost plants. J. Bacteriol. 168: 512–22

Lorenz M, Hillisch A, Goodman SD, Diekmann S (1999) Global structure similarities of intact and nicked DNA complexed with IHF measured in solution by fluorescence resonance energy transfer. Nucleic Acids Res. 27: 4619–25

Luijsterburg MS, White MF, van Driel R, Dame RT (2008) The major architects of chromatin: architectural proteins in bacteria, archaea and eukaryotes. Crit. Rev. Biochem. Mol. Biol. 43: 393–418

Lupas AN, Martin J (2002) AAA proteins. Curr. Opin. Struct. Biol. 12: 746–53

Macchi R, Montesissa L, Murakami K, Ishihama A, De Lorenzo V, Bertoni G (2003) Recruitment of $\sigma^{54}$-RNA polymerase to the Pu promoter of *Pseudomonas putida* through integration host factor-mediated positioning switch of alpha subunit carboxyl-terminal domain on an UP-like element. J. Biol. Chem. 278: 27695–702

Malnoy M, Martens S, Norelli JL, Barny M-A, Sundin GW, Smits THM, Duffy B (2012) Fire blight: applied genomic insights of the pathogen and host. Annu. Rev. Phytopathol. 50: 475–94

Mangan MW, Lucchini S, Danino V, Cróinín TO, Hinton JCD, Dorman CJ (2006) The integration host factor (IHF) integrates stationary-phase and virulence gene expression in *Salmonella enterica* serovar Typhimurium. Mol. Microbiol. 59: 1831–47

Mangan MW, Lucchini S, Ó Cróinín T, Fitzgerald S, Hinton JCD, Dorman CJ (2011) Nucleoid-associated protein HU controls three regulons that coordinate virulence, response to stress and general physiology in *Salmonella enterica* serovar Typhimurium. Microbiol. 157: 1075–87

Mann R a, Smits THM, Bühlmann A, Blom J, Goesmann A, Frey JE, Plummer KM, Beer S V, Luck J, Duffy B, et al (2013) Comparative genomics of 12 strains of *Erwinia amylovora* identifies a pan-genome with a large conserved core. PLoS One 8: e55644

Mascher T (2013) Signaling diversity and evolution of extracytoplasmic function (ECF) σ factors. Curr. Opin. Microbiol. 16: 148–55

McNally RR, Toth IK, Cock PJ a, Pritchard L, Hedley PE, Morris J a, Zhao Y, Sundin GW (2012) Genetic characterization of the HrpL regulon of the fire blight pathogen *Erwinia amylovora* reveals novel virulence factors. Mol. Plant Pathol. 13: 160–73

Meng X, Bonasera JM, Kim JF, Nissinen RM, Beer S V (2006) Apple proteins that interact with DspA/E, a pathogenicity effector of *Erwinia amylovora*, the fire blight pathogen. Mol. Plant Microbe Interact. 19: 53–61

Merighi M, Majerczak DR, Stover EH, Coplin DL (2003) The HrpX/HrpY two-component system activates *hrpS* expression, the first step in the regulatory cascade controlling the Hrp regulon in *Pantoea stewartii* subsp. *stewartii*. Mol. Plant Microbe Interact. 16: 238–48

Merighi M, Majerczak DR, Zianni M, Tessanne K, Coplin DL (2006) Molecular characterization of *Pantoea stewartii* subsp. *stewartii* HrpY, a conserved response regulator of the Hrp type III secretion system, and its interaction with the *hrpS* promoter. J. Bacteriol. 188: 5089–100

Metzger M, Bellemann P, Bugert P, Geider K (1994) Genetics of galactose metabolism of *Erwinia amylovora* and its influence on polysaccharide synthesis and virulence of the fire blight pathogen. J. Bacteriol. 176: 450–9

Miller HI, Friedman DI (1980) An *E. coli* gene product required for λ site-specific recombination. Cell 20: 711–719

Miller HI, Kikuchi A, Nash HA, Weisberg RA, Friedman DI (1979) Site-specific recombination of bacteriophage lambda: the role of host gene products. Cold Spring Harb. Symp. Quant. Biol. 43: 1121–6

Mirkin SM, Lyamichev VI, Drushlyak KN, Dobrynin VN, Filippov SA, Frank-Kamenetskii MD DNA H form requires a homopurine-homopyrimidine mirror repeat. Nature 330: 495–7

Model P, Jovanovic G, Dworkin J (1997) The *Escherichia coli* phage-shock-protein (*psp*) operon. Mol. Microbiol. 24: 255–61

Murtin C, Engelhorn M, Geiselmann J, Boccard F (1998) A quantitative UV laser footprinting analysis of the interaction of IHF with specific binding sites: re-evaluation of the effective concentration of IHF in the cell. J. Mol. Biol. 284: 949–61

Navarre WW, Porwollik S, Wang Y, McClelland M, Rosen H, Libby SJ, Fang FC (2006) Selective silencing of foreign DNA with low GC content by the H-NS protein in *Salmonella*. Science (80- ) 313: 236–8

Nissinen RM, Ytterberg a J, Bogdanove AJ, VAN Wijk KJ, Beer S V (2007) Analyses of the secretomes of *Erwinia amylovora* and selected hrp mutants reveal novel type III secreted proteins and an effect of HrpJ on extracellular harpin levels. Mol. Plant. Pathol. 8: 55–67

Norelli JL, Jones AL, Aldwinckle HS (2003) Fire blight management in the twenty first century using new technologies. Plant Dis. 87: 756–765

Nozaki S, Yamada Y, Ogawa T (2009) Initiator titration complex formed at *datA* with the aid of IHF regulates replication timing in *Escherichia coli*. Genes Cells 14: 329–41

O'Toole R, Milton DL, Hörstedt P, Wolf-Watz H (1997) RpoN of the fish pathogen *Vibrio* (*Listonella*) *anguillarum* is essential for flagellum production and virulence by the water-borne but not intraperitoneal route of inoculation. Microbiol. 143: 3849–59

Oh C-S, Beer S V (2005) Molecular genetics of *Erwinia amylovora* involved in the development of fire blight. FEMS Microbiol. Lett. 253: 185–192

Oh C-S, Kim JF, Beer S V (2005) The Hrp pathogenicity island of *Erwinia amylovora* and identification of three novel genes required for systemic infectiondouble dagger. Mol. Plant Pathol. 6: 125–38

Ortiz-Martín I, Thwaites R, Mansfield JW, Beuzón CR (2010) Negative regulation of the Hrp type III secretion system in *Pseudomonas syringae* pv. *phaseolicola*. Mol. Plant Microbe Interact. 23: 682–701

Oshima T, Ishikawa S, Kurokawa K, Aiba H, Ogasawara N (2006) *Escherichia coli* histone-like protein H-NS preferentially binds to horizontally acquired DNA in association with RNA polymerase. DNA Res. 13: 141–53

Ö sterberg S, del Peso-Santos T, Shingler V (2011) Regulation of alternative sigma factor use. Annu. Rev. Microbiol. 65: 37–55

Péchy-Tarr M, Bottiglieri M, Mathys S, Lejbølle KB, Schnider-Keel U, Maurhofer M, Keel C (2005) RpoN ($\sigma^{54}$) controls production of antifungal compounds and biocontrol activity in *Pseudomonas fluorescens* CHA0. Mol. Plant Microbe Interact. 18: 260–72

Peng JL, Dong HS, Dong HP, Delaney TP, Bonasera JM, Beer S V (2003) Harpin-elicited hypersensitive cell death and pathogen resistance require the *NDR1* and *EDS1* genes. Physiol. Mol. Plant Pathol. 62: 317–326

Pérez-Martín J, de Lorenzo V (1996) In vitro activities of an N-terminal truncated form of XylR, a $\sigma^{54}$-dependent transcriptional activator of *Pseudomonas putida*. J. Mol. Biol. 258: 575–87

Perino C, Gaudriault S, Vian B, Barny M a (1999) Visualization of harpin secretion *in planta* during infection of apple seedlings by *Erwinia amylovora*. Cell Microbiol. 1: 131–41

Popham PL, Pike SM, Novacky A (1995) The effect of harpin from *Erwinia amylovora* on the plasmalemma of suspension-cultured tobacco cells. Physiol. Mol. Plant Pathol. 47: 39–50

Porter ME, Dorman CJ (1997) Positive regulation of *Shigella flexneri* virulence genes by integration host factor. J. Bacteriol. 179: 6537–50

Prieto AI, Kahramanoglou C, Ali RM, Fraser GM, Seshasayee ASN, Luscombe NM (2012) Genomic analysis of DNA binding and gene regulation by homologous nucleoid-associated proteins IHF and HU in *Escherichia coli* K12. Nucleic Acids Res. 40: 3524–37

Rappas M, Schumacher J, Beuron F, Niwa H, Bordes P, Wigneshweraraj S, Keetch CA, Robinson C V, Buck M, Zhang X (2005) Structural insights into the activity of enhancer-binding proteins. Science 307: 1972–5

Raymundo AK, Ries SM (1981) Motility of *Erwinia amylovora*. Phytopathol. 71: 45–49
Raymundo AK, Ries SM (1980) Chemotaxis of *Erwinia amylovora*. Phytopathol. 70: 1066–69
Reitzer L, Schneider BL (2001) Metabolic context and possible physiological themes of $\sigma^{54}$-dependent genes in *Escherichia coli*. Microbiol. Mol. Biol. Rev. 65: 422–44
Rice PA, Yang S, Mizuuchi K, Nash HA (1996) Crystal structure of an IHF-DNA complex: a protein-induced DNA U-turn. Cell 87: 1295–306
Santero E, Hoover TR, North AK, Berger DK, Porter SC, Kustu S (1992) Role of integration host factor in stimulating transcription from the $\sigma^{54}$-dependent *nifH* promoter. J. Mol. Biol. 227: 602–20
Schumacher J, Joly N, Rappas M, Zhang X, Buck M (2006) Structures and organisation of $AAA^{+}$ enhancer binding proteins in transcriptional activation. J. Struct. Biol. 156: 190–9
Sebaihia M, Bocsanczy AM, Biehl BS, Quail MA, Perna NT, Glasner JD, DeClerck GA, Cartinhour S, Schneider DJ, Bentley SD, et al (2010) Complete genome sequence of the plant pathogen *Erwinia amylovora* strain ATCC 49946. J. Bacteriol. 192: 2020–1
Shen H, Keen NT (1993) Characterization of the promoter of avirulence gene D from *Pseudomonas syringae* pv. *tomato*. J. Bacteriol. 175: 5916–24
Smits THM, Rezzonico F, Duffy B (2011) Evolutionary insights from *Erwinia amylovora* genomics. J. Biotechnol. 155: 34–39
Smits THM, Rezzonico F, Kamber T, Blom J, Goesmann A, Frey JE, Duffy B (2010) Complete genome sequence of the fire blight pathogen *Erwinia amylovora* CFBP 1430 and comparison to other *Erwinia* spp. Mol. Plant Microbe Interact. 23: 384–93
Stonehouse E, Kovacikova G, Taylor RK, Skorupski K (2008) Integration host factor positively regulates virulence gene expression in *Vibrio cholerae*. J. Bacteriol. 190: 4736–48
Studholme DJ, Dixon R (2003) Domain architectures of $\sigma^{54}$-dependent transcriptional activators. J. Bacteriol. 185: 1757–67
Swinger KK, Rice PA (2004) IHF and HU: flexible architects of bent DNA. Curr. Opin. Struct. Biol. 14: 28–35
Tampakaki AP, Panopoulos NJ (2000) Elicitation of hypersensitive cell death by extracellularly targeted $HrpZ_{Psph}$ produced *in planta*. Mol. Plant Microbe Interact. 13: 1366–74
Taylor M, Butler R, Chambers S, Casimiro M, Badii F, Merrick M (1996) The RpoN-box motif of the RNA polymerase sigma factor sigma N plays a role in promoter recognition. Mol. Microbiol. 22: 1045–54
Teter B, Goodman SD, Galas DJ (2000) DNA bending and twisting properties of integration host factor determined by DNA cyclization. Plasmid 43: 73–84
Thompson LS, Webb JS, Rice SA, Kjelleberg S (2003) The alternative sigma factor RpoN regulates the quorum sensing gene *rhlI* in *Pseudomonas aeruginosa*. FEMS Microbiol. Lett. 220: 187–95
Thomson S V (2000) Epidemiology of fire blight. In: Vanneste, J.L. (Ed.), Fire Blight: The disease and its causative agent, *Erwinia amylovora*. 9–36
Travers A (1997) DNA-protein interactions: IHF--the master bender. Curr. Biol. 7: R252–4
Triplett LR, Zhao Y, Sundin GW (2006) Genetic differences between blight-causing *Erwinia* species with differing host specificities, identified by suppression subtractive hybridization. Appl. Environ. Microbiol. 72: 7359–64
Vanneste JL (2000) Fire Blight: The disease and its causative agent, *Erwinia amylovora*. CABI Publishing, New York

Venisse J-S, Barny M-A, Paulin J-P, Brisset M-N (2003) Involvement of three pathogenicity factors of *Erwinia amylovora* in the oxidative stress associated with compatible interaction in pear. FEBS Lett. 537: 198–202

Venisse JS, Gullner G, Brisset MN (2001) Evidence for the involvement of an oxidative stress in the initiation of infection of pear by *Erwinia amylovora*. Plant Physiol. 125: 2164–72

Walker JE, Saraste M, Runswick MJ, Gay NJ (1982) Distantly related sequences in the α- and β-subunits of ATP synthase, myosin, kinases and other ATP-requiring enzymes and a common nucleotide binding fold. EMBO J. 1: 945–51

Wang D, Korban SS, Zhao Y (2010) Molecular signature of differential virulence in natural isolates of *Erwinia amylovora*. Phytopathol. 100: 192–8

Wang J (2004) Nucleotide-dependent domain motions within rings of the RecA/$AAA^+$ superfamily. J. Struct. Biol. 148: 259–67

Wang YK, Lee JH, Brewer JM, Hoover TR (1997) A conserved region in the $\sigma^{54}$-dependent activator DctD is involved in both binding to RNA polymerase and coupling ATP hydrolysis to activation. Mol. Microbiol. 26: 373–86

Wei BL, Brun-Zinkernagel AM, Simecka JW, Prüss BM, Babitzke P, Romeo T (2001) Positive regulation of motility and *flhDC* expression by the RNA-binding protein CsrA of *Escherichia coli*. Mol. Microbiol. 40: 245–56

Wei Z, Kim JF, Beer S V (2000) Regulation of hrp genes and type III protein secretion in *Erwinia amylovora* by HrpX/HrpY, a novel two-component system, and HrpS. Mol. Plant Microbe Interact. 13: 1251–62

Wei ZM, Beer S V (1995) *hrpL* activates *Erwinia amylovora hrp* gene transcription and is a member of the ECF subfamily of sigma factors. J. Bacteriol. 177: 6201–10

Wei ZM, Laby RJ, Zumoff CH, Bauer DW, He SY, Collmer A, Beer S V (1992a) Harpin, elicitor of the hypersensitive response produced by the plant pathogen *Erwinia amylovora*. Science 257: 85–8

Wei ZM, Sneath BJ, Beer S V (1992b) Expression of *Erwinia amylovora hrp* genes in response to environmental stimuli. J. Bacteriol. 174: 1875–82

Weilbacher T, Suzuki K, Dubey AK, Wang X, Gudapaty S, Morozov I, Baker CS, Georgellis D, Babitzke P, Romeo T (2003) A novel sRNA component of the carbon storage regulatory system of *Escherichia coli*. Mol. Microbiol. 48: 657–70

Wikström P, O'Neill E, Ng LC, Shingler V (2001) The regulatory N-terminal region of the aromatic-responsive transcriptional activator DmpR constrains nucleotide-triggered multimerisation. J. Mol. Biol. 314: 971–84

Wyman C, Rombel I, North AK, Bustamante C, Kustu S (1997) Unusual oligomerization required for activity of NtrC, a bacterial enhancer-binding protein. Science 275: 1658–61

Xiao Y, Heu S, Yi J, Lu Y, Hutcheson SW (1994) Identification of a putative alternate sigma factor and characterization of a multicomponent regulatory cascade controlling the expression of *Pseudomonas syringae* pv. *syringae* Pss61 *hrp* and *hrmA* genes. J. Bacteriol. 176: 1025–36

Xie Z, Chen Z (2000) Harpin-induced hypersensitive cell death is associated with altered mitochondrial functions in tobacco cells. Mol. Plant Microbe Interact. 13: 183–90

Yang SW, Nash HA (1995) Comparison of protein binding to DNA *in vivo* and *in vitro*: defining an effective intracellular target. EMBO J. 14: 6292–300

Yap M-N, Yang C-H, Barak JD, Jahn CE, Charkowski AO (2005) The *Erwinia chrysanthemi* type III secretion system is required for multicellular behavior. J. Bacteriol. 187: 639–48

Zhang N, Joly N, Burrows PC, Jovanovic M, Wigneshweraraj SR, Buck M (2009) The role of the conserved phenylalanine in the $\sigma^{54}$-interacting GAFTGA motif of bacterial enhancer binding proteins. Nucleic Acids Res. 37: 5981–92

Zhang X, Chaney M, Wigneshweraraj SR, Schumacher J, Bordes P, Cannon W, Buck M (2002) Mechanochemical ATPases and transcriptional activation. Mol. Microbiol. 45: 895–903

Zhao K, Liu M, Burgess RR (2010) Promoter and regulon analysis of nitrogen assimilation factor, $\sigma^{54}$, reveal alternative strategy for *E. coli* MG1655 flagellar biosynthesis. Nucleic Acids Res. 38: 1273–83

Zhao Y, He S-Y, Sundin GW (2006) The *Erwinia amylovora avrRpt2*$_{EA}$ gene contributes to virulence on pear and AvrRpt2$_{EA}$ is recognized by *Arabidopsis* RPS2 when expressed in *Pseudomonas syringae*. Mol. Plant Microbe Interact. 19: 644–54

Zhao Y, Qi M (2011) Comparative genomics of *Erwinia amylovora* and related *Erwinia* Species - what do we learn? Genes 2: 627–639

Zhao Y, Sundin GW, Wang D (2009a) Construction and analysis of pathogenicity island deletion mutants of *Erwinia amylovora*. Can. J. Microbiol. 55: 457–64

Zhao Y, Wang D, Nakka S, Sundin GW, Korban SS (2009b) Systems level analysis of two-component signal transduction systems in *Erwinia amylovora*: role in virulence, regulation of amylovoran biosynthesis and swarming motility. BMC Genomics 10: 245

Zou L, Zeng Q, Lin H, Gyaneshwar P, Chen G, Yang C-H (2012) SlyA regulates type III secretion system (T3SS) genes in parallel with the T3SS master regulator HrpL in *Dickeya dadantii* 3937. Appl. Environ. Microbiol. 78: 2888–95

Zwet T, Keil HL (1979) Fire Blight: a bacterial disease of rosaceous plants. Agricultural Handbook, U.S. Govt. Print, Washington